Astrofisica Nucleare e Subnucleare

“GRB” Astrophysics

Exercise #2

- Find David Band' GRB parametrization in paper (1993) and in XSPEC model

$$f_{\rm BAND}(E) = A\left(\frac{E}{100}\right)^{\alpha}\exp\left(-\frac{E(2+\alpha)}{E_{\rm peak}}\right) \quad \text{if} \quad \mathrm{E} < \mathrm{E_c}$$

$$f_{\rm BAND}(E) = A\left[\frac{(\alpha-\beta)E_{\rm peak}}{100(2+\alpha)}\right]^{\alpha-\beta}\exp\left(\beta-\alpha\right)\left(\frac{E}{100}\right)^{\beta} \quad \text{if} \quad \mathrm{E} \geq \mathrm{E_c},$$

where

$$E_c = (\alpha-\beta)\frac{E_{\rm peak}}{2+\alpha} \equiv (\alpha-\beta)E_0.$$

- Band et al. 1993 ApJ 413, 281
- Find other papers on spectral evolution of GRBs
  - Ford et al 1995, (II) Peak energy evolution in bright, long bursts
  - Preece et al 1996 (III) Low-Energy Behavior of Time-averaged Spectra
  - Preece et al. 1998 (IV) Time-resolved High-Energy Spectroscopy

GRB: where are they?

The great debate (1995)

Flux: 10^{-7} erg cm^{-2} s^{-1}

Distance: 1 Gpc

Energy: 10^{51} erg

Distance: 100 kpc

Energy: 10^{43} erg

Cosmological - Galactic?

Need a new type of observation!

Astrofisica Nucleare e Subnucleare

Position sensitive detectors

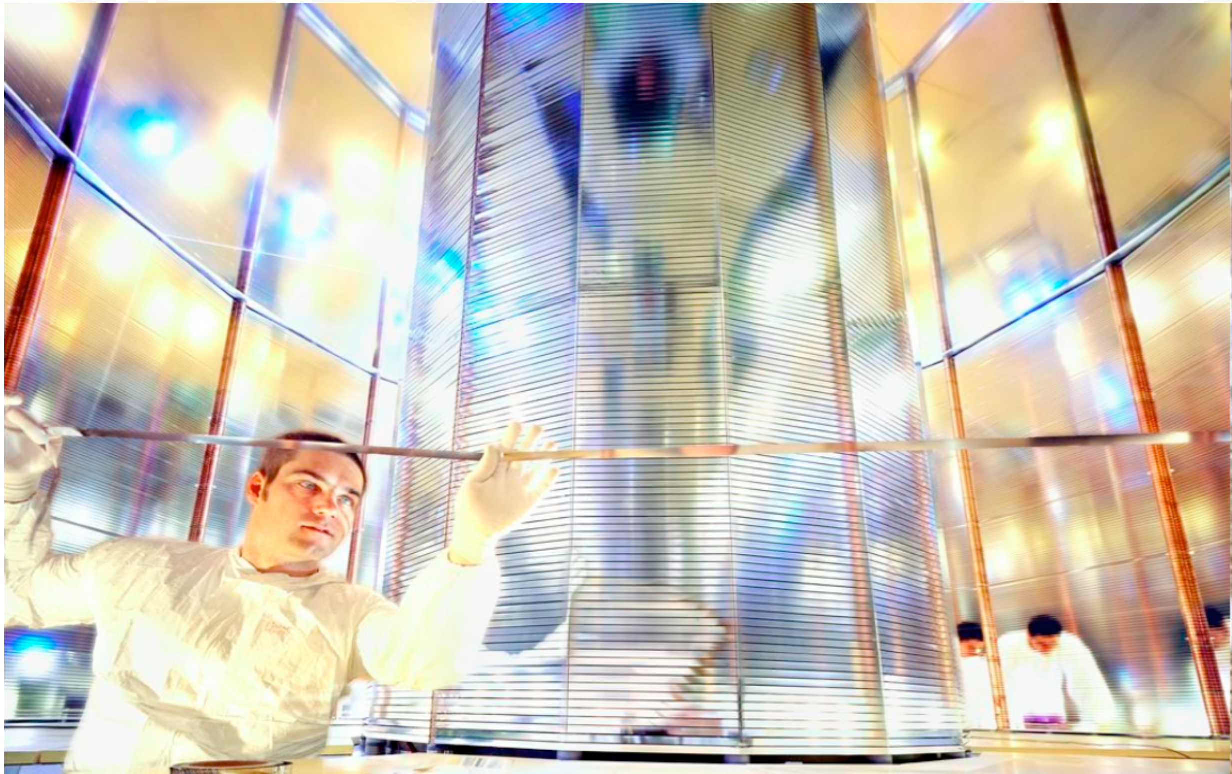


Detectors for Particle Physics

Scintillators and Gaseous detector

D. Bortoletto
University of Oxford & Purdue University

Tracking

- Particle detection has many aspects:
  - Particle counting
  - Particle Identification = measurement of mass and charge of the particle
  - Tracking
- Charged particles are deflected by B fields:

$$\vec{F} = q\vec{v} \times \vec{B}$$

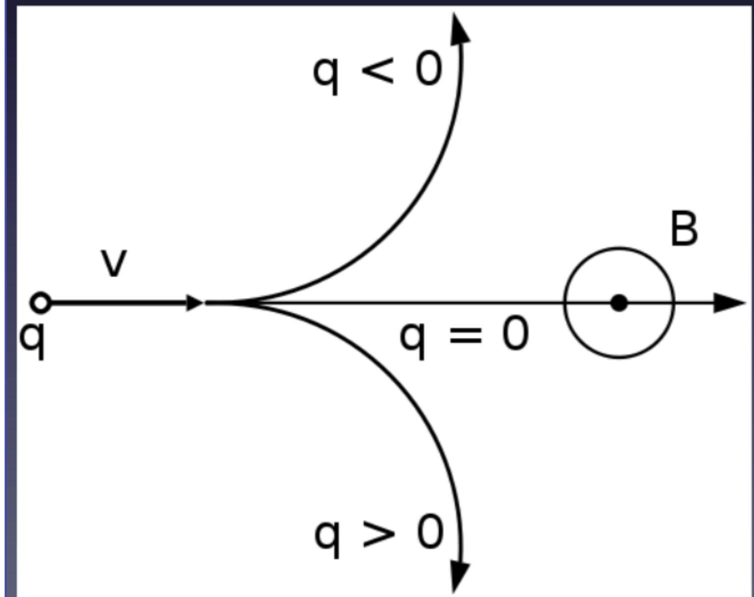

$$\rho = \frac{p_T}{q|B|} = \frac{\gamma m_0 \beta c}{q|B|}$$

- By measuring the radius of curvature we can determine the momentum of a particle
- If we can measure also β independently we can determine the particle mass.

Signal creation

- Charged particle traversing matter leave excited atoms, electron-ion pairs (gases) and electrons-hole pairs (solids)

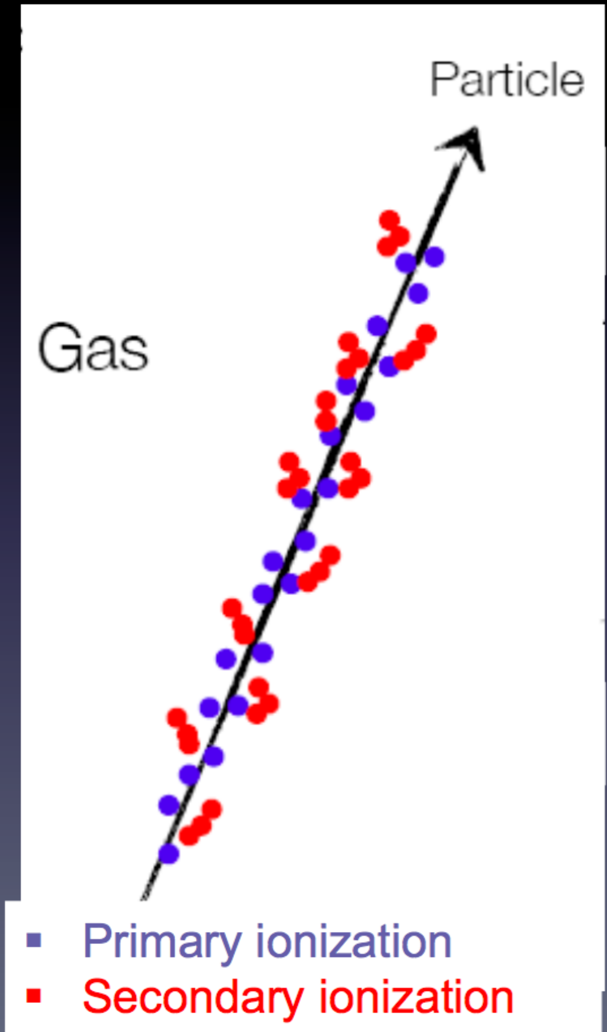

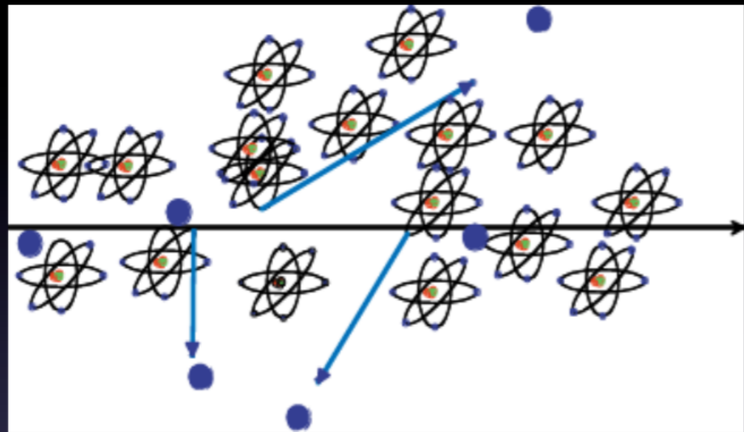

- Excitation: Photons emitted by the excited atoms in transparent materials can be detected with photon detectors
- Ionization: By applying an electric field in the detector volume, the ionization electrons and ions can be collected on electrodes and readout

Astrofisica Nucleare e Subnucleare

Gas Detectors

Primary and secondary ionization

- Coulomb interactions between E field of the particle and of the molecules of the medium produce electron-ion pairs.

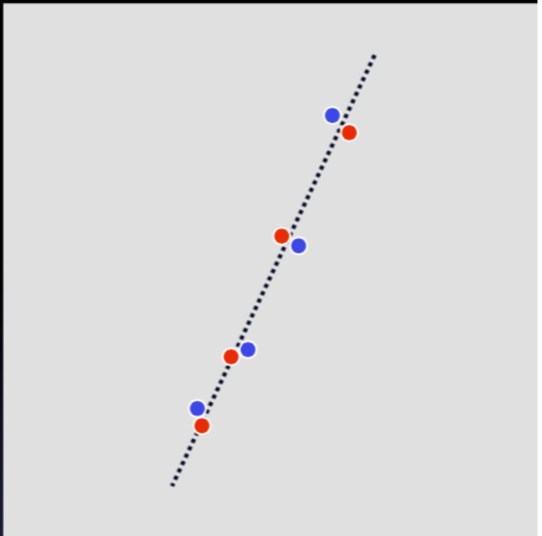

- Minimum ionizing particles in argon NTP
  - $\langle n_P \rangle$: 25 cm^{-1}
- Primary electrons can ionize the medium producing local e-ion clusters. Electron can have energy to produce a long trail (delta electron).
- Total number of ion pairs n_T:
  - *E:* energy loss
  - w_i : average energy per ion pair

$$n_T = \frac{\Delta E}{w_i}$$

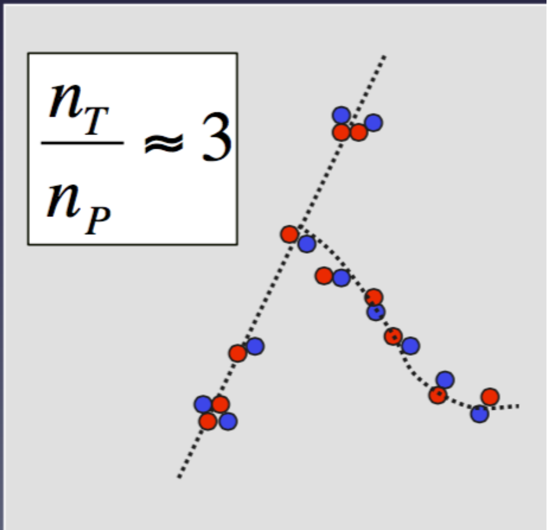

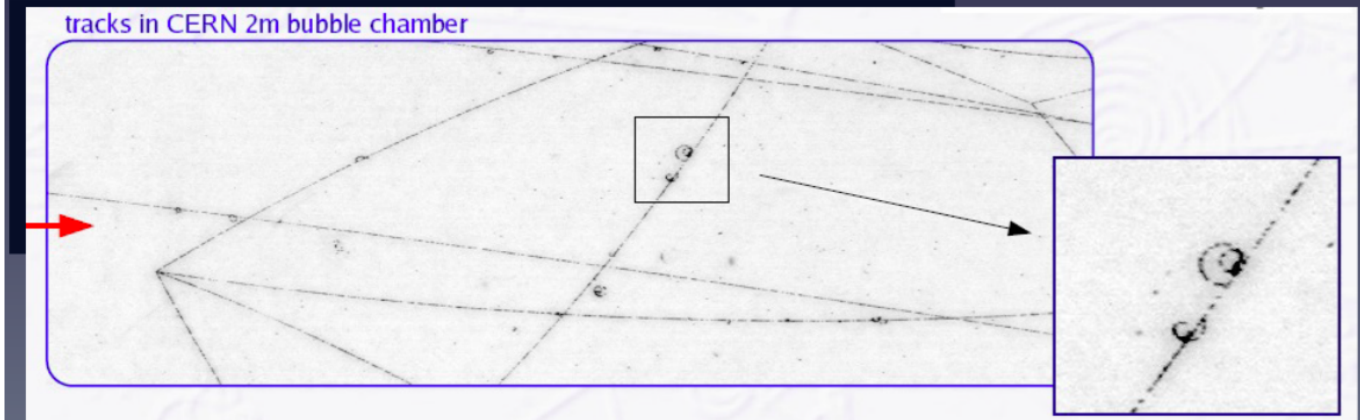

Ionization statistics

- Multiple ionizing collisions follow Poisson's statistics:

$$\langle n_p \rangle = \frac{L}{\lambda}$$

$$\lambda = \frac{1}{n_e \sigma_I}$$

$$P_{n_P}^{\langle n_P \rangle} = \frac{\langle n_p \rangle^{n_p} e^{-\langle n_p \rangle}}{n_p!}$$

σ_I: Ionization x-section
n_e: Electron density
L: Thickness

Typical values of the mean free path **λ**

- He 0.25 cm
- Air 0.052 cm
- Xe 0.023 cm

GAS (STP)	thickness	ε (%)
Helium	1 mm	45
	2 mm	70
Argon	1 mm	91.8
	2 mm	99.3

- Efficiency:

$$\varepsilon = 1 - P_0^{\langle n_p \rangle} = 1 - e^{-\langle n_p \rangle}$$

- Other important parameters are:
  - Recombination and electron attachment due to Electro-negative gases which bind electrons; e.g.: O_2, Freon, Cl_2, SF_6 ... →influences detection efficiency
  - Diffusion→ Influences the spatial resolution
  - Mobility of charges → Influences the timing behavior of gas detectors
  - Electronic noise in amplifier is typically 1000 e- (ENC)→Amplification is needed → Important for the gain factor of the gas detector ...

Diffusion & Drift

E = 0: Thermal diffusion

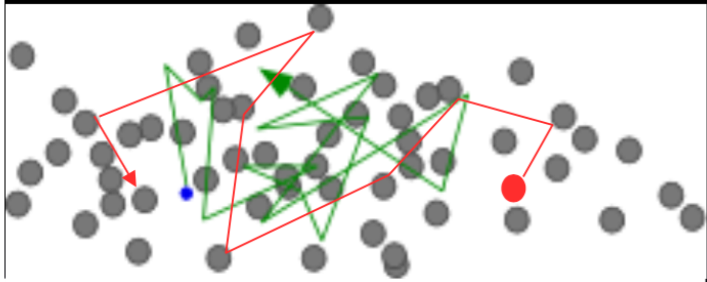

$$D = \frac{1}{3} v \lambda = \frac{2}{3\sqrt{\pi}} \frac{1}{P\sigma_0} \sqrt{\frac{(kT)^3}{m}}$$

E >0: Charge Transport and Thermal diffusion

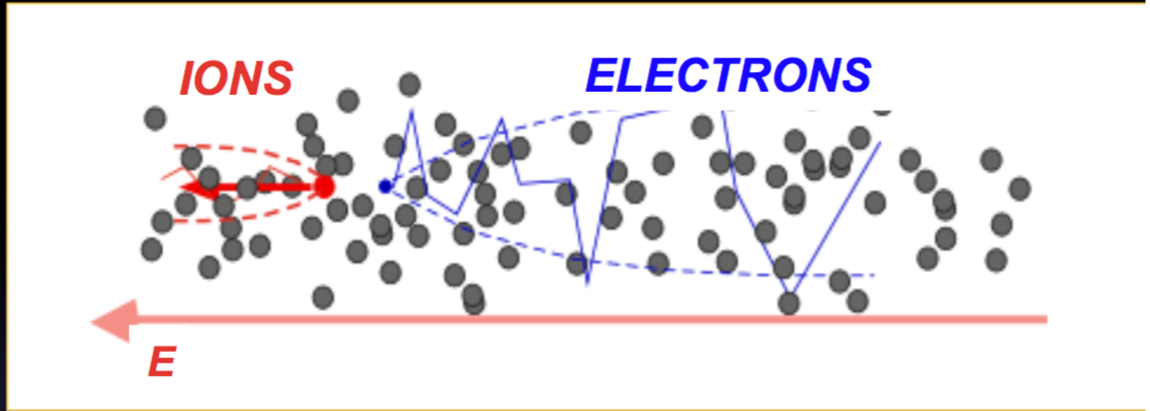

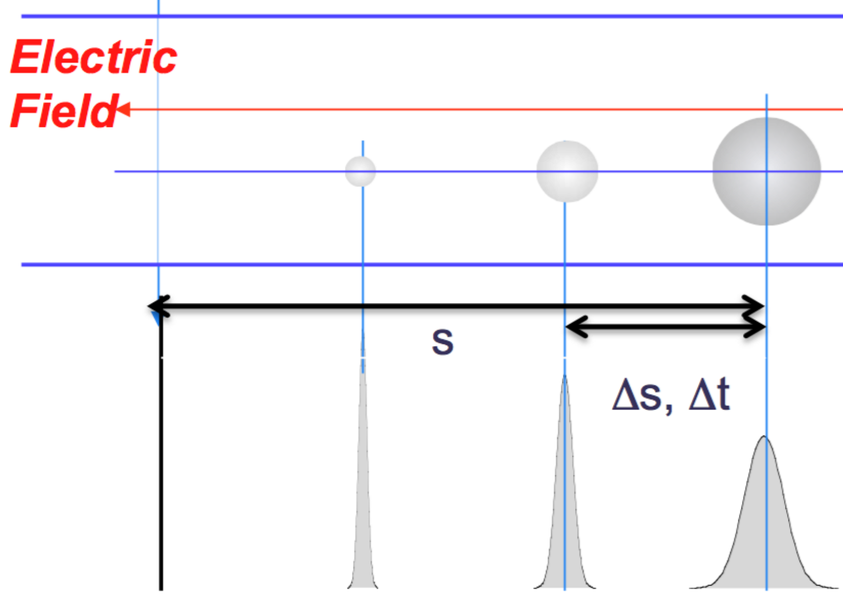

Drift velocity: $v_D = \frac{\Delta s}{\Delta t}$

Space diffusion rms:

$$\sigma_x = \sqrt{2Dt} = \sqrt{2D \frac{s}{v_D}}$$

Diffusion in a gas

- Diffusion is evaluated using the classical theory of gases.
- Due to multiple collisions the distribution of charge at time t in a length dx after a distance x is given by a Gaussian

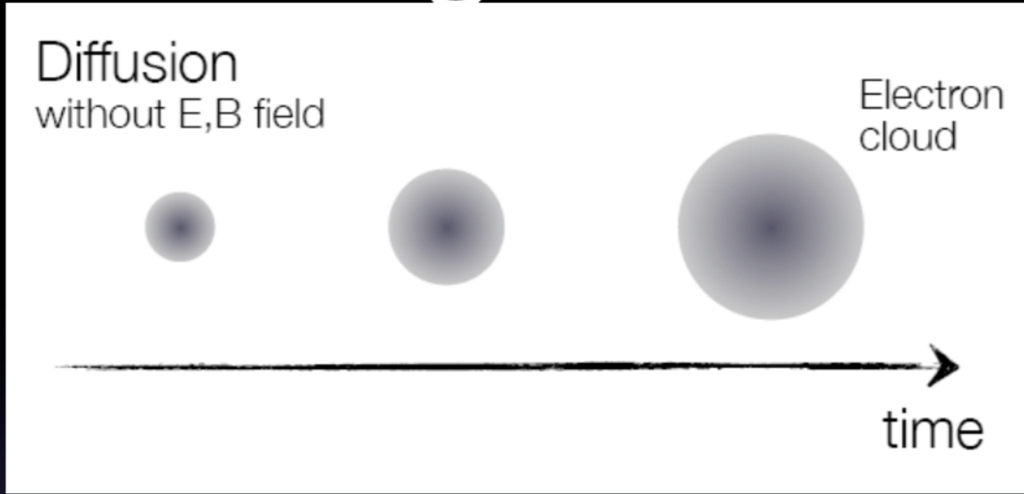

$$\frac{dN}{dx} = \frac{N_0}{\sqrt{4\pi Dt}} \exp\left(-\frac{x^2}{4Dt}\right)$$

- Linear diffusion $\sigma_x = \sqrt{2Dt}$

D=diffusion coefficient depends on the pressure P and the temperature T

$$D = \frac{1}{3} v\lambda = \frac{2}{3\sqrt{\pi}} \frac{1}{P\sigma_0} \sqrt{\frac{(kT)^3}{m}}$$

- The Mean-free path of electrons/ions in the path

$$\lambda = \frac{1}{\sqrt{2}} \frac{kT}{\sigma_0 P}$$

- The mean velocity is given by the Maxwell distribution where m is the mass of the particle

$$v = \sqrt{\frac{8kT}{\pi m}}$$

Avalanche Multiplication

- The primary ionization signal is very small in a gas layer: in 1 cm of Ar/CO_2 (70:30) at NTP only **~100** electron–ion pairs are created →use an "internal gas amplification" mechanism to increase signal
- Large E fields →large electron kinetic energy →avalanche formation
  - **$dn = n\,\alpha\,dx$** **α=Townsend Coefficient**
  - **$n(x) = n_0\,e^{\alpha x}$** n(x)=electrons at location x
- Gain or Amplification is:

$$G = \frac{n}{n_0} = e^{\alpha x}$$

- Raether's limit $G \approx 10^8$, since after that sparking can occur

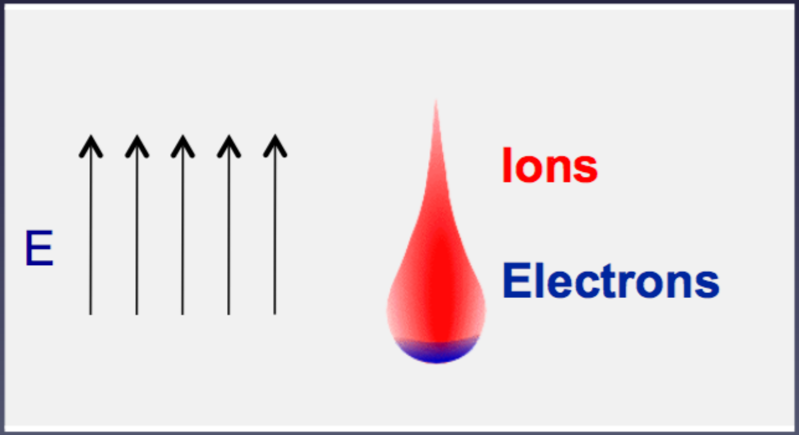

Drop-like shape of an avalanche

Gas amplification factor

- Ionization mode: full charge collection; no amplification; G=1
- Proportional mode: multiplication; signal proportional to original ionization ⇒ measurement of dE/dx. Secondary avalanches needs quenching; G ≈10^4-10^5
- Limited Proportional (Saturated, Streamer mode): strong photo-emission; Require strong quenchers. High gain 10^{10}⇒ large signal, simple electronics
- Geiger mode: Massive photo emission. Full length of anode affected. Discharge stopped by HV cut

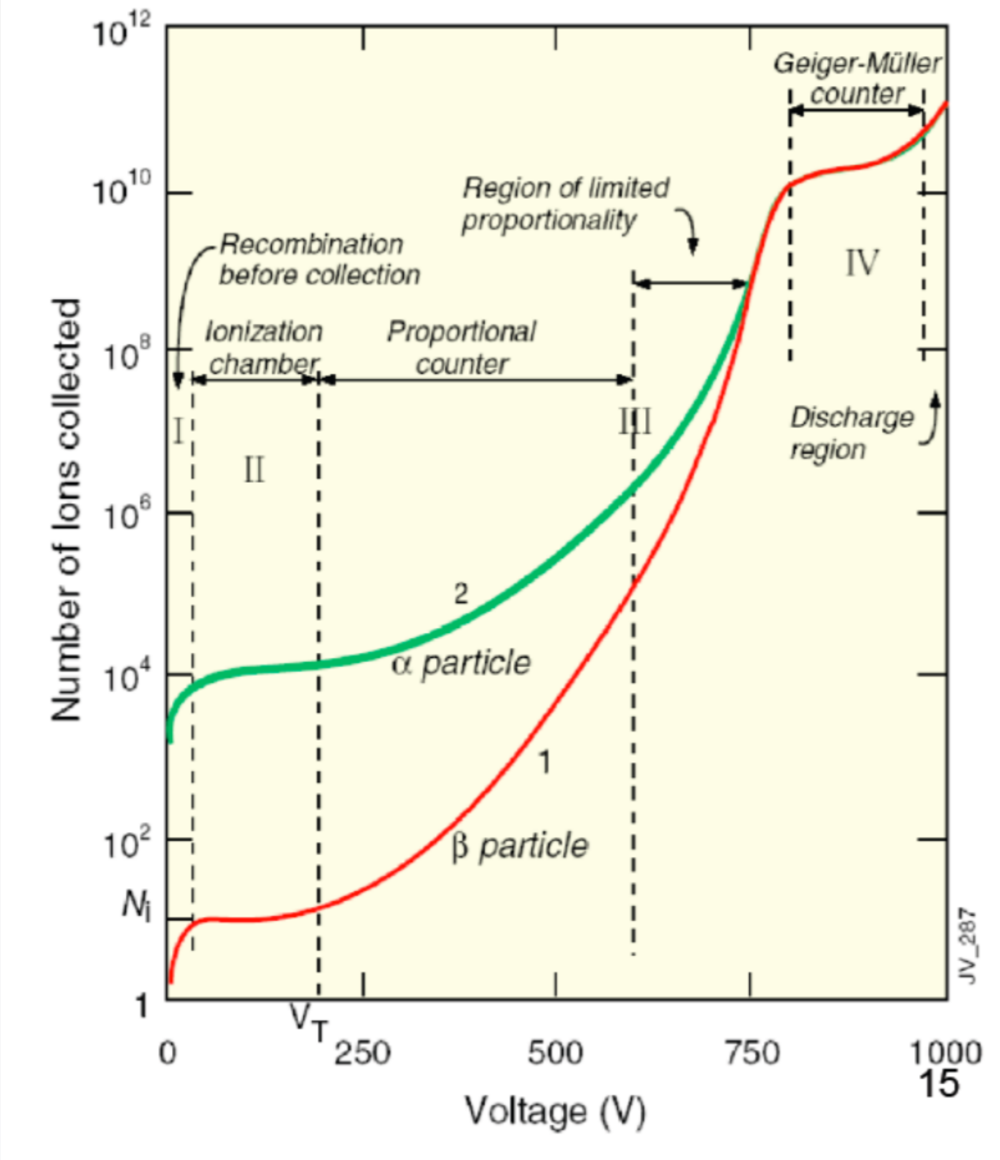

15

Multiwire proportional chambers

- A proportional counter does not provide the position of the incident particle
- Charpak developed of multi-wire proportional chamber

G. Charpak Nobel price ('92)

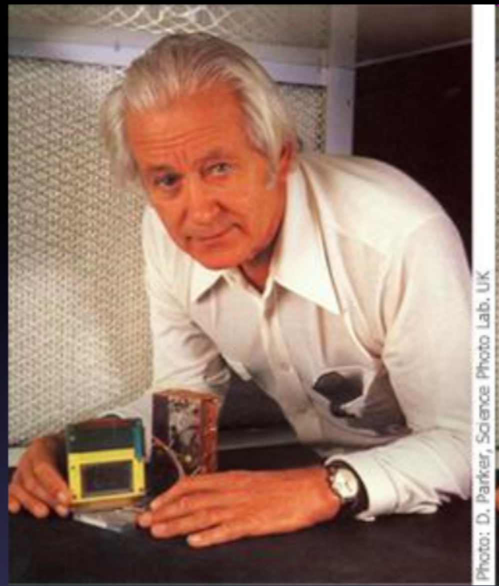

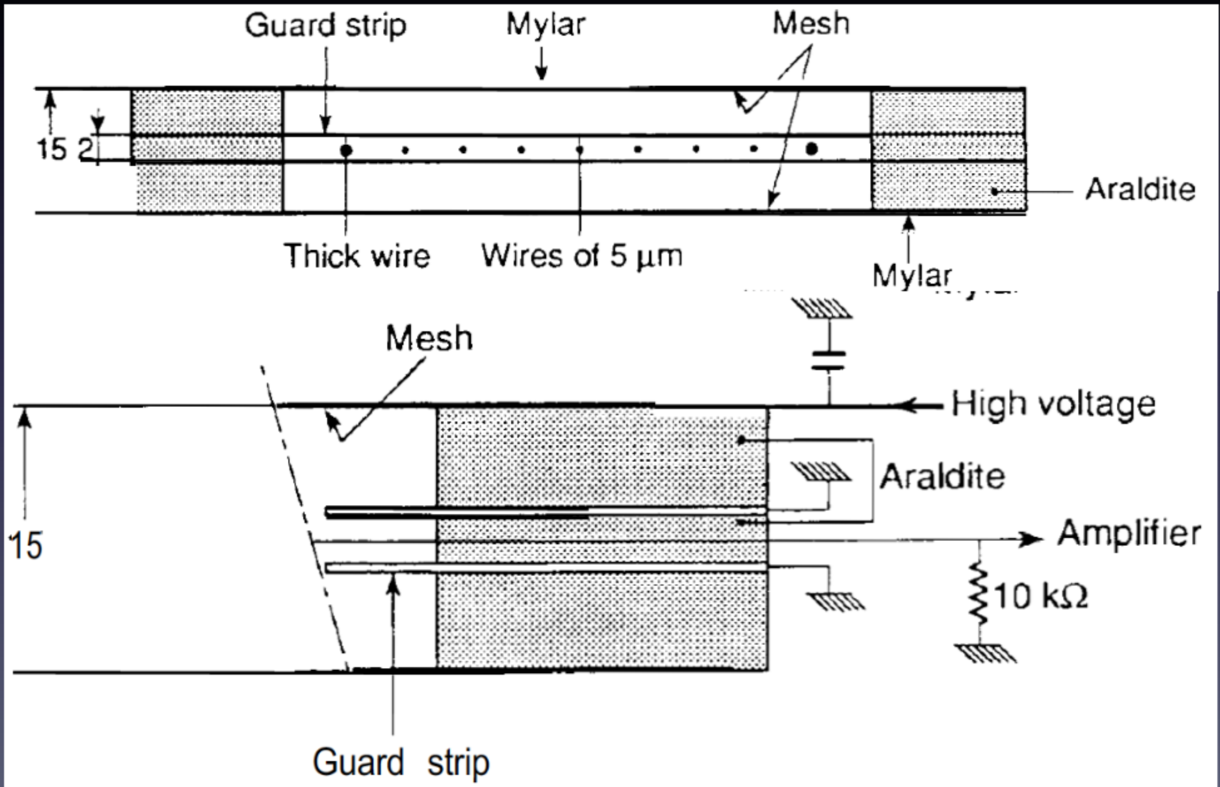

Construction details of the original design of Charpak's multi-wire chambers (from Nobel lecture)

Anode wire =20μ diameter
d=2 mm

2D MWPC

- Two coordinates (x,y) of the track hit can be determined from the position of the anode wire and the signal induced on the cathode strips (or wires)
  - High spatial resolutions due to center of gravity
  - Resolve ambiguities using strip pattern

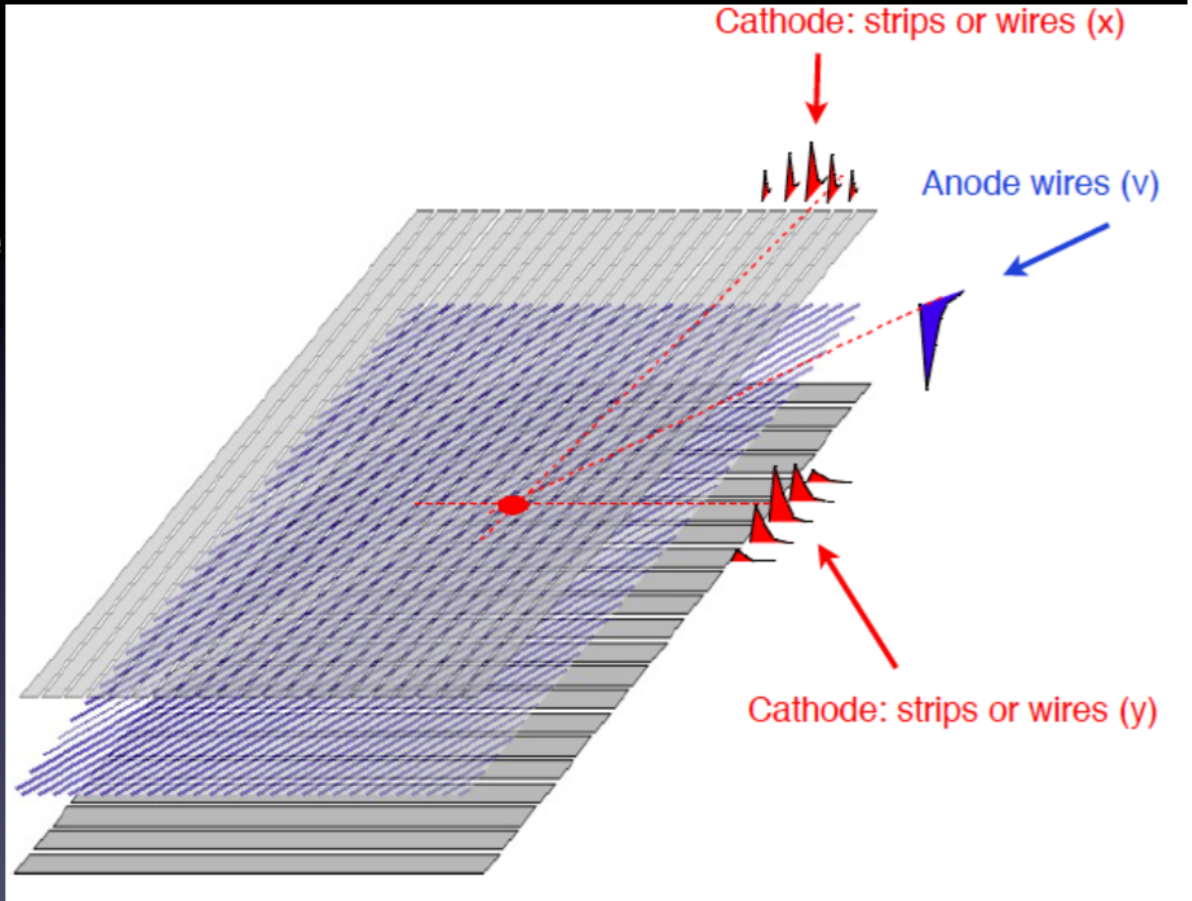

Micromegas and GEM

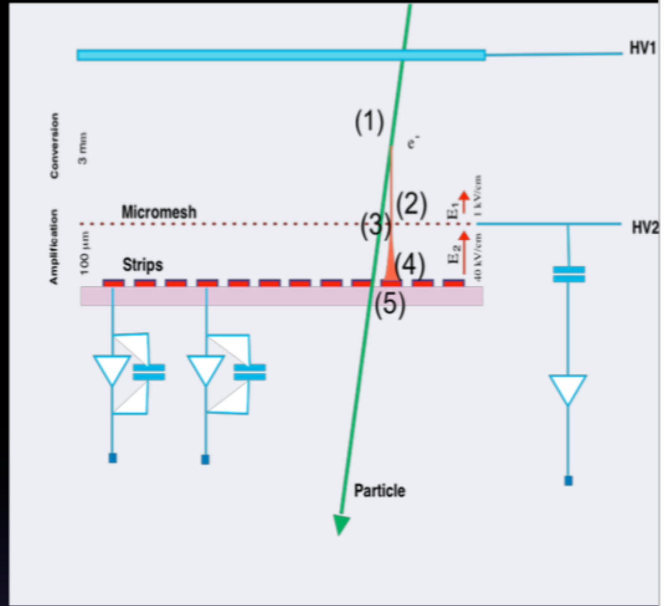

- Micromegas
  - Gas volume divided in two by metallic micro-mesh
  - Gain = 10^4 and a fast signal of 100ns.
- GEM (Gas Electron Multipliers, Sauli 1996)
  - Thin insulating Kapton foil coated with metal film
  - Chemically produced holes pitch ≈100 µm
  - Electrons are guided by high drift field of GEM which generates avalanche
    - Electric field strength is in the order of some 10 kV/cm
    - Avalanche gain of 100 – 1000

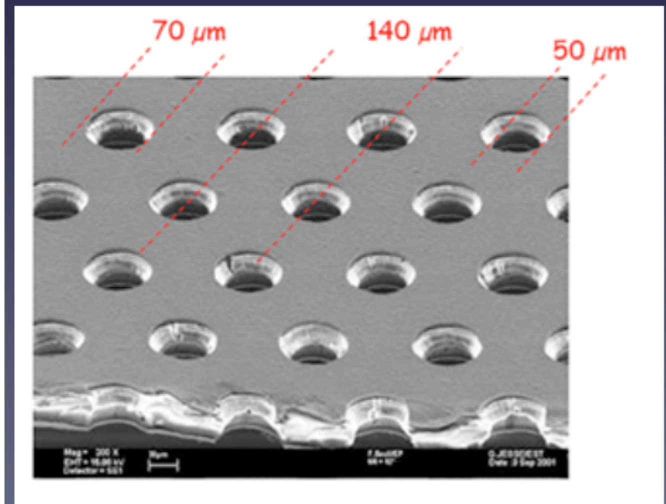

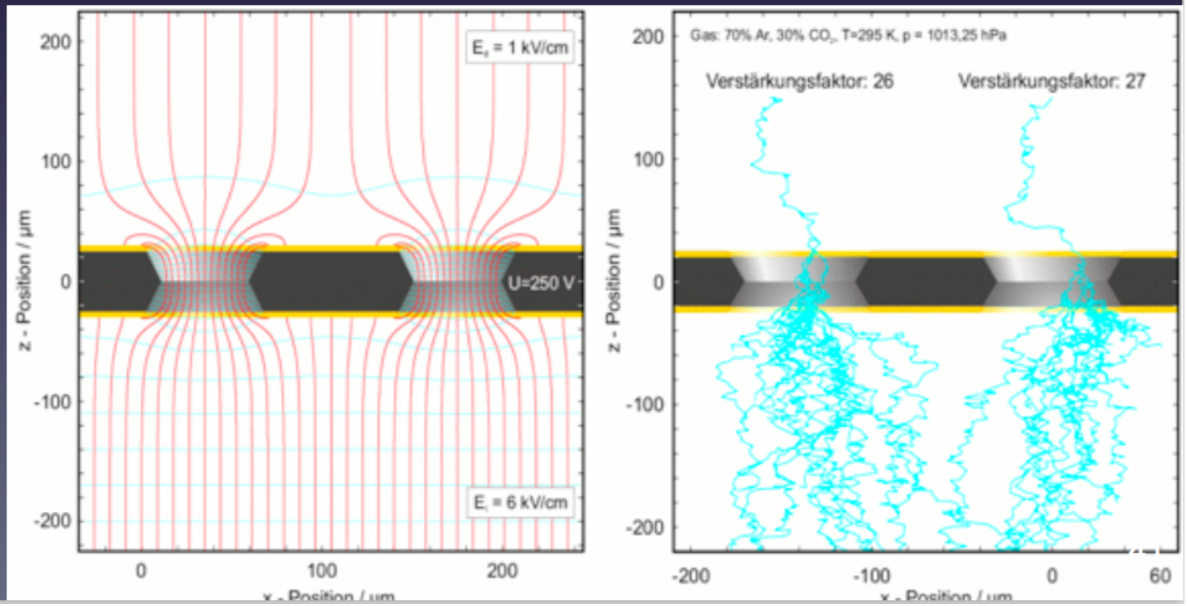

Drift chambers

- Obtain spatial information by measuring the electrons drift time
  - time measurement started by an external (fast) detector, i.e. scintillator counter
  - electrons drift to the anode (sense wire), in the field created by the cathodes
  - the electron arrival at the anode stops the time measurement

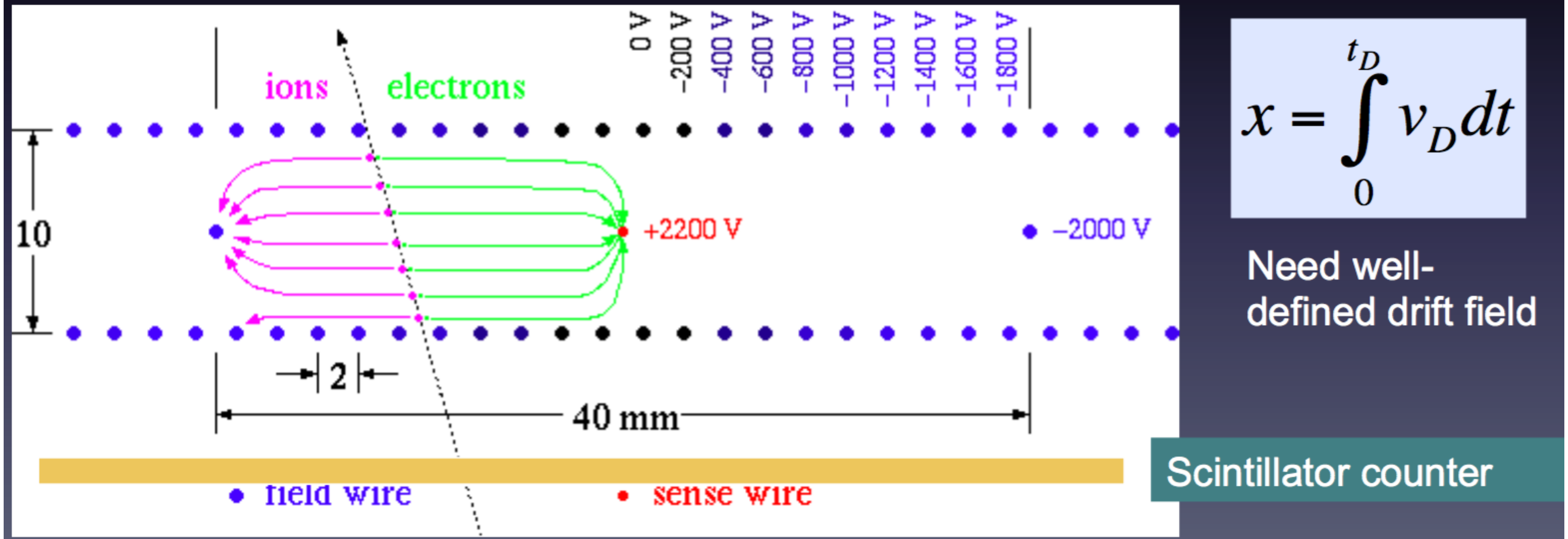

$$x = \int_0^{t_D} v_D dt$$

Need well-defined drift field

J. Heintze, 1971

Time Projection chamber (TPC)

- D.R. Nygren in 1976
- Full 3-D reconstruction
  - XY: MWPC and pads of MWPC at the endcap
  - Z: from drift time measurement (several meters)
    - Field cage for very homogenous electric field
- Typical resolution
  - z and y ≈mm, x=150-300 μm
  - dE/dx ≈5-10%
- Advantages:
  - Complete track information → good momentum resolution
  - Good particle ID by dE/dx
- Challenges
  - Long drift time limited rate
  - Large volume (precision)
  - Large voltages (discharges)
  - Large data volume
  - Difficult operation at high rate

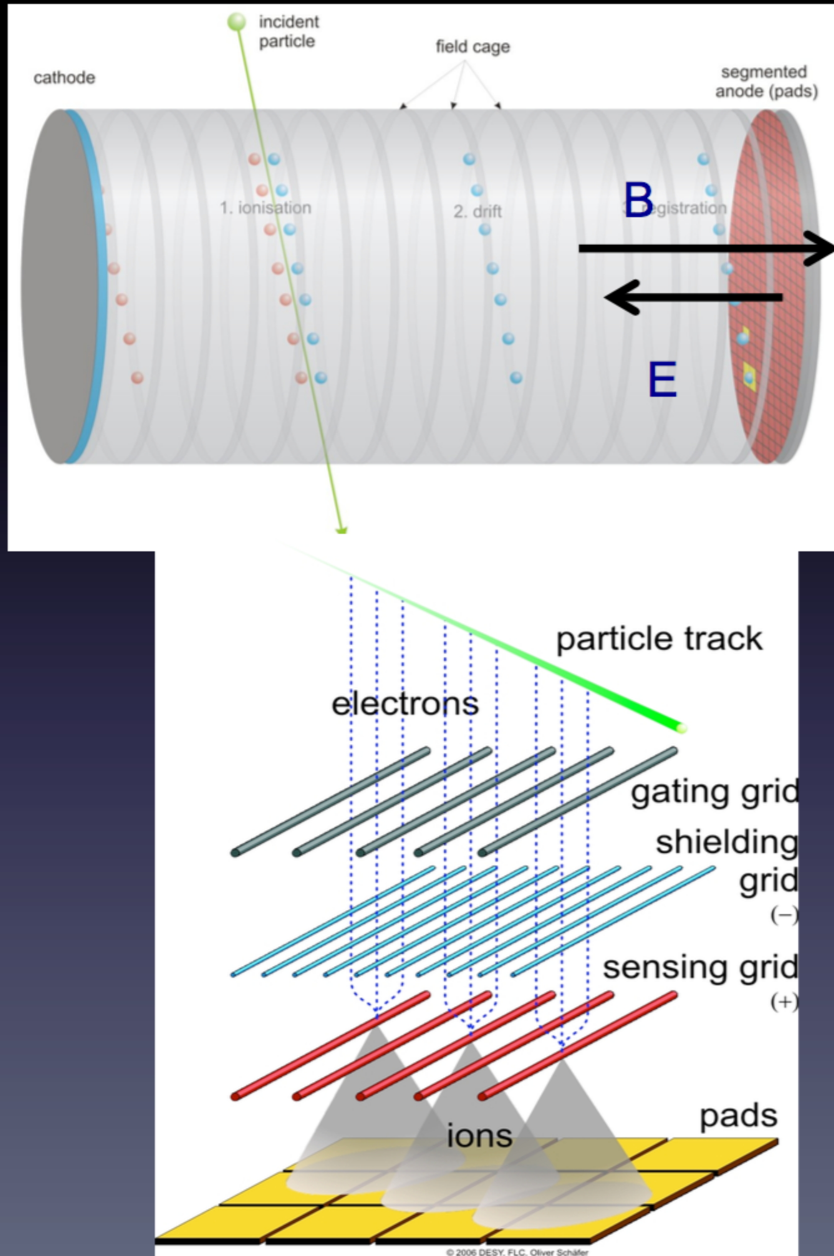

Strumentazioni per l'astrofisica
(prima parte)

Rivelazione di raggi X/γ in condizioni astronomiche

partly adapted from G. Malaguti's Lessons
Istituto Nazionale di Astrofisica (INAF) IASF-Bologna

Telescopi in banda X e γ

Incidenza radente (E<20 keV, presto anche ad energie maggiori) – configurazione di tipo Wolter I

E≈20-100 keV: collimatori, coded masks
E≈0.2-10 MeV: Compton Telescopes
E>10 MeV: Pair Telescopes (tracking chambers)
(gia' discussi)

Telescopi per astronomia γ vs Energia

Detection of Gamma Radiation

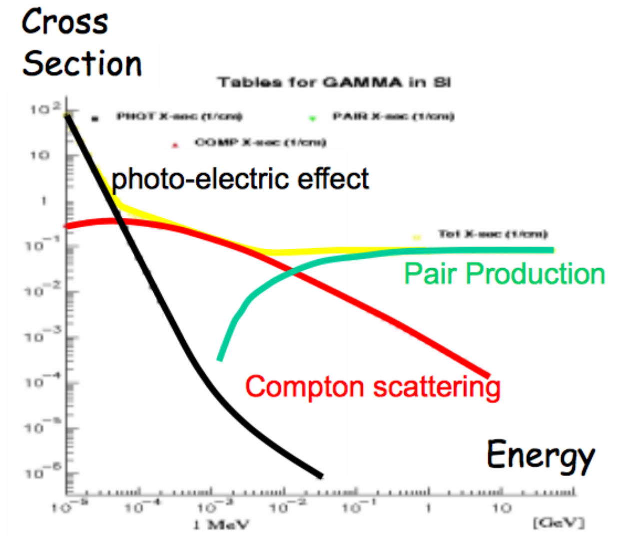

Photoeffect(< 100 keV)

Photons effectively blocked and stopped

Telescopes:

Collimators
Coded Mask Systems

Compton Scattering (0.2-10 MeV)
Photon Crossection Minimum
Scattered photons with long range
Telescope:
Compton Camera Coincidence System

Pair Creation (> 10 MeV)
Photons completely converted to e^+e^-

Telescope:
Tracking chambers to visualize the pairs

Scanning with Slat Collimators

- Imaging the sky with non-imaging X-ray instruments as a goal
- Linear scanning means position is determined in one direction
- At least a second scanning, preferentially in the direction perpendicular to the previous one
- First all-sky survey in X-rays by Uhuru (1970-72): 2 prop. counters with metal collimators (0.5°×5°, 5°×5° FWHM)

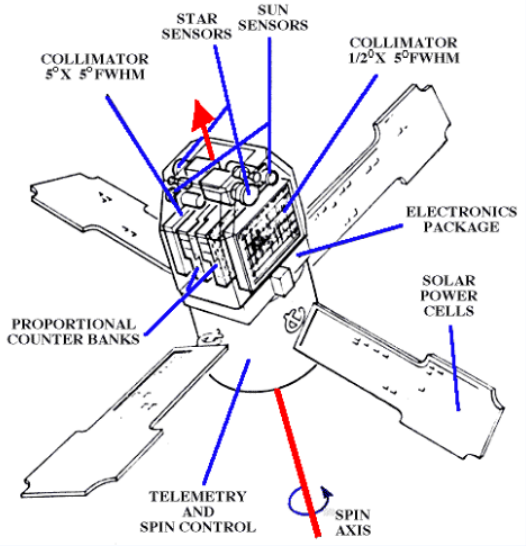

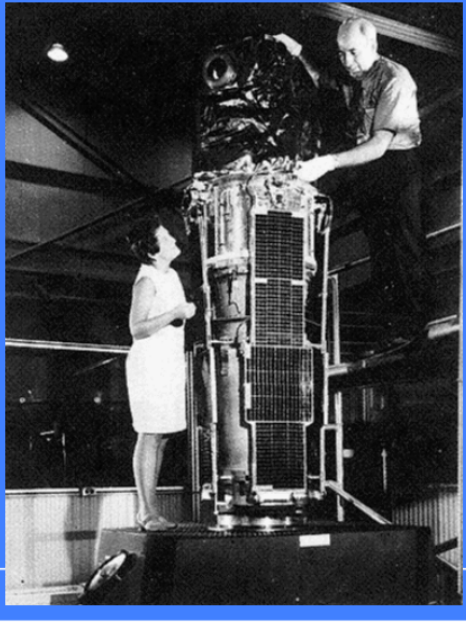

Scanning Grid Collimators

- Two or more plane ("grid" of absorbing rods) collimators to improve angular resolution

- Higher resolution with three or more grids (e.g., 4 in HEAO-1 A-3 experiment)

- Two-dimensional measurements need scans in two or more directions

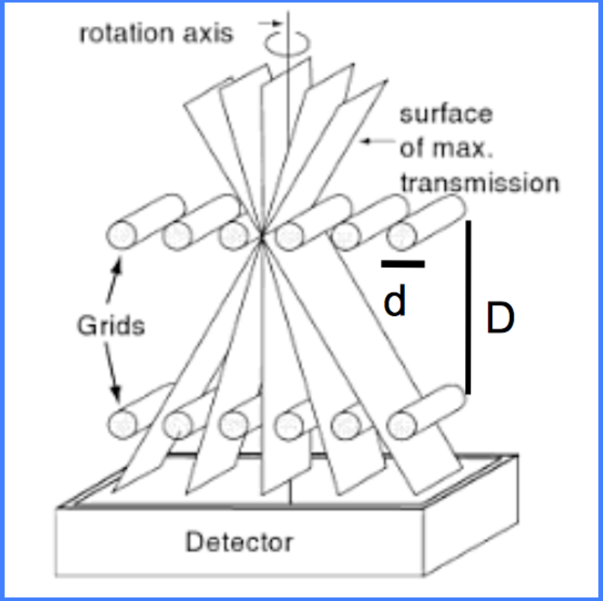

Double-grid collimator
Transmission Function of triangular shape
Angular resolution: d/D

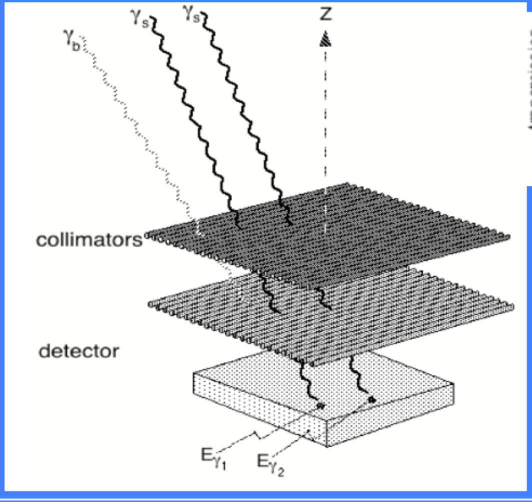

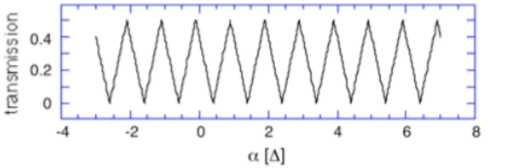

Modulation curve

Sensibilità - 1

- Sensibilità = flusso minimo rivelabile
  - Emissione nel continuo: fotoni cm^{-2} s^{-1} keV^{-1}
  - Emissione di righe: fotoni cm^{-2} s^{-1}
- C_S = Tasso di conteggi di sorgente
- C_{Bkg} = Tasso di conteggi di fondo

assumendo una statistica poissoniana

$$SNR = n_\sigma = \frac{C_S}{\sqrt{C_S + C_{Bkg}}}$$

In realta' quello che si misura e' (S+B)-B in un dato intervallo di tempo

$$S = (S+B) - B \longrightarrow \sigma_S^2 = \sigma_{S+B}^2 + \sigma_B^2 =$$

$$= (\sqrt{(S+B)})^2 + (\sqrt{B})^2 = S + B + B = S + 2B$$

$$SNR = S/\sigma_S = S/\sqrt{(S+2B)}$$

Detector Project

GLAST Project

For SWG discussion , Huntsville, 2002.9.13

Definition of Terms

- **Effective Area:**

  A_{eff}

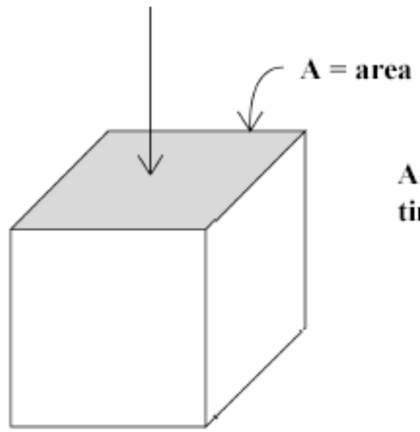

Area at normal incidence times detection efficiency.

- **Energy Resolution:**

  E_R

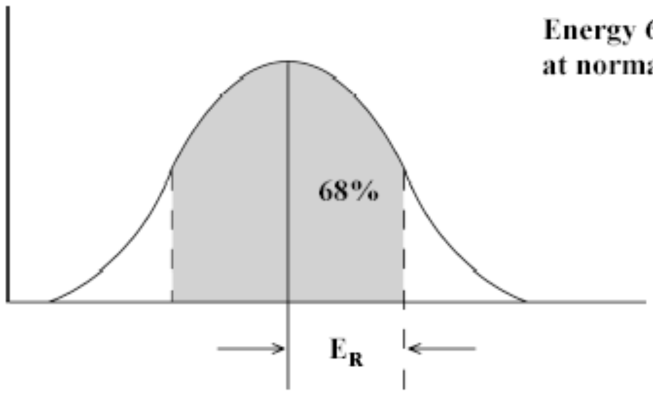

Energy 68% spread at normal incidence.

Detector Project

Definition of Terms

- **Angular Resolution:**
  Θ_R

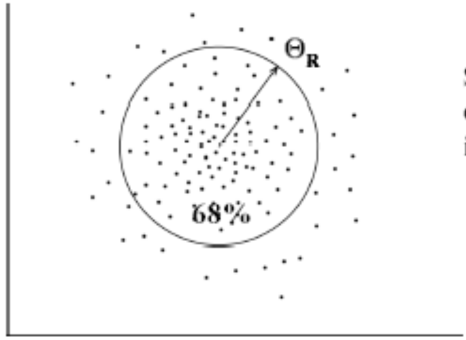

Space angle for 68% containment at normal incidence.

- **Field of View:**
  FOV

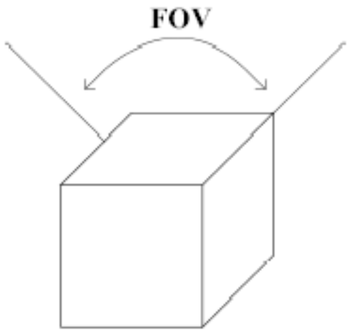

Integral effective area over solid angle divided by peak effective area.

- **Sensitivity:**

Flux of weakest source that can be detected at 5 sigma significance.

Sensibilità – 2 – "basic" dependencies

$S = \varepsilon\ A\ T\ \Delta E\ F_{src}$

$B = A\ T\ \Delta E\ F_{bkg}$

ε=efficienza di rivelazione fotoni della sorgente
A=area efficace
T=tempo di esposizione
ΔE=banda energetica
F_{src}=flusso della sorgente
F_{bkg}=fondo strumentale

$B \ll \varepsilon F_{src}$

$$SNR = \frac{S}{\sqrt{S+2B}} \approx \sqrt{S} \propto \sqrt{F_{src} T}$$

the source dominates the signal

$B \gg \varepsilon F_{src}$

$$SNR = \frac{S}{\sqrt{S+2B}} \approx S/\sqrt{2B} \propto \sqrt{T}(F_{src}/\sqrt{2F_{bkg}})$$

Backg-dominated obsn.

$$SNR = n_\sigma \approx \frac{\varepsilon \cdot \mathrm{A} \cdot \mathrm{T} \cdot \Delta\mathrm{E} \cdot \mathrm{F}}{\sqrt{\mathrm{A} \cdot \mathrm{T} \cdot \Delta\mathrm{E} \cdot \mathrm{B}}} \rightarrow F_{Min} = \frac{n_\sigma}{\varepsilon}\sqrt{\frac{B}{\mathrm{A} \cdot \mathrm{T} \cdot \Delta\mathrm{E}}}$$

to give an idea of the main dependencies of the limiting flux (sensitivity)

In the "real world", the background is not only instrumental but also cosmic

S=source flux density [counts/m^2 s]
A=area of the detector
Ω=solid angle subtended by the beam of the telescope on the sky
B_1=instrumental (particle) background [counts/s]
B_2=cosmic background (XRB) [phot/m^2 s ster]
T=exposure time
SOURCE=S×A×T (photons related to the source)
BACKGROUND=B_1×T + B_2×A×Ω×T (photons related to the backgrounds)

$$N = \sqrt{(B_1 + B_2 A\Omega) \times T}$$

$$S/N = \frac{SAT}{\sqrt{(B_1 + B_2 A\Omega) \times T}} = \frac{SA^{1/2}T^{1/2}}{\sqrt{\left(\frac{B_1}{A}\right) + \Omega B_2}}$$

$$S/N = 5 \Rightarrow S_{min} = 5\sqrt{\frac{B_1/A + \Omega B_2}{AT}}$$

Focalizzazione vs collimazione

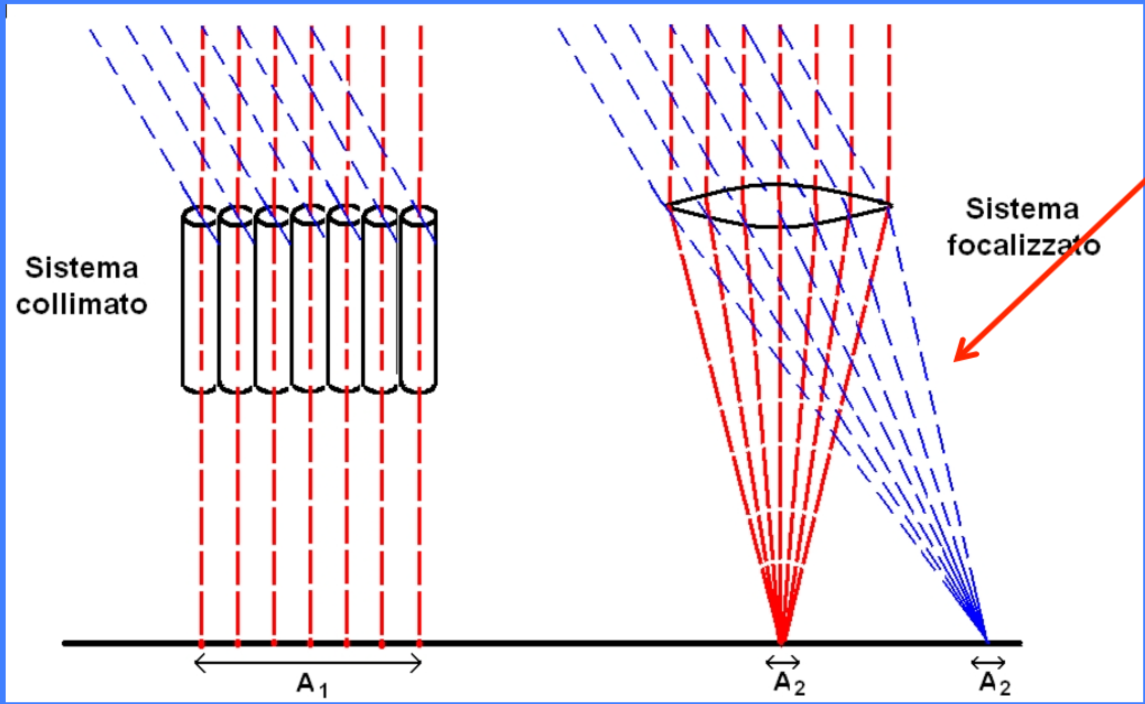

Proper imaging of X-rays below 20-40 keV

$$F_{\min} \approx n_\sigma \frac{\sqrt{2B}}{\sqrt{A_{det} T_{int} \Delta E}}$$

A_d= PSF projected on the focal plane

$$F_{\min} \approx n_\sigma \frac{\sqrt{BA_d}}{A_{eff}\sqrt{T_{int}\Delta E}}$$

Sistema collimato: limita la regione di cielo da cui puo' provenire un segnale, (quindi limita il background), non incrementandone la "densita"

Sistema focalizzato: fa corrispondere ad ogni sorgente un punto nel piano focale, e "concentra" il segnale, producendo un'immagine

$$C_B = B\, A_d\, \Delta E\, \Delta t$$

Background counts from a collimated telescope with detector area A_d, sensitive over the band ΔE, in a time interval Δt

$$\sigma(C_B) = C_B^{1/2}$$

The counts obey the Poisson statistics

$$C_S = S_E\, A_d\, \Delta E\, \Delta t\, \eta_E$$

Source counts collected from a source with flux S_E in the same conditions (QE=η_E)

$$C_{\text{meas}} = (C_S + C_B) - C_B$$

Measured counts (backg-subtracted)

$$\sigma^2(C_{\text{meas}}) = 2\sigma^2(C_B)$$

Background dominates fluctuations

$$S/N = n_\sigma = \frac{C_S}{\sqrt{2C_B}} = \frac{S_E\, A_d\, \Delta E\, \Delta t\, \eta_E}{\sqrt{2B\, A_d\, \Delta E\, \Delta t}}$$

$$S_{E,\min} = \frac{n_\sigma}{\eta_E} \frac{\sqrt{2B}}{\sqrt{A_d\, \Delta t\, \Delta E}}$$

Spatial Aperture Modulation

- **Alternative to temporal modulation**
- **Requires two-dimensional position-sensitive detectors**
- **The spatial modulation is achieved by a pattern of holes in an otherwise absorbing plate, providing a unique spatial code**

Coded-aperture (or coded-mask) Telescopes

Principle: the mask pattern (in the form of the shadow produced by the parallel beam of an X-ray source) is recognized by the two-dimensional position-sensitive detector. Any shift in the pattern is related to a shift of the source position.

Coded Mask Imaging

The Coded Mask Technique

is the worst possible way of making a telescope

Except when you can 't do anything better !

- Wide fields of view
- Energies too high for focussing, or too low for Compton/Tracking detector techniques
- Very good angular resolution
- The best energy resolution

Coded Mask Imaging

The principle of the camera is straightforward: photons from a certain direction in the sky project the mask on the detector; this projection has the same coding as the mask pattern, but is shifted relative to the central position over a distance uniquely correspondent to the direction of the photons. The detector accumulates the sum of a number of shifted mask patterns.
Each shift encodes the position and its strength encodes the intensity of the sky at that position.

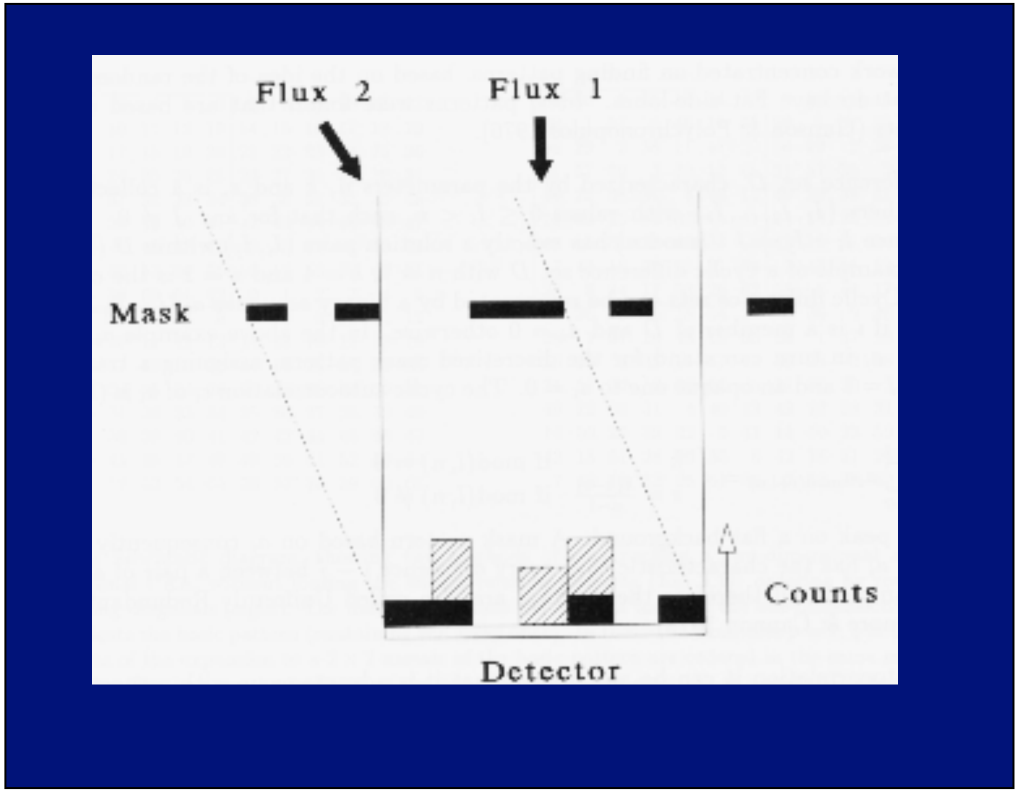

http://asd.gsfc.nasa.gov/archive/cai/coded_intr.html

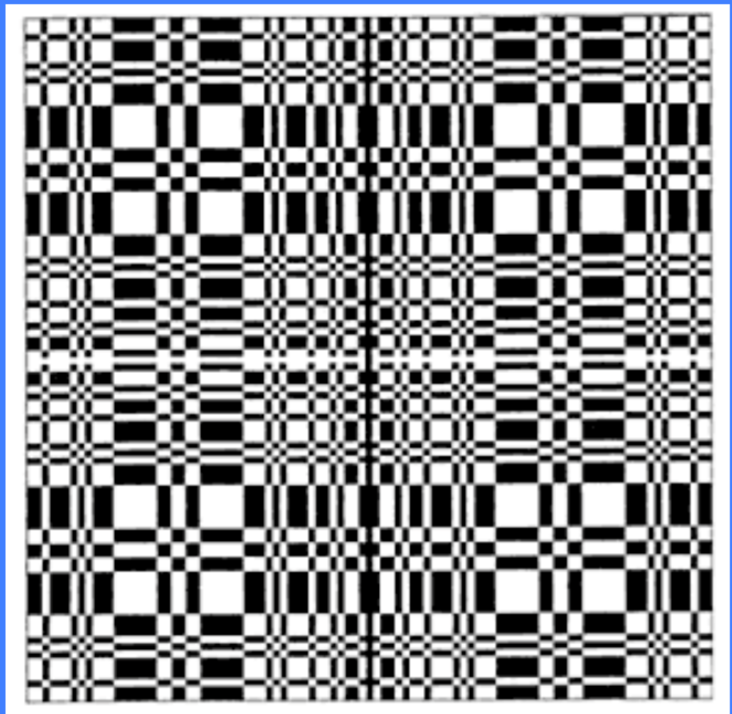

Mask of IBIS (15 keV – 10 MeV) onboard *INTEGRAL*

Coded Mask Imaging

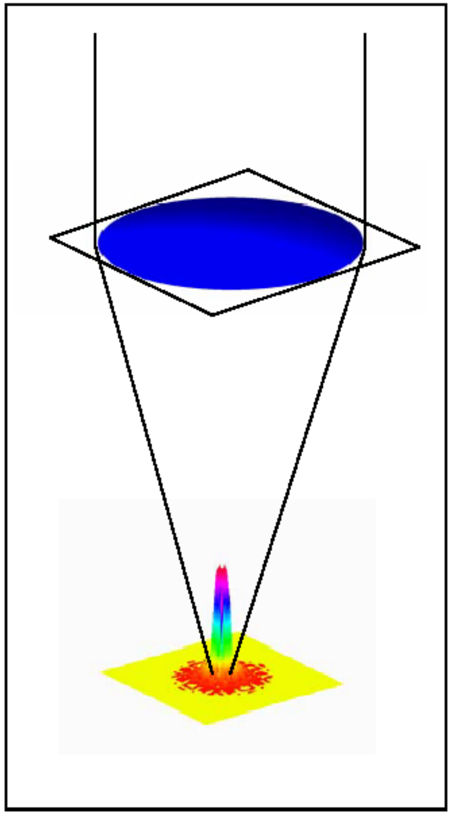

Point Source Response Function

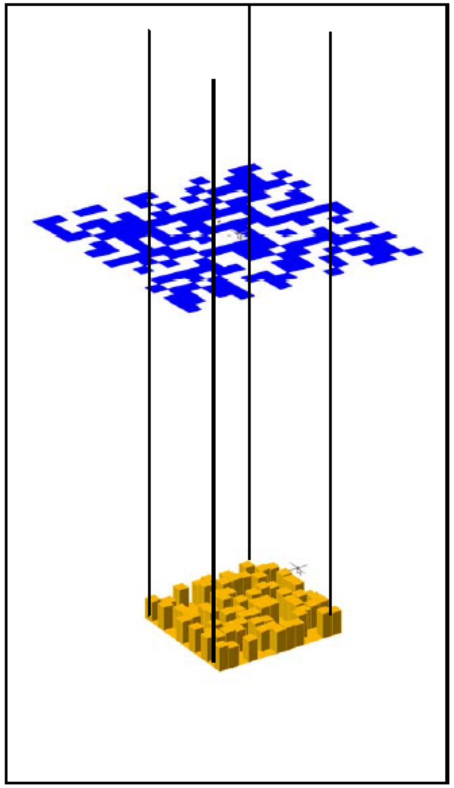

A coded mask telescope has the worst PSF imaginable

The response to a point source isn't just 'a bit blurred',

it fills the whole detector plane !

Coded-mask Telescopes

Fully-Coded Field of View (FCFOV)

Partially-Coded Field of View (PCFOV)

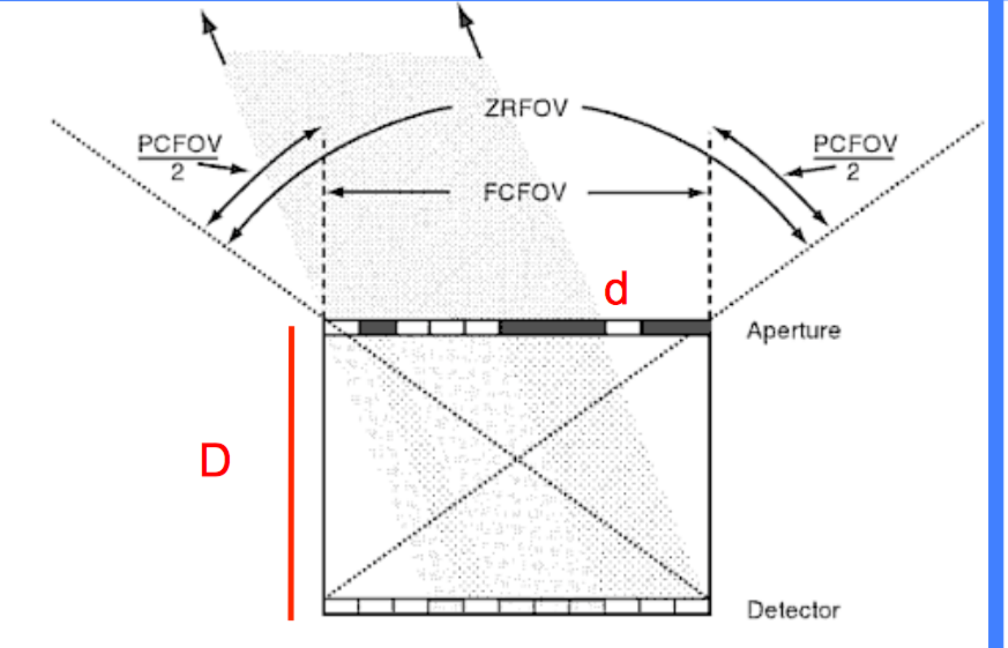

Fig. 5.2 Coded-mask box camera. Full coding is only achieved for on-axis sources

Photons from any source within this area of the sky cannot reach the detector without passing through the mask (i.e., the entire detector surface is "coded")

FCFOV for on-axis sources only

RESOLUTION=d/D

where d=length of the mask pattern (width of the holes) and D=distance mask-detector

Detector resolution should match the mask element dimension

Photons can arrive from sources outside the FCFOV ➔ partially coded FoV: only part of the mask is projected on the detector plane

Coded Mask Imaging

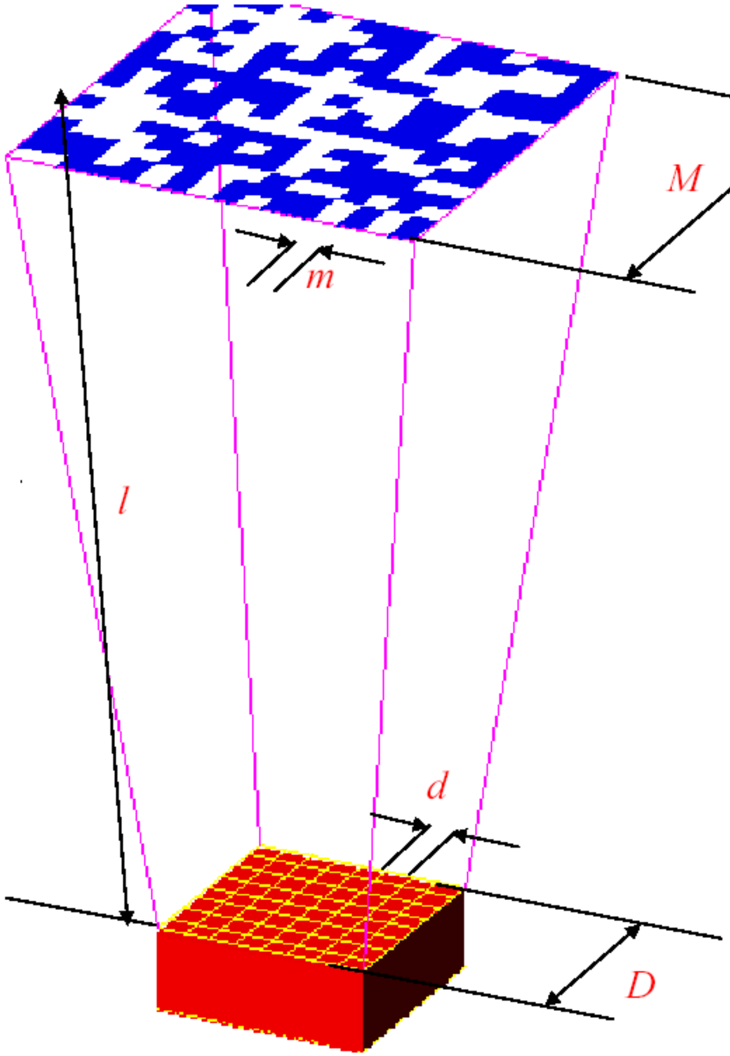

Coded mask telescopes -key parameters

- m Mask Pixel size
- d Detector Pixel size
- M Mask Size
- D Detector Size (assume $D<M$)
- l Mask-Detector Separation
- t Mask open fraction

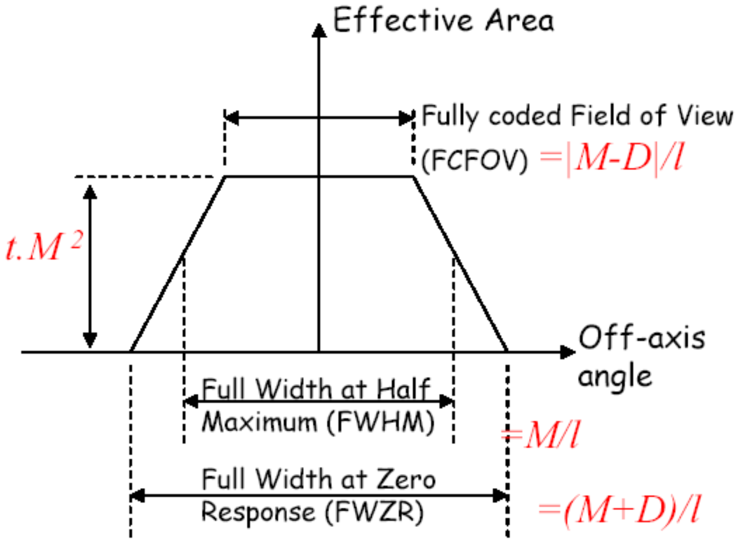

Coded Mask Imaging

'Optimum coded ' designs or 'URAs'

URAs are closely related to ' Cyclic Difference Sets '. Different families of cyclic difference sets yield Mask patterns which look quite different but which all have the desired properties - all have an ACF of the same form.

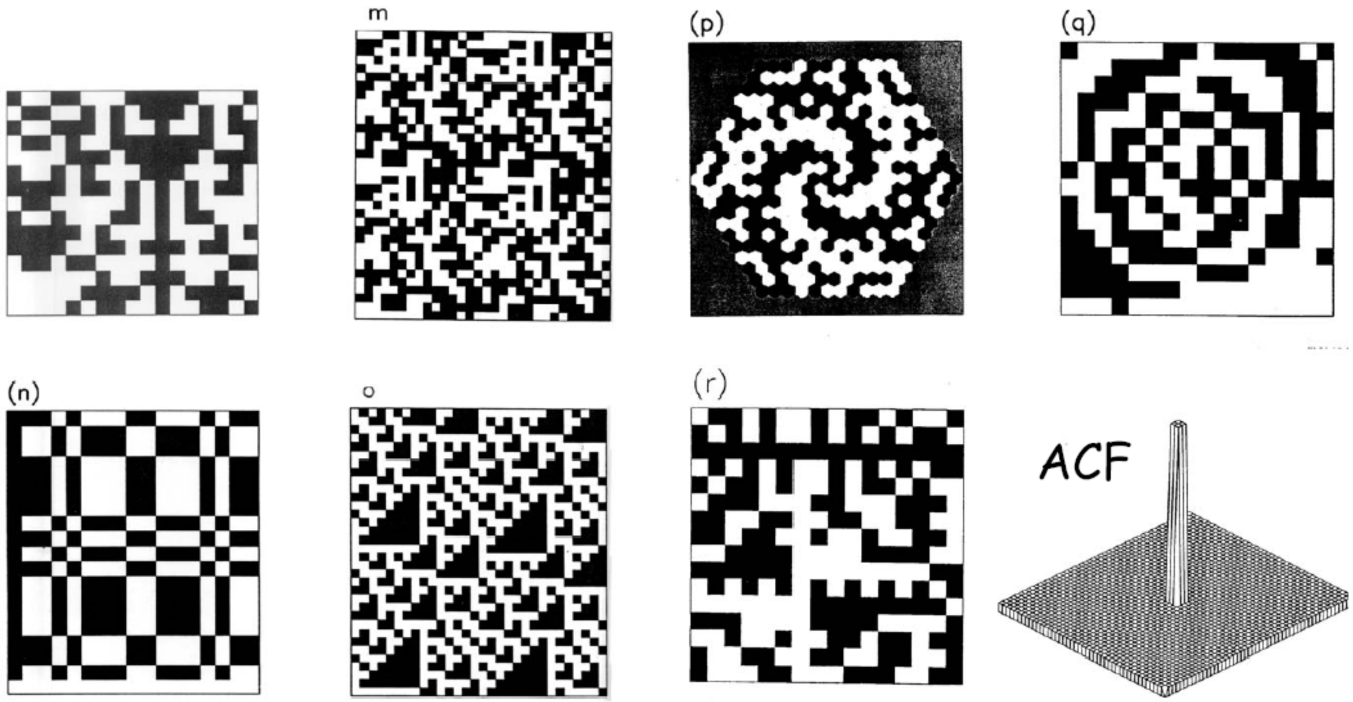

Coded Mask Imaging

Some aspects of *real* systems

Mask
- Non cyclic
- Mask Closed element absorbtion
- Mask Open element transparency
- Mask Element Thickness
- Obstructions in Mask Plane

Detector
- Detector finite position resolution
- Detector efficiency non-uniformities
- Detector response dependent on off-axis angle
- Detector background non-uniform
- Gaps in the detector plane
- Dead/inactive pixels in the detector plane

Other
- Shielding (collimation) imperfect
- Obstructions between detector and mask
- Leaks onto detector from far outside the fov

Coded Mask Imaging

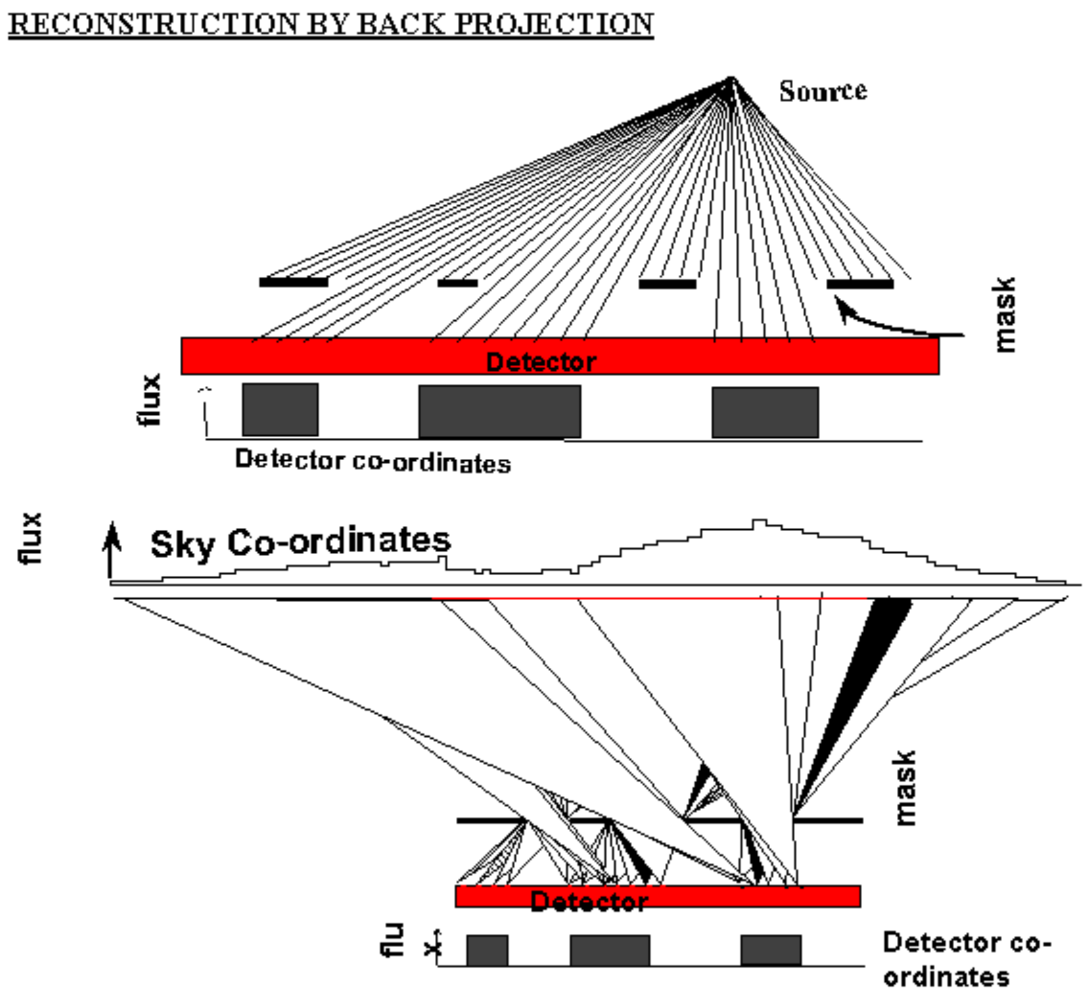

Coded Mask Imaging

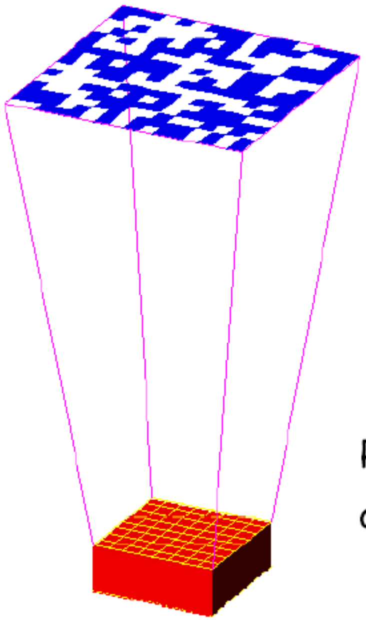

How to recover an image

Basic method :
' Correlation with the Mask Pattern '

Recorded pattern is Convolution of source distribution and the mask pattern, plus some background B

$$D = S \otimes M + B$$

Suppose we form an image as †

$$I = M \otimes D = M \otimes S \otimes M + M \otimes B$$
$$= M \otimes M \otimes S + M \otimes B$$
$$= ACF(M) \otimes S + M \otimes B$$

where ACF indicated the Autocorrellation function.
If ACF(M) were a Delta function and if $M \otimes B$ were zero we would have recovered S.

† coordinate reversals are ignored here

Image Reconstruction

The observed intensity distribution over the detector must be interpreted ("unfolded") using the **coding function** associated with the mask pattern.

$$D(x)=M(x) \times S(x)$$

D(x)=observed detector distribution
M(x)=coding function (aperture modulation function)
S(x)=sky distribution
x=(X,Y) in the respective plane

D(x) must be inverted to get S(x)
S(x) not unambiguously defined, main problem coming from Poisson statistics because of the presence of background (often dominant over the source signal)

➔ $S(x)=B_{sky}(x)+sum(S_i(x))$ = X-ray background + all the i sources in the FoV, both coded by M(x)
+ detector background (charged particles, secondary photons)

M(x) directly inverted only for few mask patterns
Typically used *correlation procedures*=correlation of the aperture code with the suitably binned intensity distribution; *mismatched filtering*=FT^{-1} of the PSF; *backprojection*=the mask pattern is projected onto the sky, marking all areas from which the photon could have arrived.

Coded Mask Imaging

Position sensitive detectors for coded mask telescopes

Detector Technology	Approx Energy Range (keV)	Examples	Notes
CCD	0.5-10	HETE-2 SXC	1-d 33 arc sec resolution !
Gas-filled Proportional Counter	2-50	Spacelab-2 TTM, SAX-WFC RXTE ASM HETE-2 WXM Integral : JEM-X	Space Shuttle Mir-Kvant Space Station 1-d 1-d
Arrays of semiconductor detectors	5-100	Legri (CZT) Integral : ISRI (CdTe)	MiniSat-01
Anger Camera	50-1000	Sigma Exite-2	On Granat Balloon
Array of Scintillator detectors	100-10000	New Hampshire DGT Integral : PIXIT	Balloon
Aray of Germanium detectors	20-10000	SAGE Integral : SPI	Balloon

BeppoSAX (1995 - 2002)

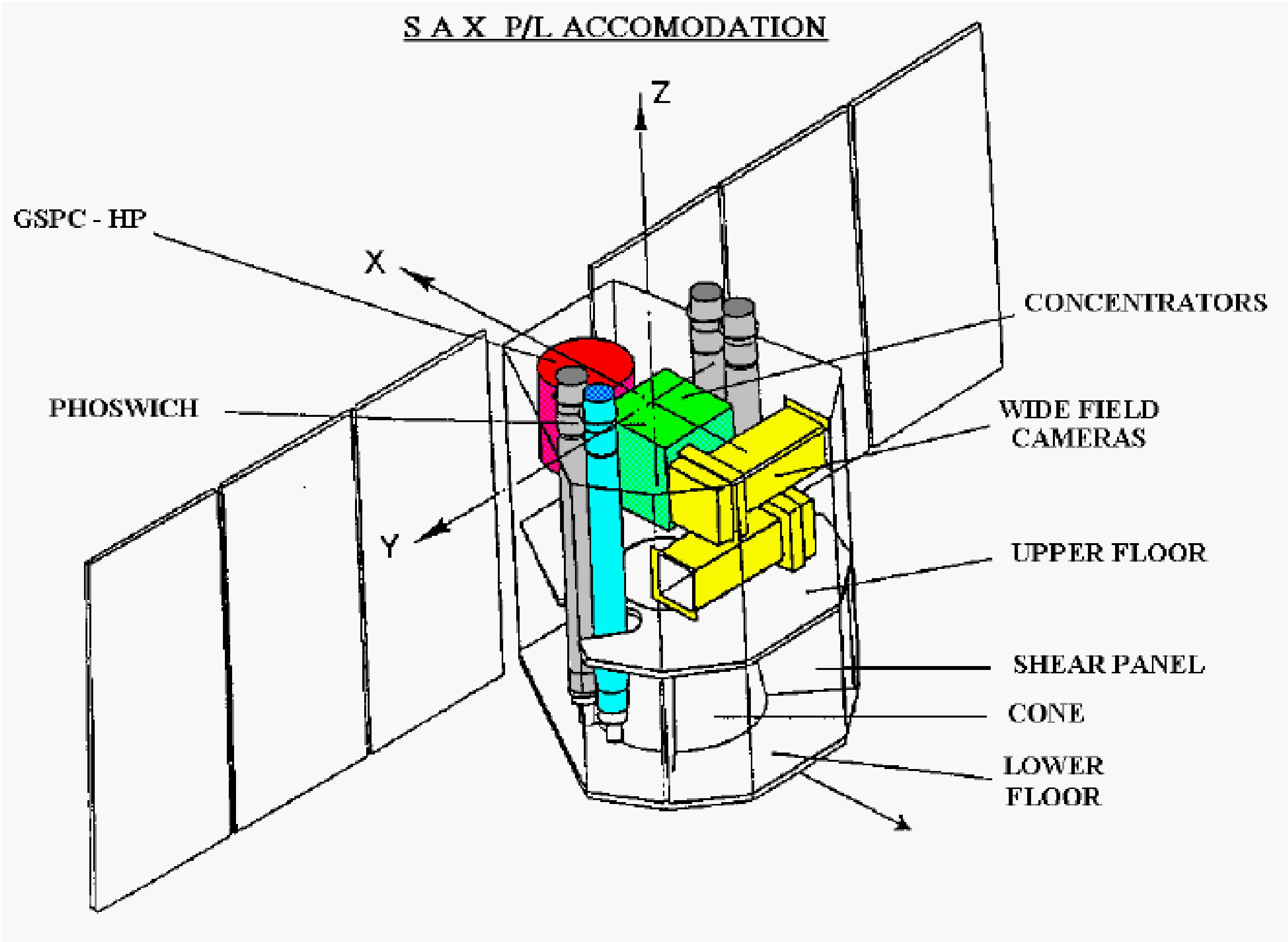

BeppoSAX

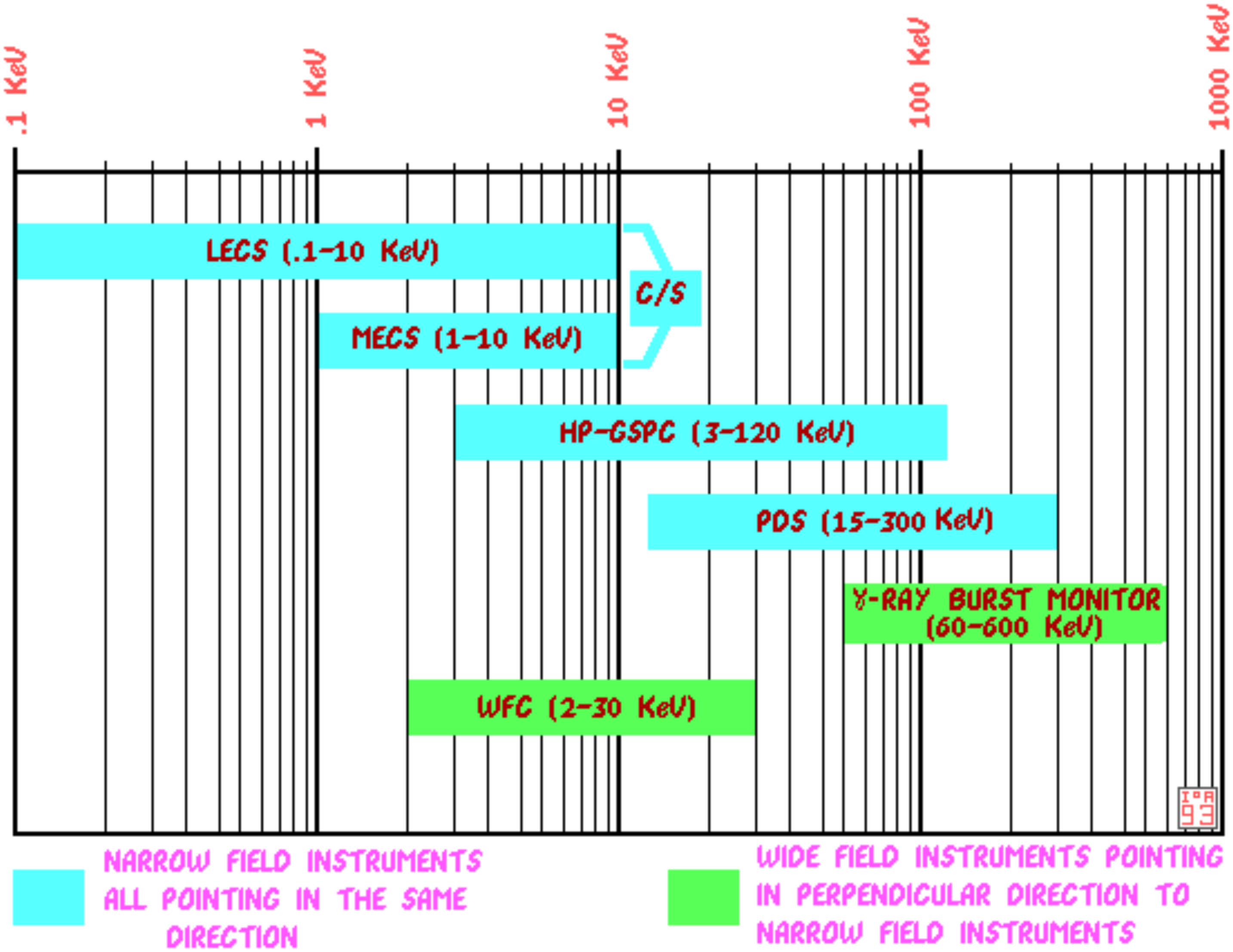

.1 KeV
1 KeV
10 KeV
100 KeV
1000 KeV
LECS (.1-10 KeV)
C/S
MECS (1-10 KeV)
HP-GSPC (3-120 KeV)
PDS (15-300 KeV)
γ-RAY BURST MONITOR (60-600 KeV)
WFC (2-30 KeV)
NARROW FIELD INSTRUMENTS ALL POINTING IN THE SAME DIRECTION
WIDE FIELD INSTRUMENTS POINTING IN PERPENDICULAR DIRECTION TO NARROW FIELD INSTRUMENTS

Phoswich detectors

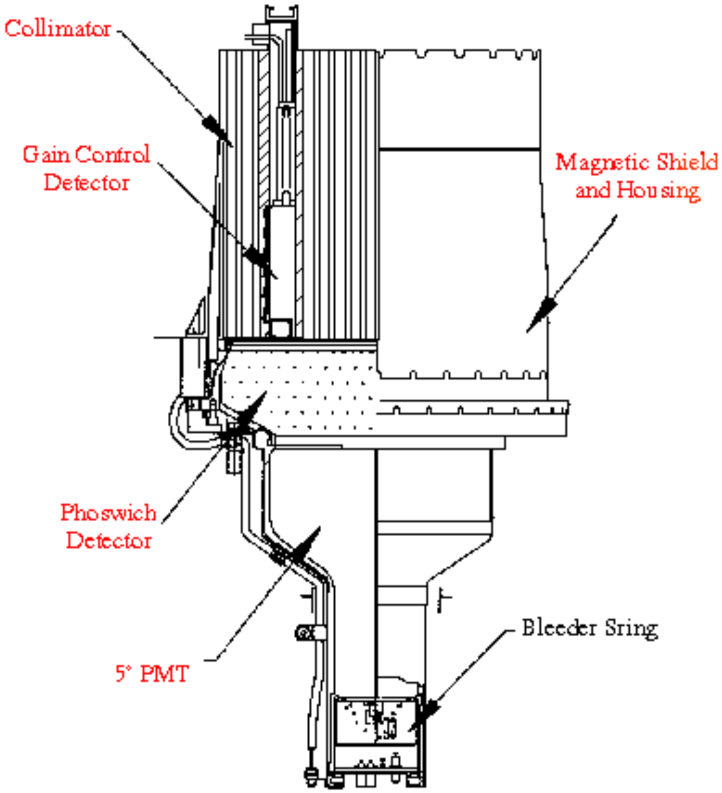

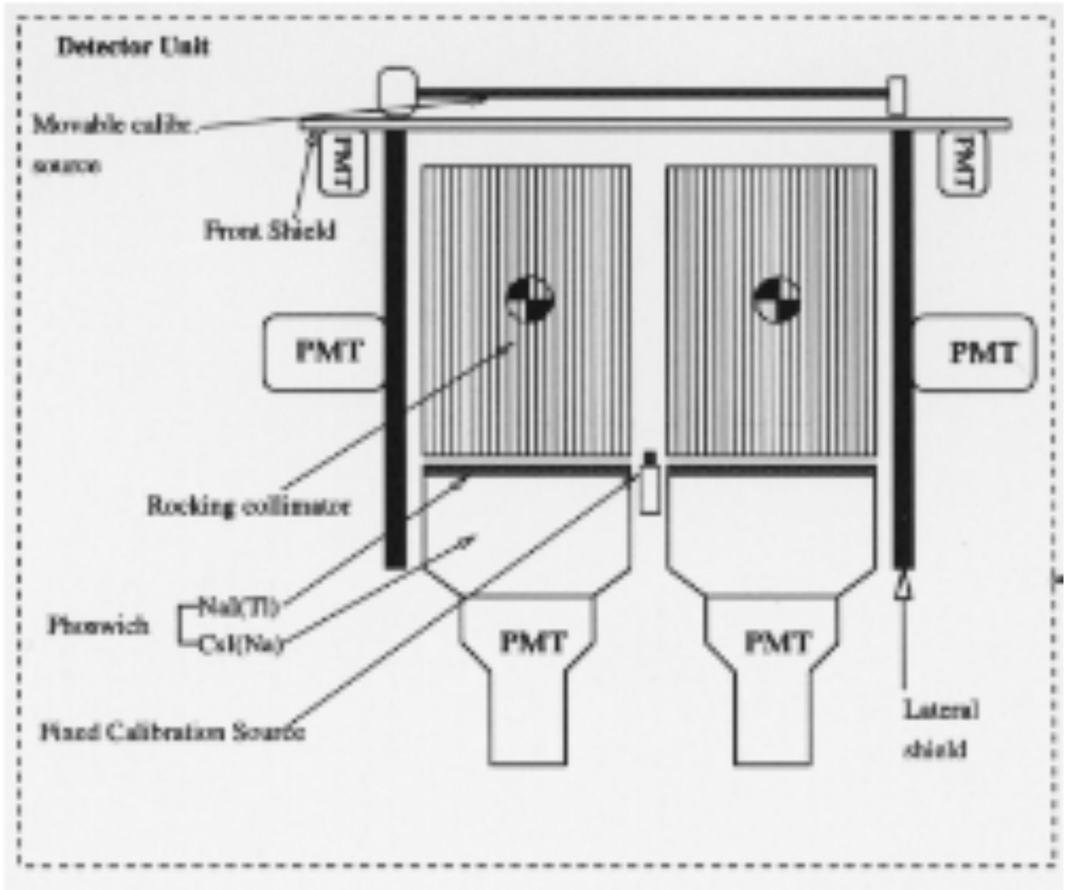

Two scintillators with different decay times. Pulse analysis can distinguish. Back scintillator used as shield at low energy, as detector at high energies.

Rivelatori a scintillazione

- "Fondamenti" del processo: il γ incidente interagisce nel cristallo creando un elevato numero di fotoni ottici
- I livelli energetici sono determinati dalla struttura del reticolo cristallino
- La band gap separa la banda di valenza dalla banda di conduzione
- Assorbendo energia, un e^- viene promosso dalla banda di valenza a quella di conduzione
- Il "drogaggio" del reticolo cristallino con impurità rende più efficiente il processo

Nel cristallo, gli elettroni possono occupare solo due livelli energetici, la **banda di valenza** e la **banda di conduzione**. Le impurita` permettono la creazione di meta-stati che sono particolarmente efficienti per la diseccitazione dalla banda di conduzione

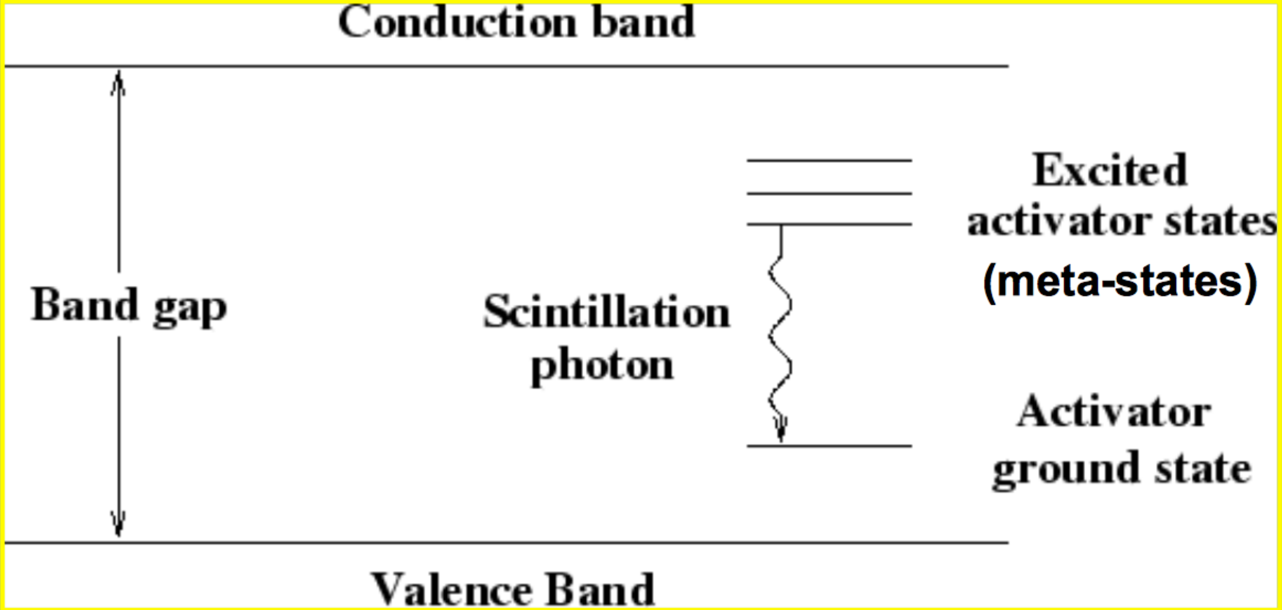

Esempio: phoswich

The Phoswich (e.g. PDS on BeppoSAX)

Phoswich is short for 'phosphor sandwich'

Phosphor is the old name for a scintillator, and more than one are sandwiched together and viewed by the same photomultiplier.

More penetrating particles can produce signal in both scintillators

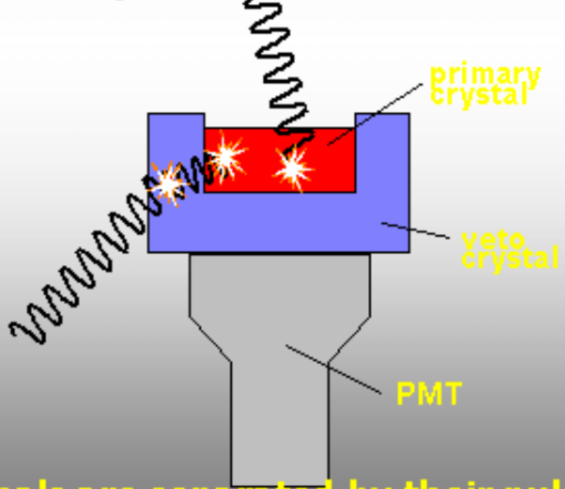

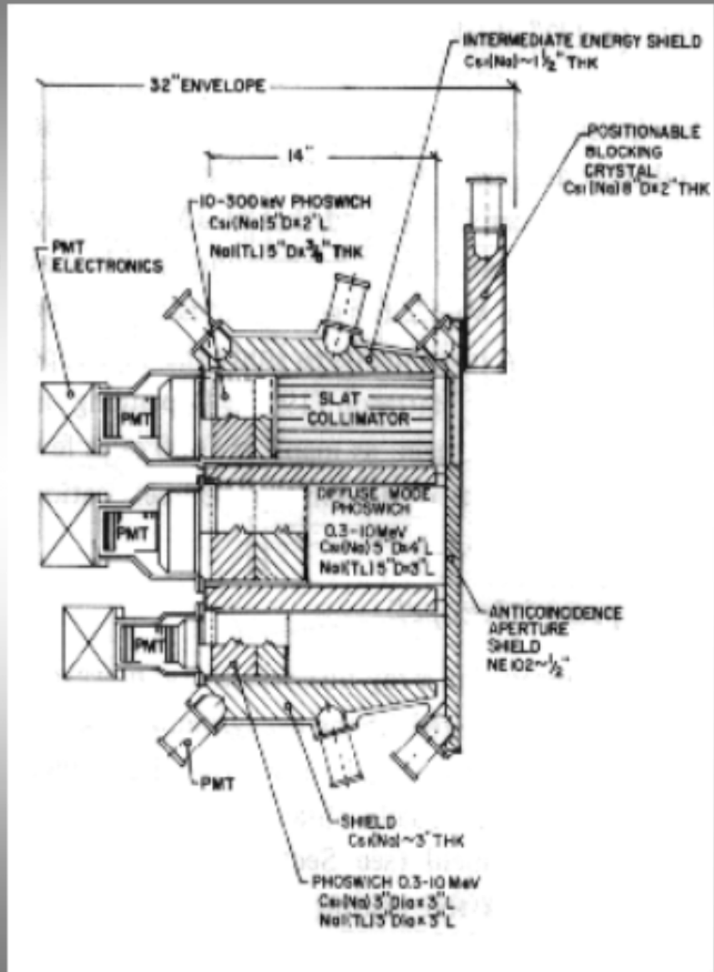

Signals are separated by their pulse shape

Different materials have different pulse shapes and are used to discriminate different events

The BeppoSAX detectors

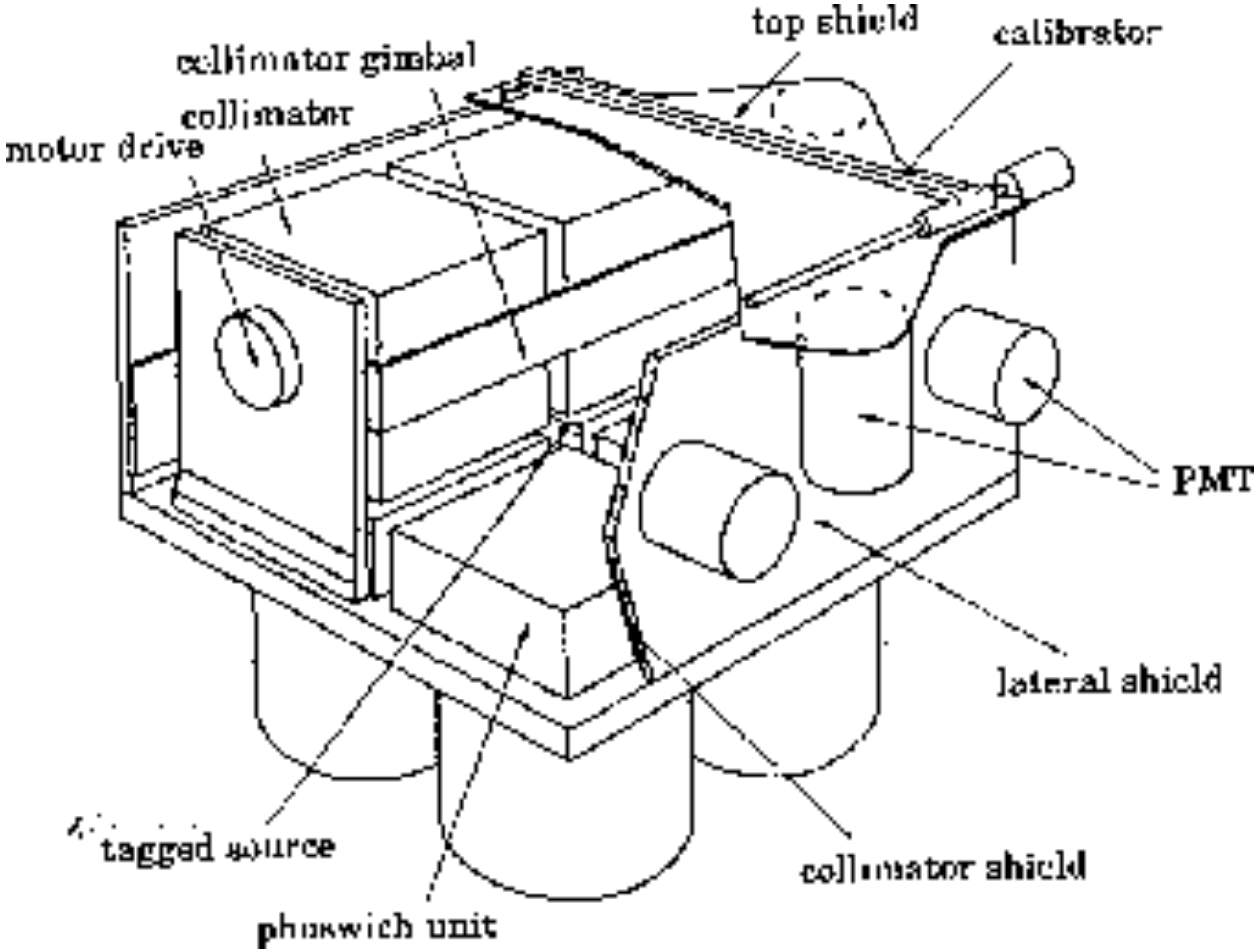

The BeppoSAX detectors

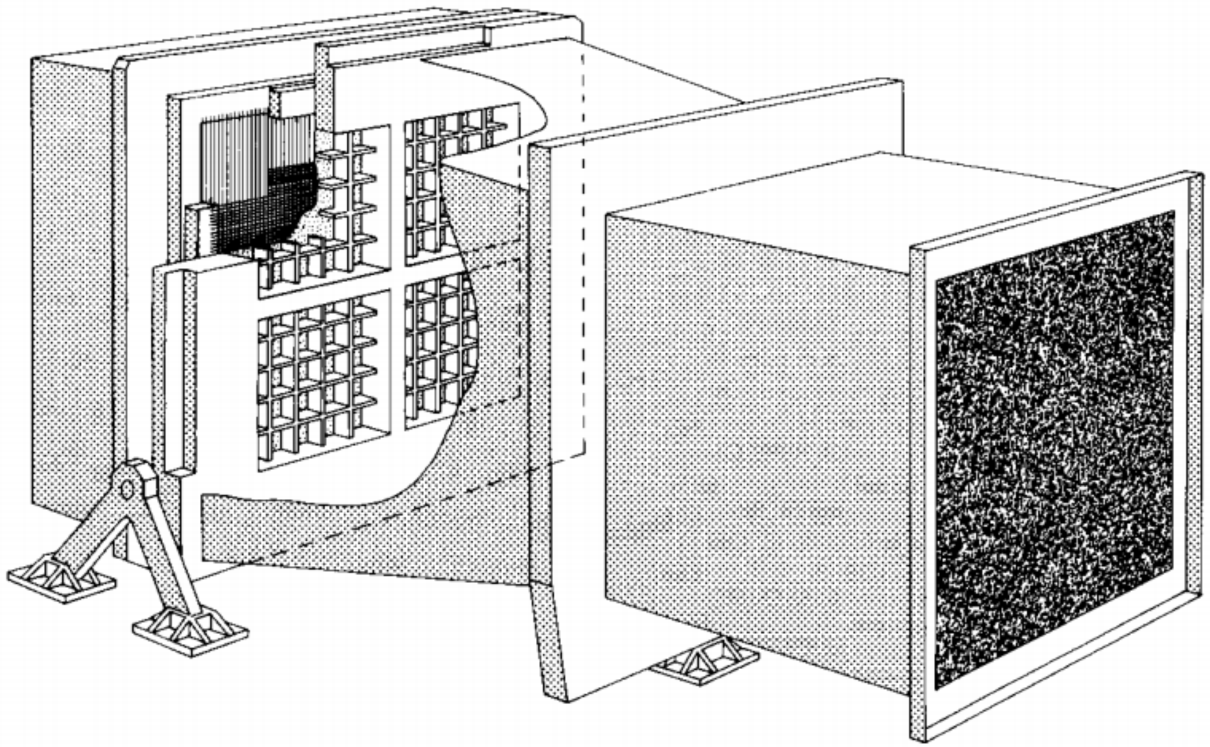

X-Ray Mirrors

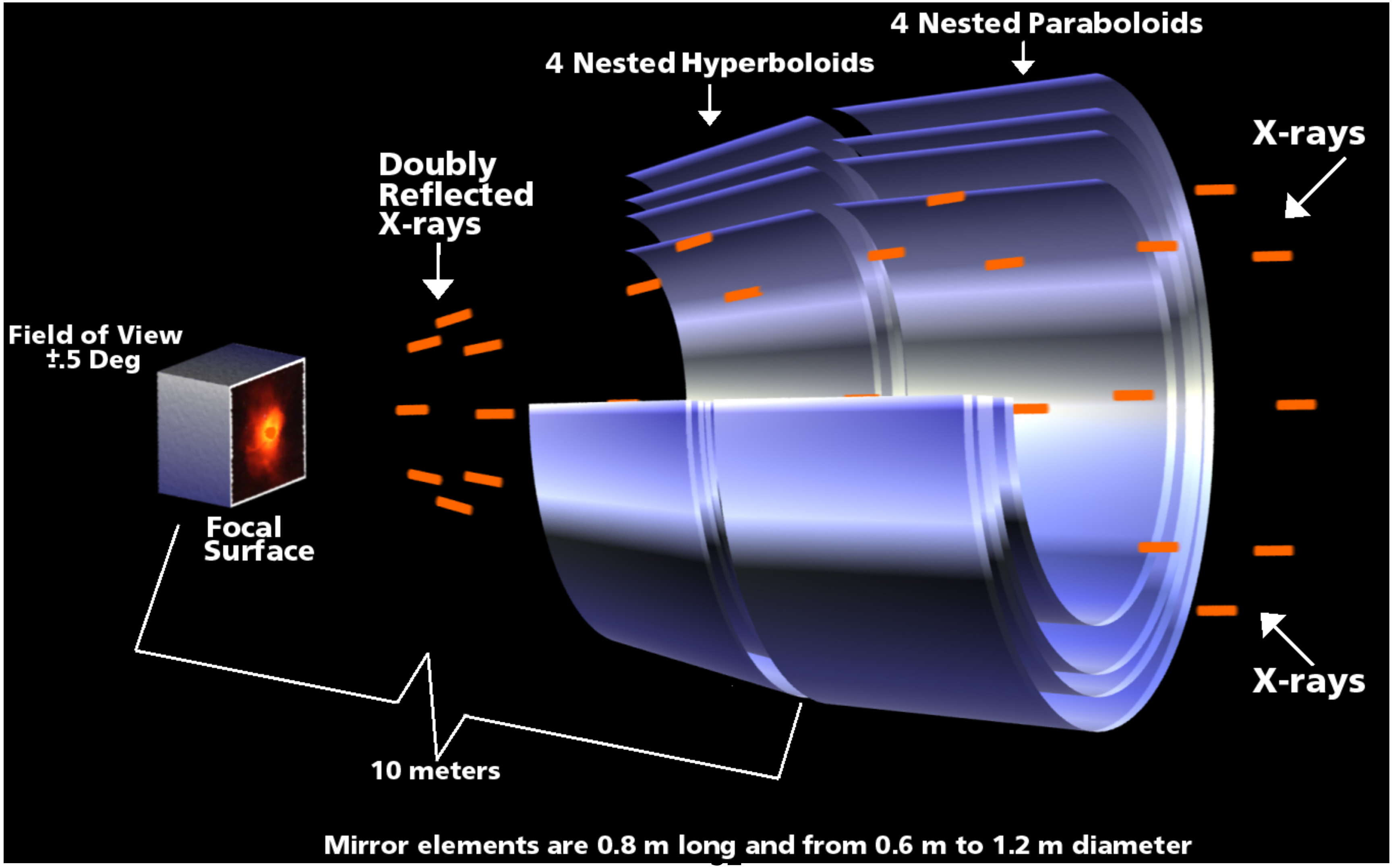

Nobel prize 2002 – R.Giacconi

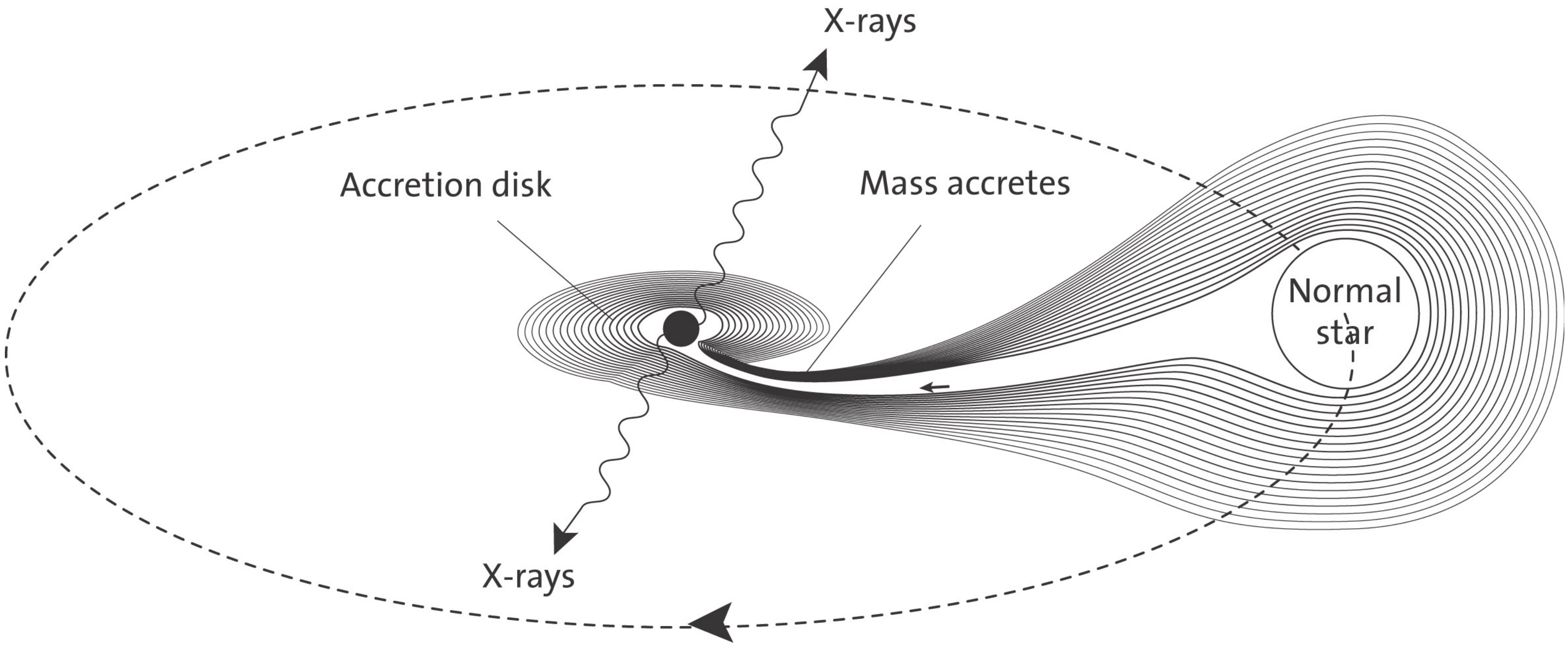

" … for pioneering contributions to astrophysics,
which have led to the discovery of cosmic X-ray sources"

Useful reference

Cambridge University Press

Handbook of Space Astronomy and Astrophysics

Martin V. Zombeck's **Handbook of Space Astronomy & Astrophysics, 2nd edition** is on-line at no cost. Published by Cambridge University Press, this handbook has become an essential reference for space astronomy and astrophysics. The complete 2nd edition (Copyright Cambridge University Press, 1982, 1990) is now available at your electronic desktop.

A 3rd edition of the Handbook of Space Astronomy & Astrophysics has been published. Fully updated, enlarged (nearly double the number of pages of the Second Edition) and including data from space-based observations, this 3rd edition is a comprehensive compilation of the facts and figures relevant to astronomy and astrophysics. As well as a

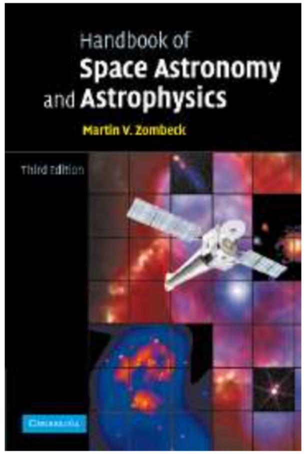

Third Edition by Martin V. Zombeck

On-line Version of the 2nd Edition

Note: All chapters now have links to related WWW resources containing extensive tabulations, images, interactive programs, etc.. Look for the link at the top of the table of contents for the given chapter.

Citation form: Zombeck, M. V., *Handbook of Astronomy and Astrophysics*, Cambridge, UK: Cambridge University Press.

- Table of Contents
- Index
- Links
- Help

http://ads.harvard.edu/books/hsaa

Why do we use X-ray optics

- To achieve the best 2-dim angular resolution
  - To distringuish nearby sources or different regions of the same source
  - To perform morphological studies
- As a collector to "gather" weak fluxes (case of limited photon statistics)
- As a concentrator, so that the image photons may interact in a small region of the detector, thus limiting the influence of the background
- To serve with high spectral resolution dispersive spectrometers such as transmission or reflection gratings
- To simultaneously measure both the source(s) of interest and the contaminating background in other (source-free) regions of the detector

X-ray optical constants

- X-rays are hard to refract or reflect: the refractive index of all materials in X-rays is very close to 1 and only slightly less than 1 ➔ X-rays are above the characteristic energy of bonded e- in atoms
- complex index of refraction of the reflector to describe the interaction X-rays /matter (see, for a review, Aschembach et al. 1985, Rep. Prog. Phys. 48, 579)

$$n=1-\delta+i\beta$$

where δ describes the phase change and β accounts for the absorption

δ and β depend on the wavelength

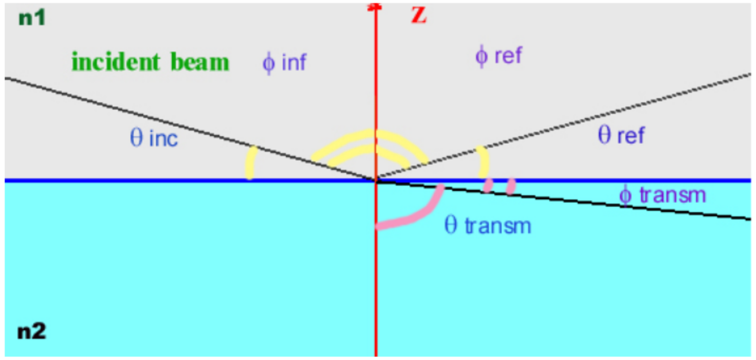

- the amplitute of reflection is described by the Fresnel's equations

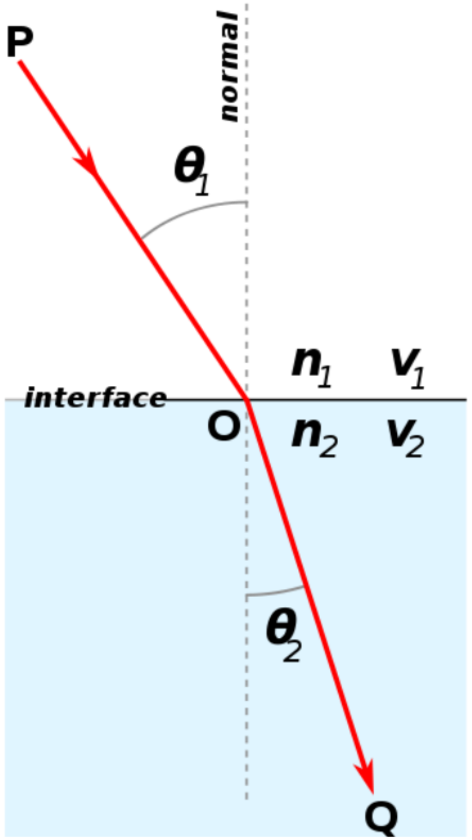

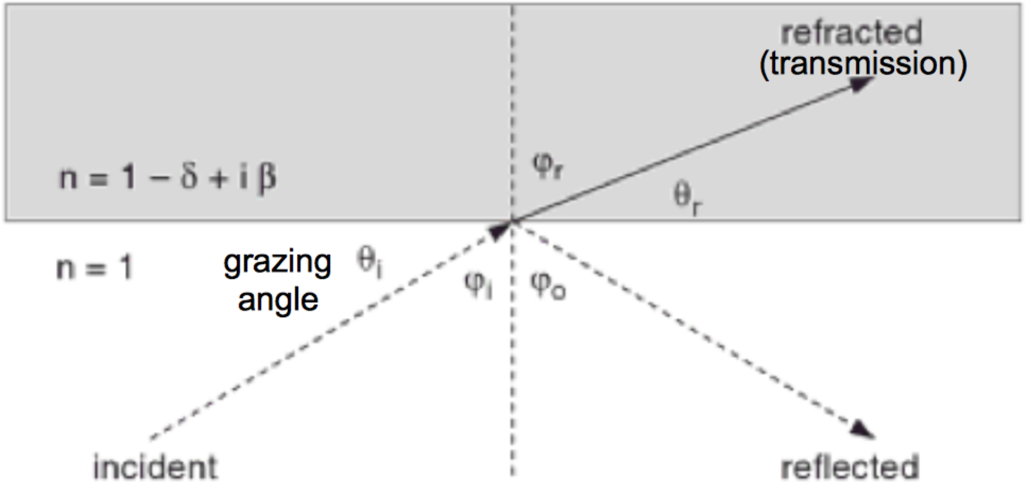

Snell's Law of Refraction:
relationship between the angles of incidence and refraction in a medium

$$n_1 \sin\theta_1 = n_2 \sin\theta_2$$

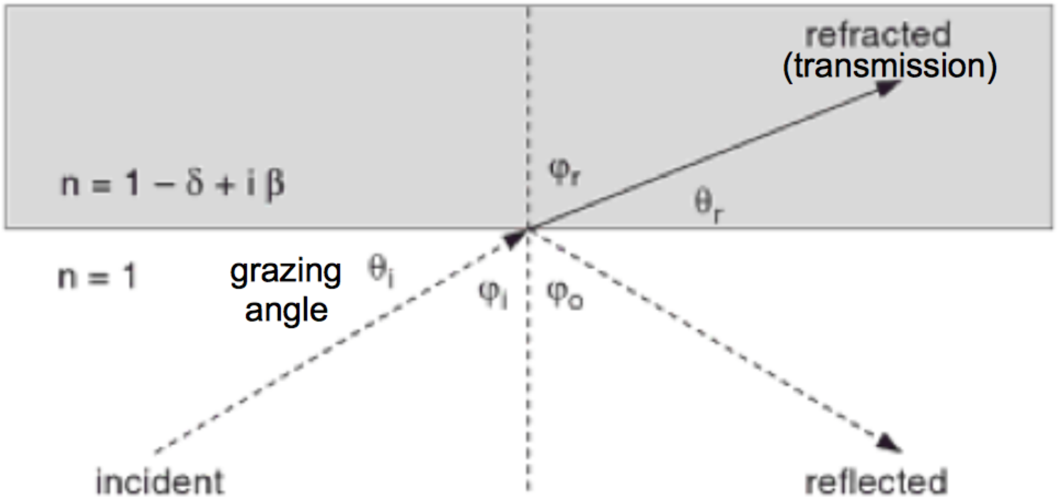

$$n_1 = 1,\ n_2 = (1-\delta) \ \rightarrow\ \sin\phi_i = (1-\delta)\sin\phi_r$$

$$\vartheta = (\pi/2) - \phi$$

$$\cos(90-\phi_i) = \cos\vartheta_i = (1-\delta)\cos(90-\phi_r) = (1-\delta)\cos\vartheta_r$$

$$\Rightarrow \cos\vartheta_i = \cos\vartheta_r(1-\delta)$$

Total reflection if no real solution for ϑ_r

$\delta>0$, $\cos\theta_r \leq 1$ ➔ There is a **critical angle θ_c** below which refraction is impossible and total external reflection occurs (grazing angle, $\theta_i=\theta_c$)

Extreme case for low θr values

$$1 = \cos\vartheta_r = \cos\vartheta_c / (1-\delta) \rightarrow \cos\vartheta_c = 1-\delta$$

Total X-ray reflection at grazing incidence

- Real part of n slightly less than unity for matter at X-rays, =1 in vacuum (total external reflection); $\delta << 1$

- Snell's law ($n1 \cos\theta_1 = n2 \cos\theta_2$) to find a critical angle for total reflection

- (Total) external reflection in vacuum for angles < critical angle: $\cos\theta_{crit} = 1 - \delta$

- X-ray partially reflected also for $\theta > \theta_{crit}$; also, some absorption in the material

- $\cos(\theta_{crit}) = 1 - \theta_{crit}^2/2 = 1 - \delta \xrightarrow{\text{low angles}} \theta_{crit} = \sqrt{2\delta}$

- Far from fluorescent edges: $\delta \approx \dfrac{N_0 Z r_e \rho \lambda^2}{2\pi A}$

where N_0=Avogadro's number
Z=atomic number
r_e=electron radius
ρ=density
λ=wavelength of the incoming photon
A=atomic weight

Critical angle:

- Inversely dependent on energy
- Higher Z materials reflect higher energies, for a fixed grazing angle
- Higher Z materials have a larger critical angle at any energy

- For heavy elements, Z/A≈0.5, and if δ<<1:

$$\theta_{crit} \approx \sqrt{2\delta} \approx 5.6\lambda\sqrt{\rho}$$

where λ[Å] and ρ[g/cm³], and θ[arcmin]

$$\theta_{crit} \propto \sqrt{\rho} / E$$

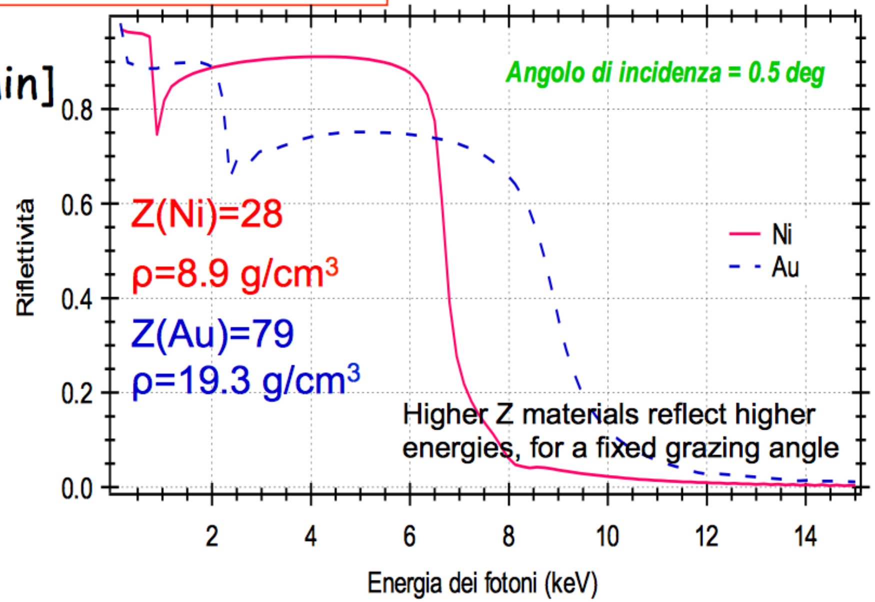

- Some reflectivity is lost due to scattering related to the presence of micro-roughness at the surface

- Use of heavy materials (but attention at the absorption edges…)

X-ray mirrors with parabolic profile

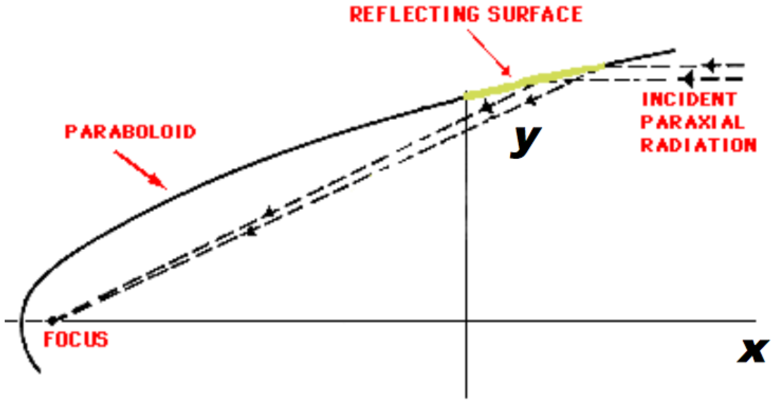

- perfect on-axis focusing
- off-axis images <u>strongly</u> affected by coma

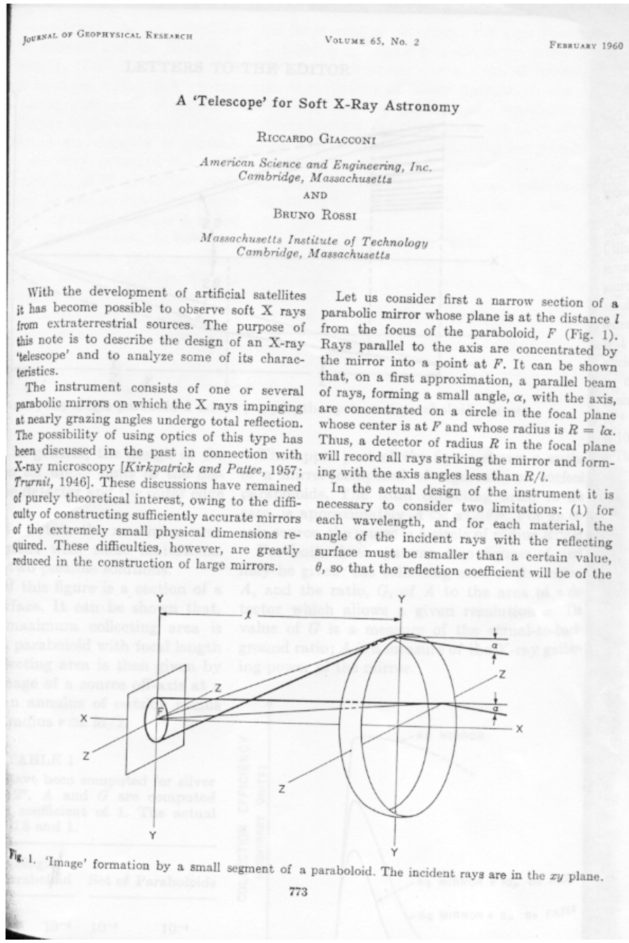

JOURNAL OF GEOPHYSICAL RESEARCH VOLUME 65, No. 2 FEBRUARY 1960

A 'Telescope' for Soft X-Ray Astronomy

RICCARDO GIACCONI

American Science and Engineering, Inc.
Cambridge, Massachusetts

AND

BRUNO ROSSI

Massachusetts Institute of Technology
Cambridge, Massachusetts

With the development of artificial satellites it has become possible to observe soft X rays from extraterrestrial sources. The purpose of this note is to describe the design of an X-ray 'telescope' and to analyze some of its characteristics.

The instrument consists of one or several parabolic mirrors on which the X rays impinging at nearly grazing angles undergo total reflection. The possibility of using optics of this type has been discussed in the past in connection with X-ray microscopy [*Kirkpatrick and Pattee*, 1957; *Trurnit*, 1946]. These discussions have remained of purely theoretical interest, owing to the difficulty of constructing sufficiently accurate mirrors of the extremely small physical dimensions required. These difficulties, however, are greatly reduced in the construction of large mirrors.

Let us consider first a narrow section of a parabolic mirror whose plane is at the distance l from the focus of the paraboloid, F (Fig. 1). Rays parallel to the axis are concentrated by the mirror into a point at F. It can be shown that, on a first approximation, a parallel beam of rays, forming a small angle, α, with the axis, are concentrated on a circle in the focal plane whose center is at F and whose radius is $R = l\alpha$. Thus, a detector of radius R in the focal plane will record all rays striking the mirror and forming with the axis angles less than R/l.

In the actual design of the instrument it is necessary to consider two limitations: (1) for each wavelength, and for each material, the angle of the incident rays with the reflecting surface must be smaller than a certain value, θ, so that the reflection coefficient will be of the

Fig. 1. 'Image' formation by a small segment of a paraboloid. The incident rays are in the xy plane.

Wolter, 1952

Wolter's solution to the X-ray imaging

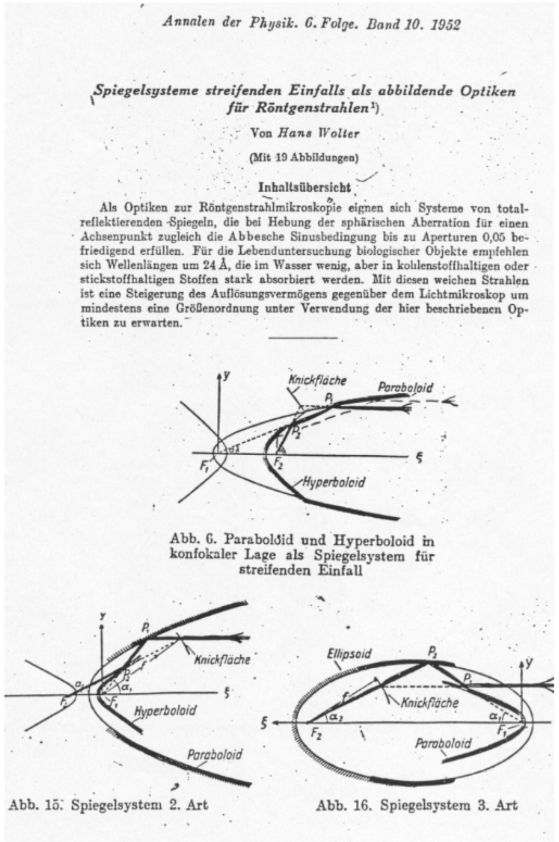
Annalen der Physik. 6. Folge. Band 10. 1952

Spiegelsysteme streifenden Einfalls als abbildende Optiken für Röntgenstrahlen[1])

Von *Hans Wolter*

(Mit 19 Abbildungen)

Inhaltsübersicht

Als Optiken zur Röntgenstrahlmikroskopie eignen sich Systeme von totalreflektierenden Spiegeln, die bei Hebung der sphärischen Aberration für einen Achsenpunkt zugleich die Abbesche Sinusbedingung bis zu Aperturen 0,05 befriedigend erfüllen. Für die Lebenduntersuchung biologischer Objekte empfehlen sich Wellenlängen um 24 Å, die im Wasser wenig, aber in kohlenstoffhaltigen oder stickstoffhaltigen Stoffen stark absorbiert werden. Mit diesen weichen Strahlen ist eine Steigerung des Auflösungsvermögens gegenüber dem Lichtmikroskop um mindestens eine Größenordnung unter Verwendung der hier beschriebenen Optiken zu erwarten.

Abb. 6. Paraboloid und Hyperboloid in konfokaler Lage als Spiegelsystem für streifenden Einfall

Abb. 15. Spiegelsystem 2. Art

Abb. 16. Spiegelsystem 3. Art

H. Wolter, Ann. Der Phys., NY10, 94 (1952)

Fine for X-ray astronomy

Applied in solar X-ray telescopes

Not adopted

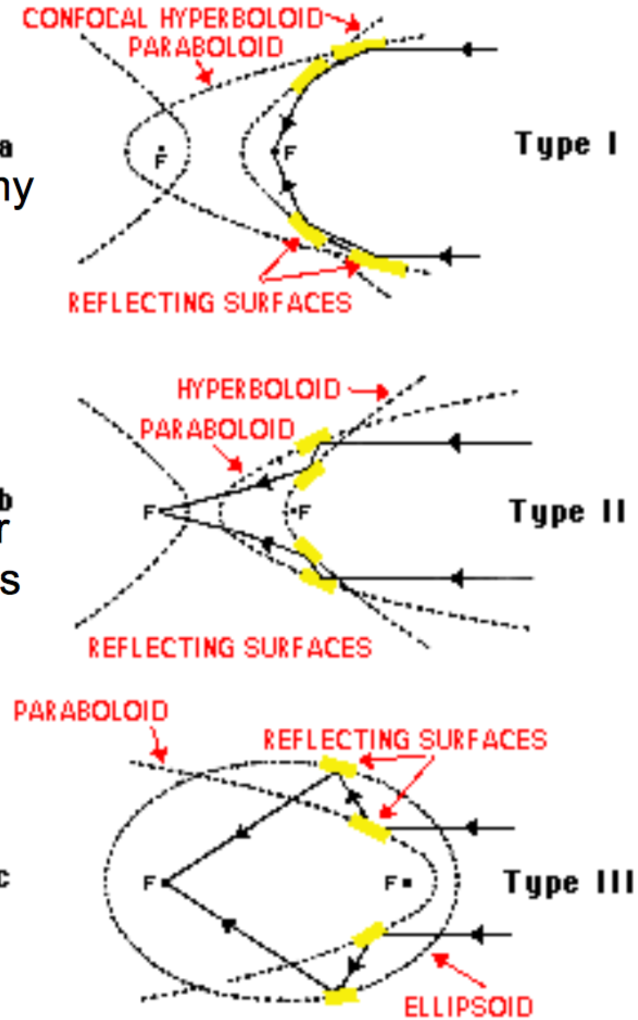

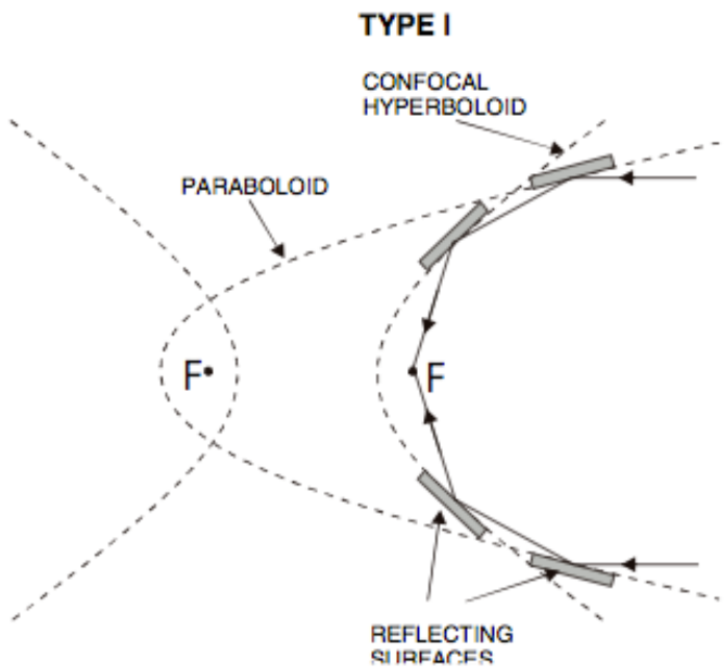

Wolter-I optics
Paraboloid ➔ Hyperboloid

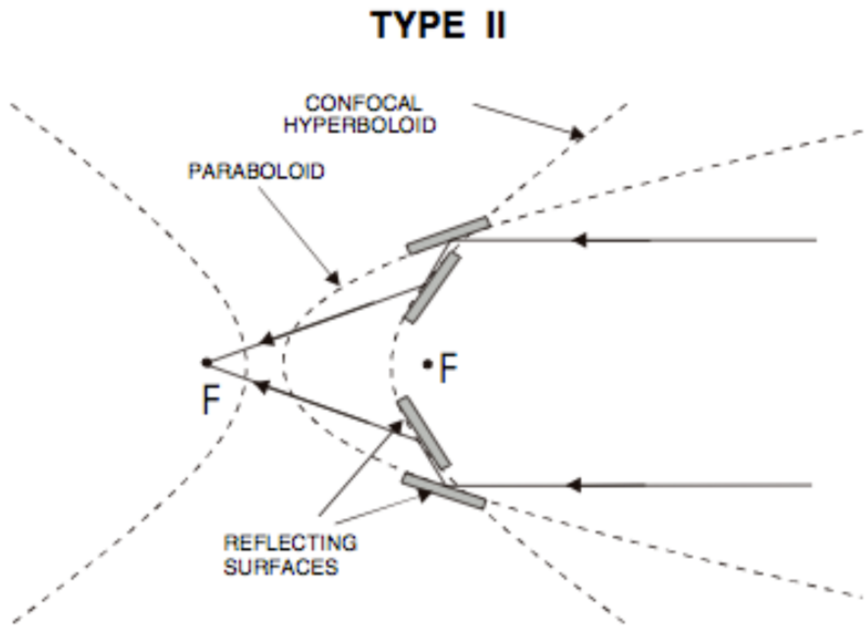

Wolter-II optics
Paraboloid ➔ Hyperboloid (ext. surface)

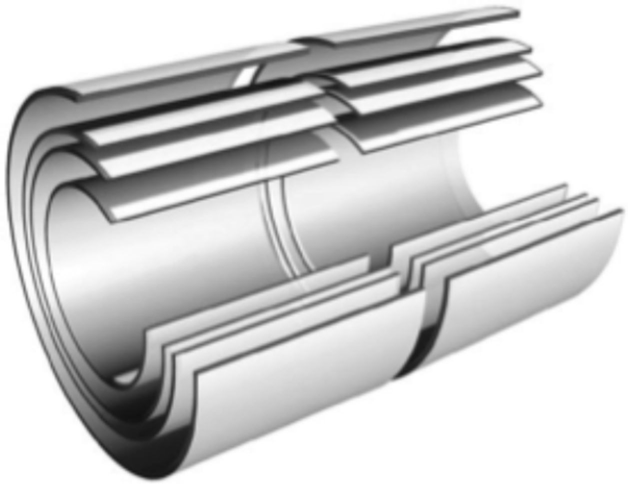

X-Ray Mirrors

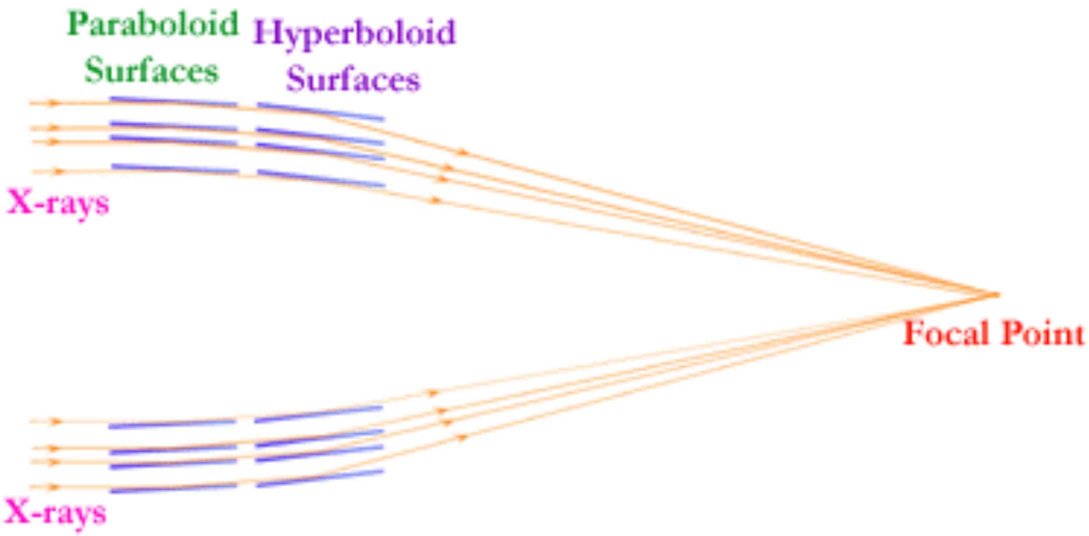

$$\cos\phi = 1 - \delta$$

$$\delta = 2.70 \times 10^{-6} \frac{Z_e}{A} \rho \lambda^2$$

Cf Aschembach et al. 1985

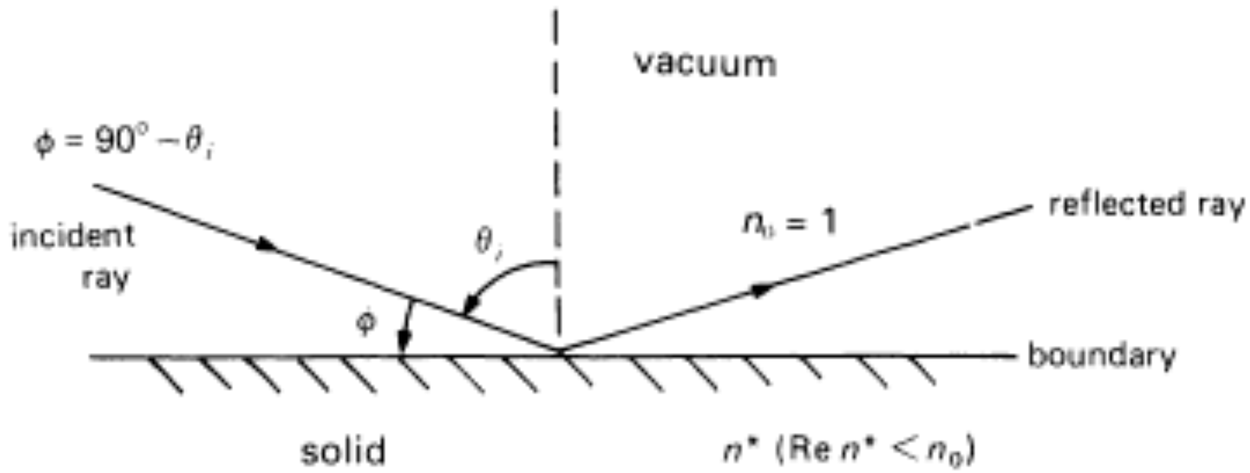

A_{geom} x Reflectivity

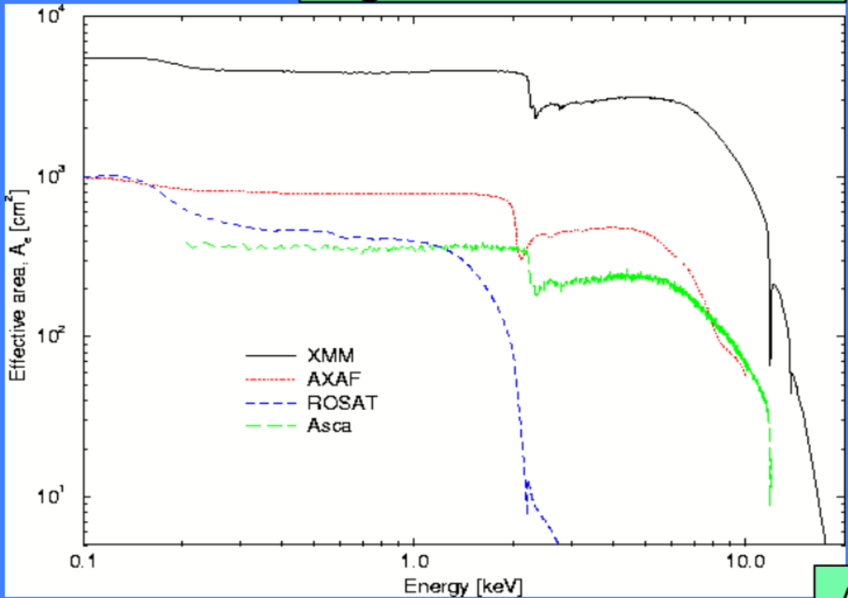

x

QE

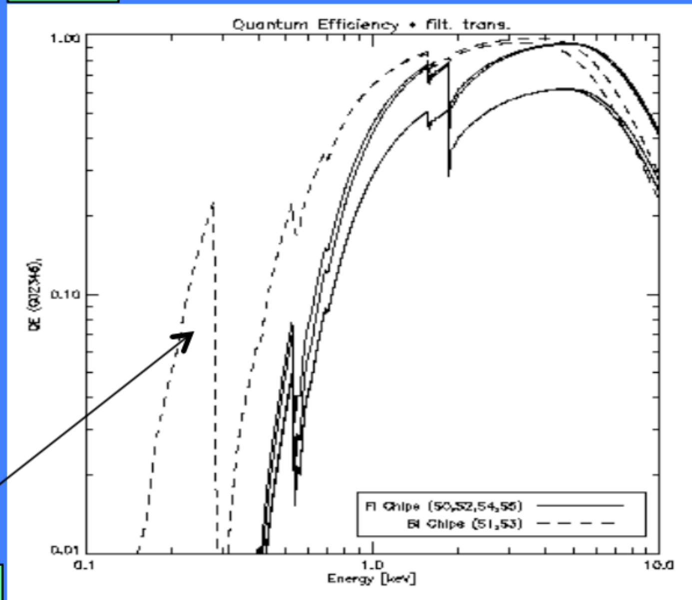

=

$A_{effective}$

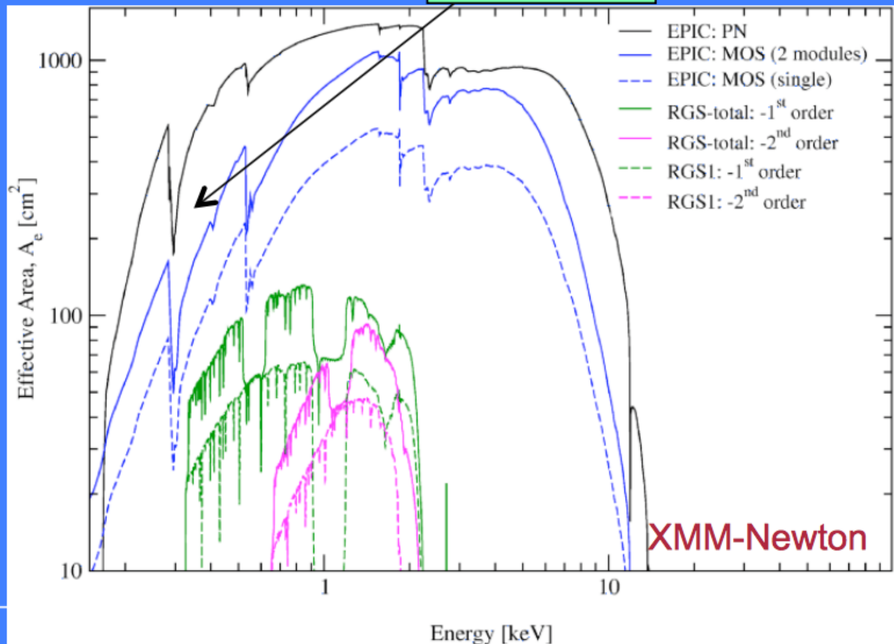

CCD

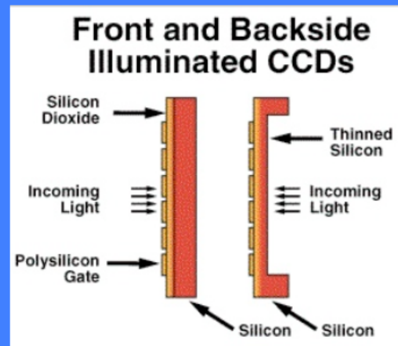

Focalizzazione vs collimazione

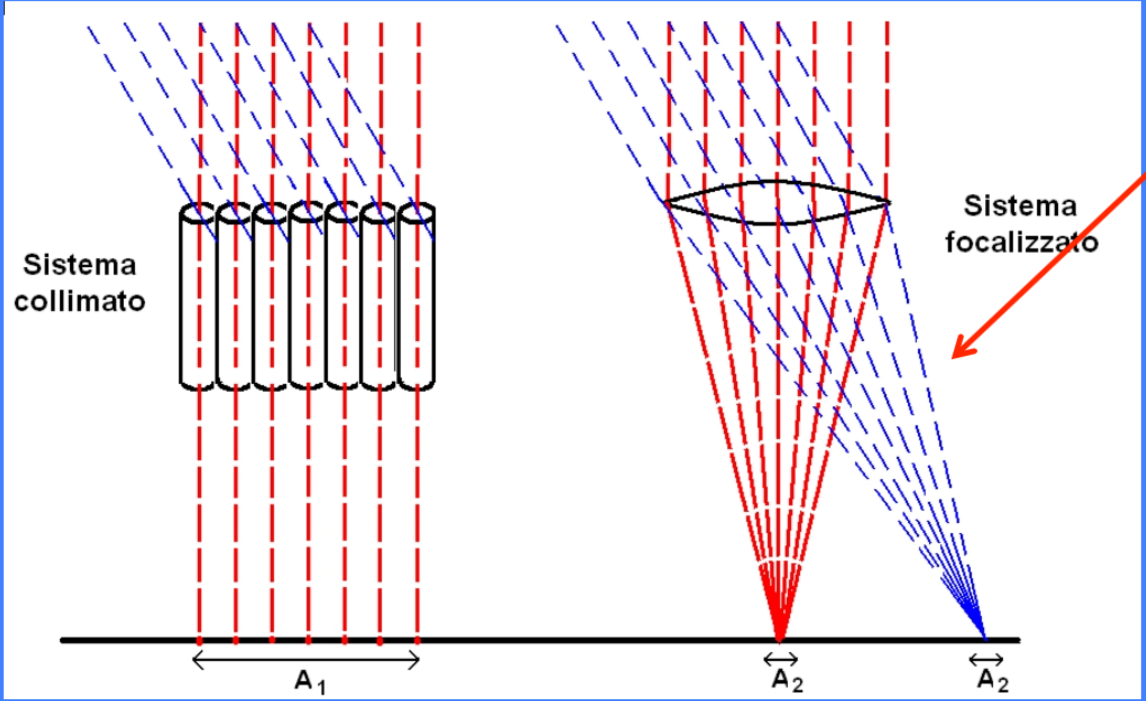

Proper imaging of X-rays below 20-40 keV

$$F_{\min} \approx n_\sigma \frac{\sqrt{2B}}{\sqrt{A_{\det} T_{\rm int} \Delta E}}$$

A_d= PSF projected on the focal plane

$$F_{\min} \approx n_\sigma \frac{\sqrt{BA_d}}{A_{eff}\sqrt{T_{\rm int}\Delta E}}$$

Sistema collimato: limita la regione di cielo da cui puo' provenire un segnale, (quindi limita il background), non incrementandone la "densita"

Sistema focalizzato: fa corrispondere ad ogni sorgente un punto nel piano focale, e "concentra" il segnale, producendo un'immagine

$$C_S = S_E\, A_e\, \Delta E\, \Delta t\, \eta_E$$

Detected signal

$$C_B = B\, \varepsilon\, A_d\, \Delta E\, \Delta t$$

Background signal (ε: region of the detector where B counts are focused)

$$S/N = n_\sigma = \frac{C_S}{\sqrt{C_S + 2C_B}} \approx \frac{S_E\, A_e\, \Delta E\, \Delta t\, \eta_E}{\sqrt{2B\, \varepsilon\, A_d\, \Delta E\, \Delta t}}$$

$$S_{E,\min} = \frac{n_\sigma}{\eta_E}\, \frac{1}{\mathrm{A_e}} \sqrt{\frac{2B\, \varepsilon\, A_d}{\Delta t\, \Delta E}}$$

Weak sources

Old slide but *Chandra* and XMM-*Newton* still working

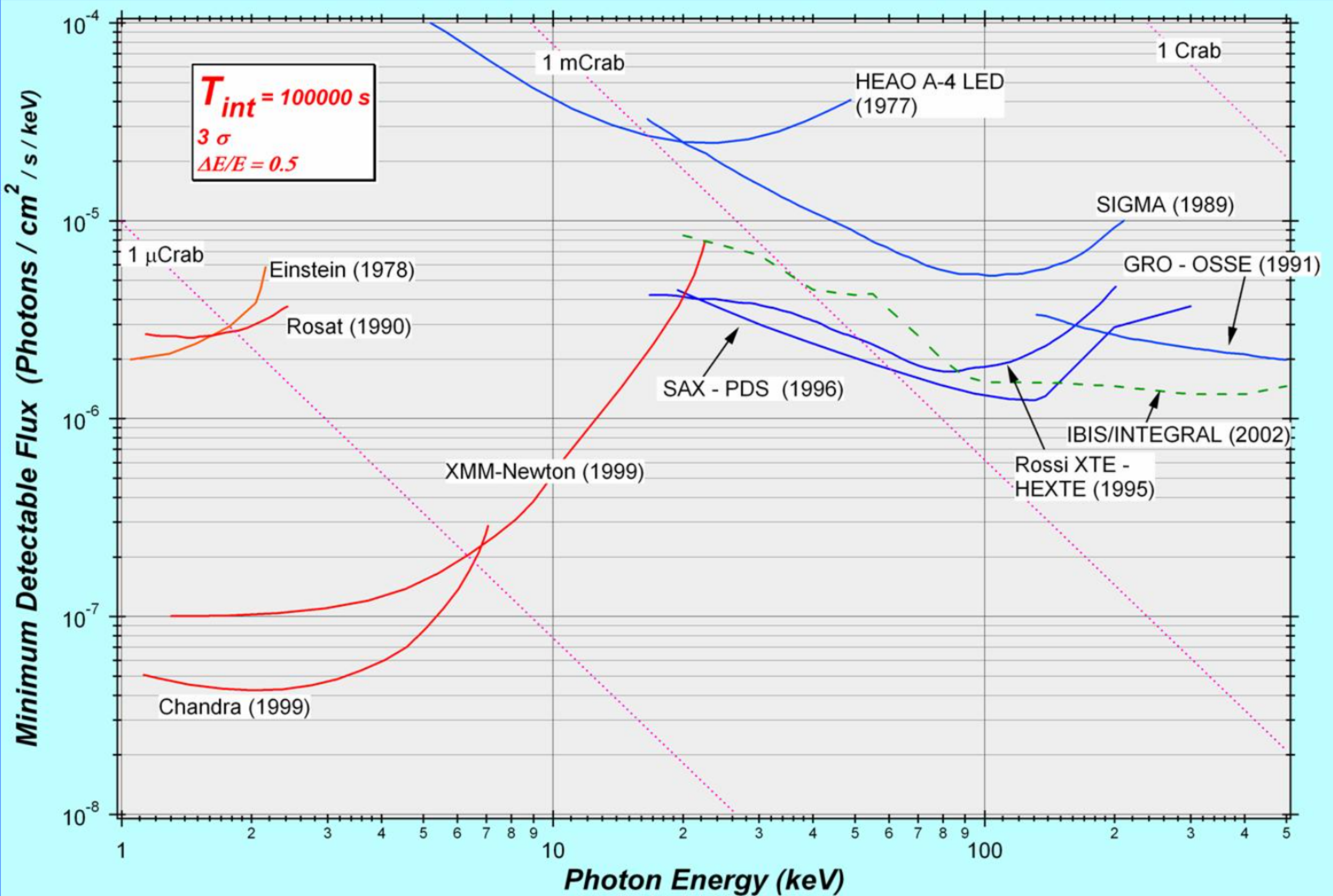

The GRB phenomenon

• simultaneous detection of GRBs by GRBM and WFC
→ very accurate localization (few arcmin)

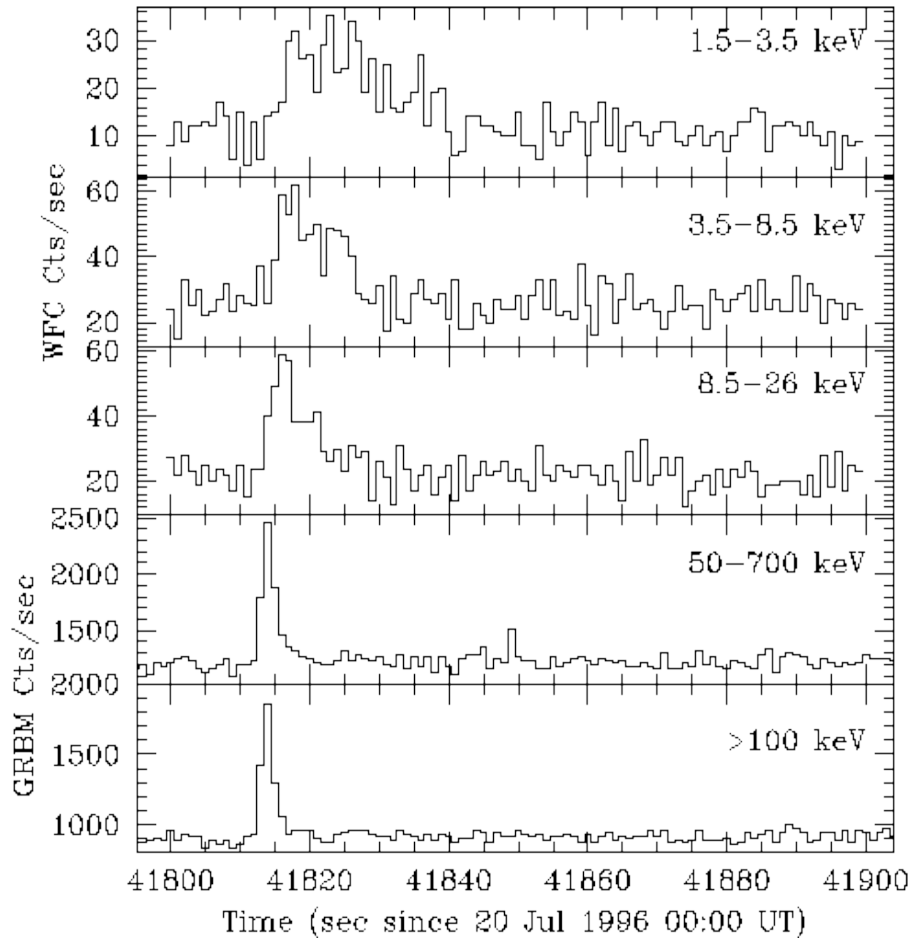

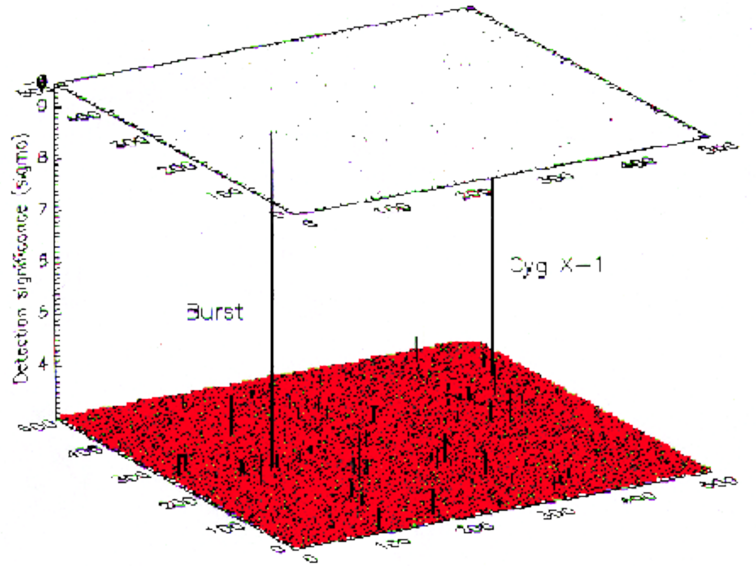

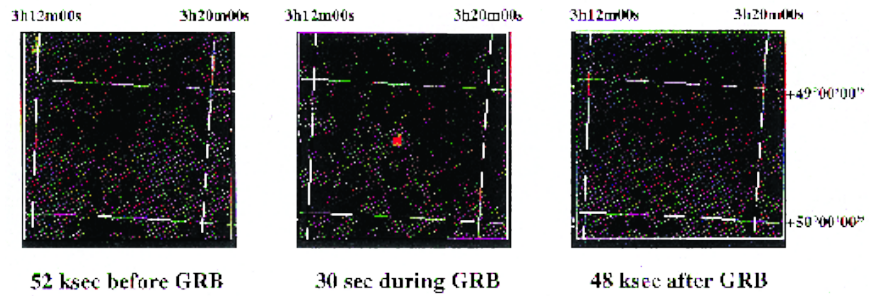

GRB960720, Piro et al., A&A, 1998

The GRB phenomenon

- in 1997, thanks to BeppoSAX observations, discovery of fading X-ray, optical, radio emission following the GRB

- photons received during the classical GRB phenomenon are then called "prompt emission" and the subsequent fading emission is called "afterglow emission"

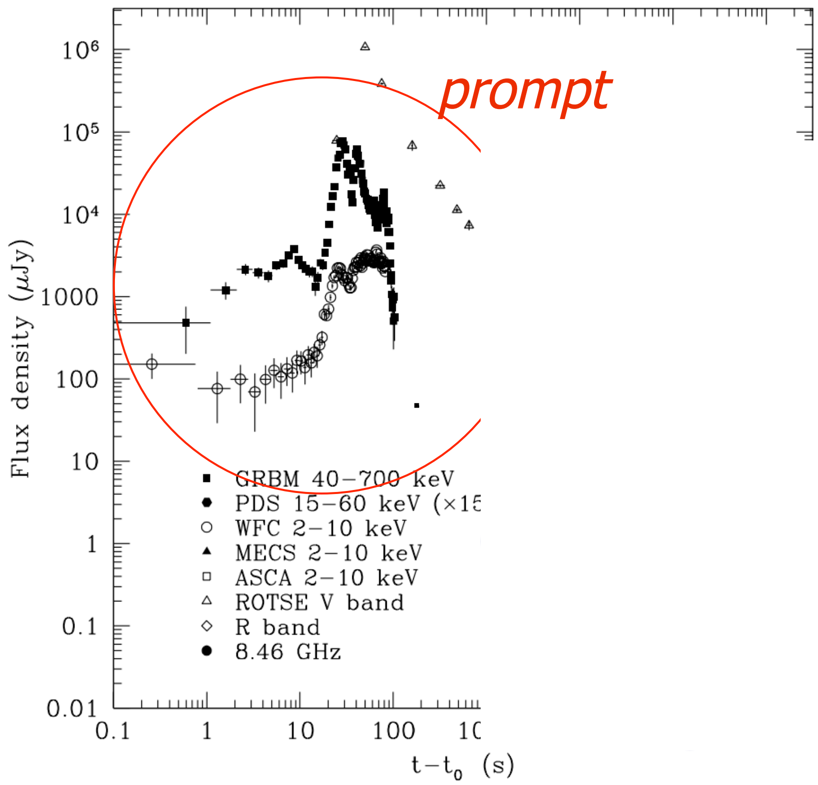

Adapted from Maiorano et al., A&A, 2005

GRB970228 – first good localization

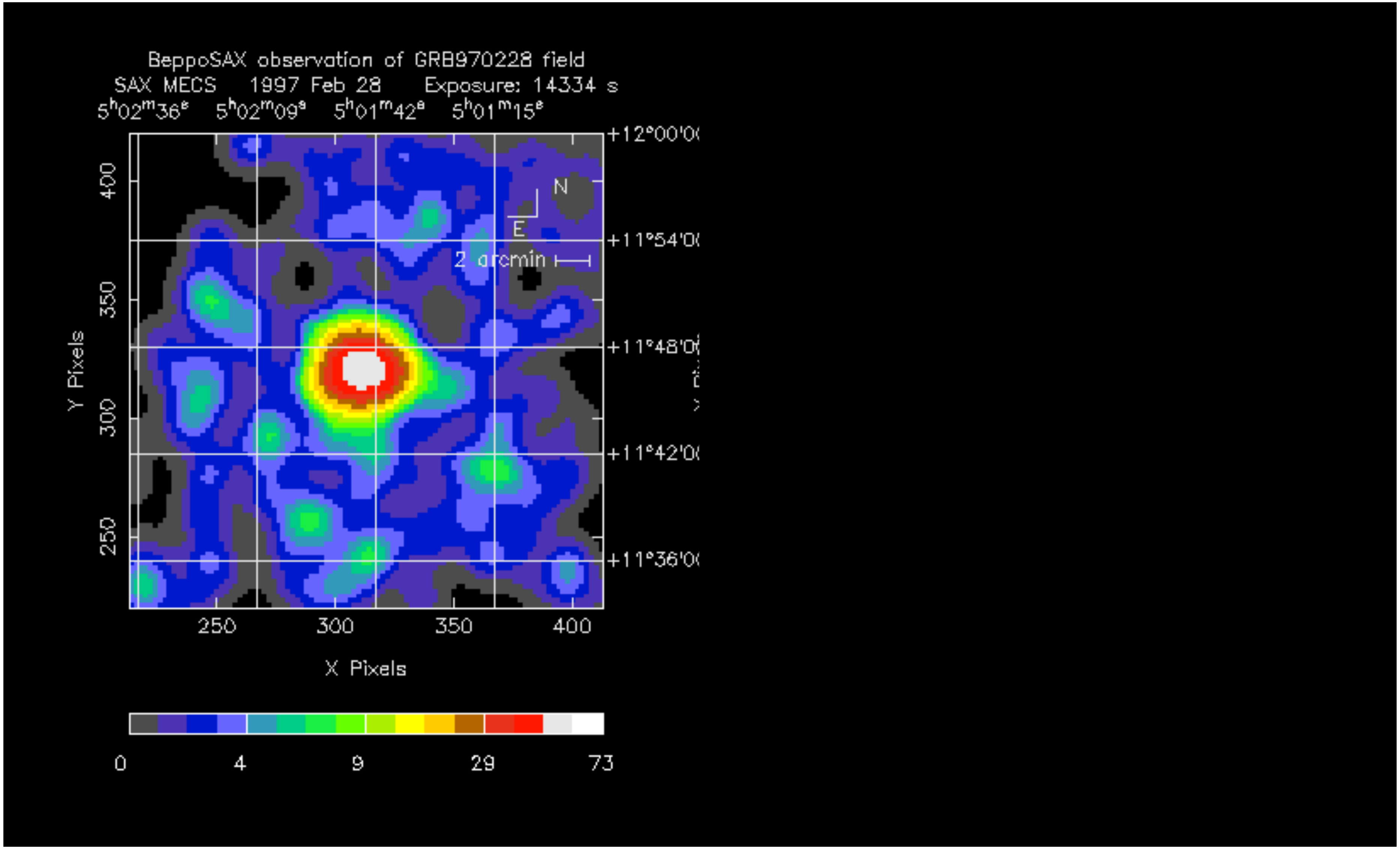

BeppoSAX

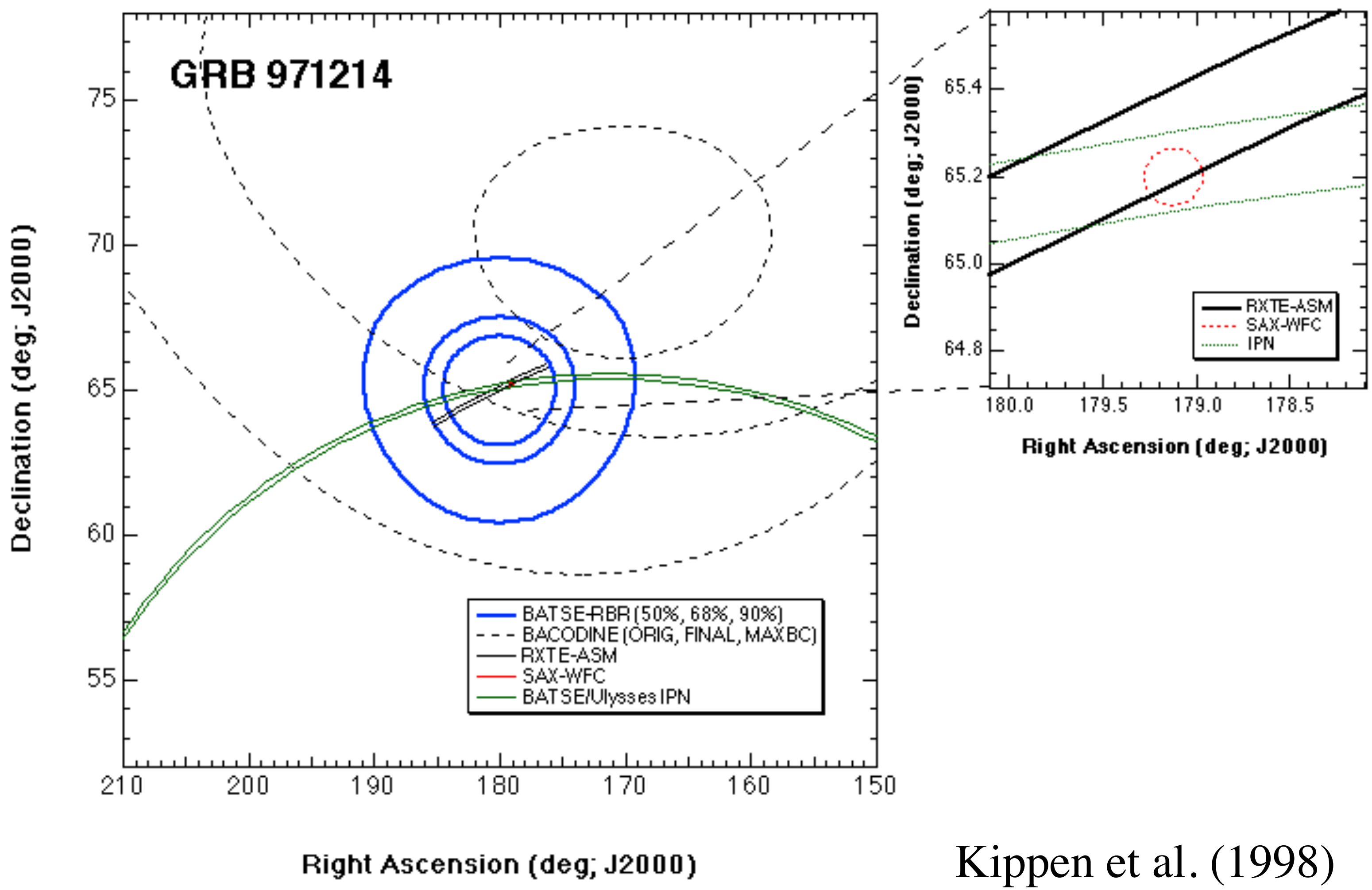

Kippen et al. (1998)

Afterglow Observations

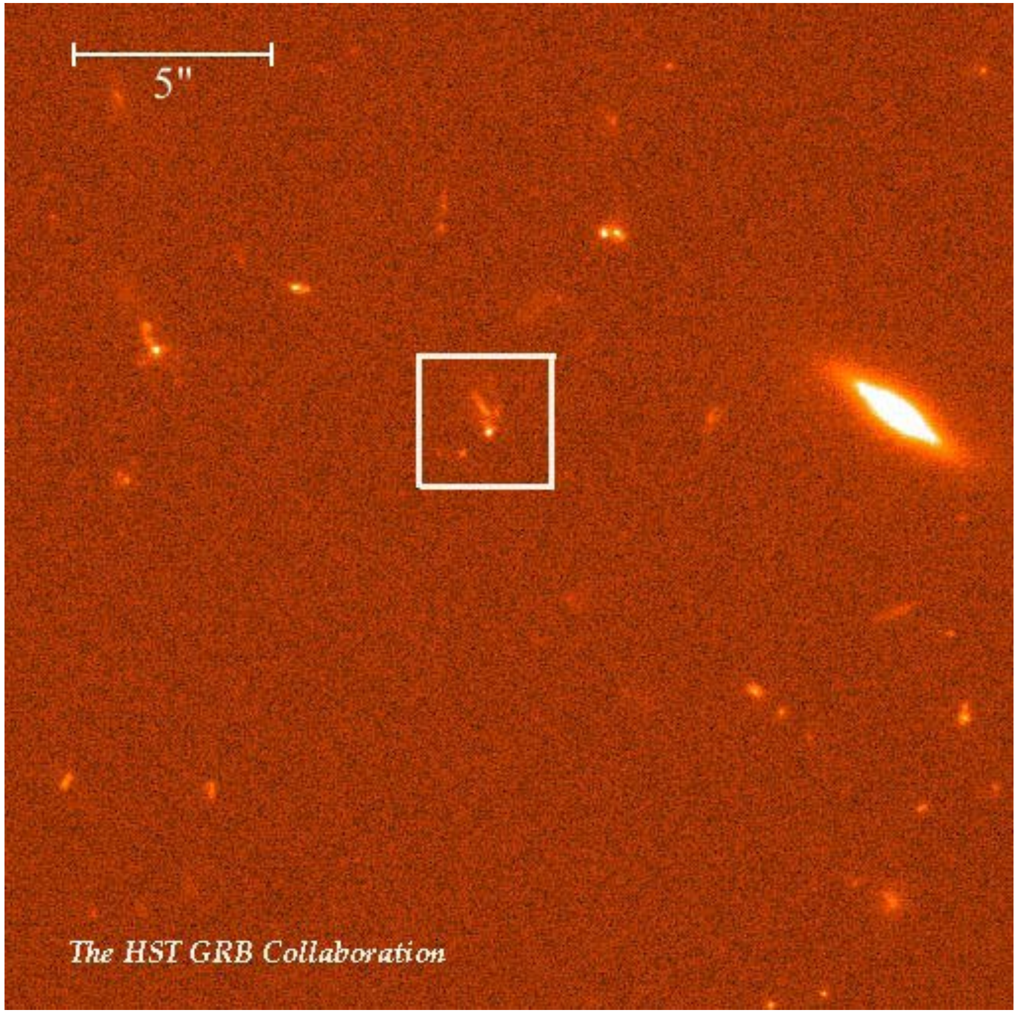

Identificazione delle Host Galaxies

Fruchter et al (1999)

BeppoSAX and the Afterglows

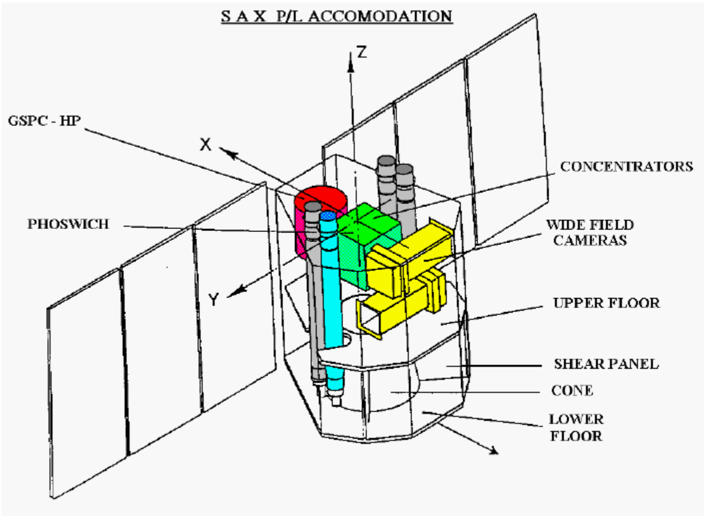

- Good Angular resolution (< arcmin)
- Observation of the X-Afterglow

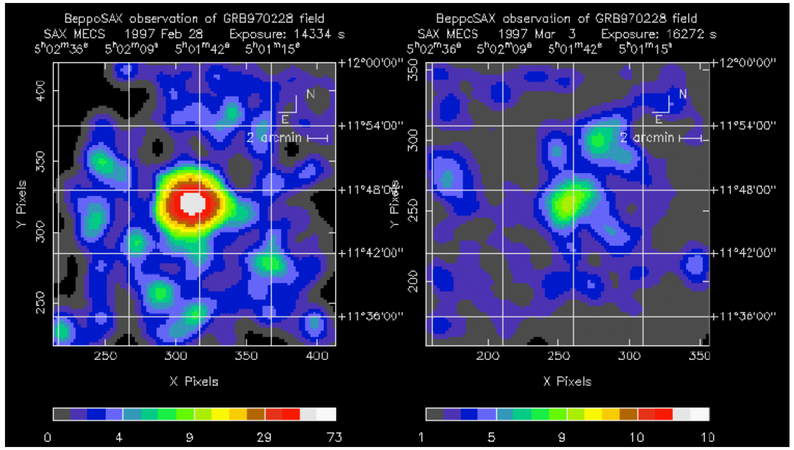

Costa et al. (1997)

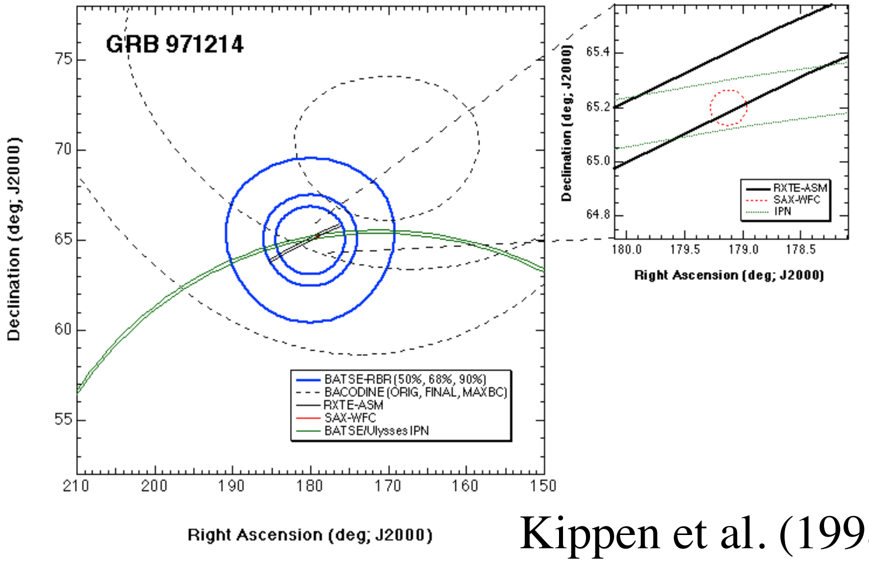

Kippen et al. (1998)

- Optical Afterglow (HST, Keck)
- Direct observation of the host galaxies
- Distance determination

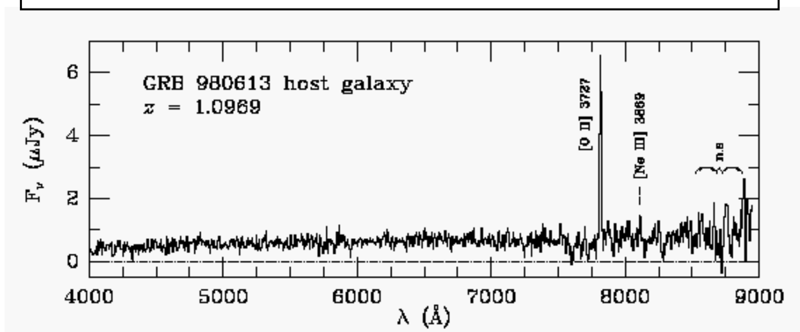

Djorgoski et al. (2000)

The compactness problem

Light curve variability ~ 1 ms

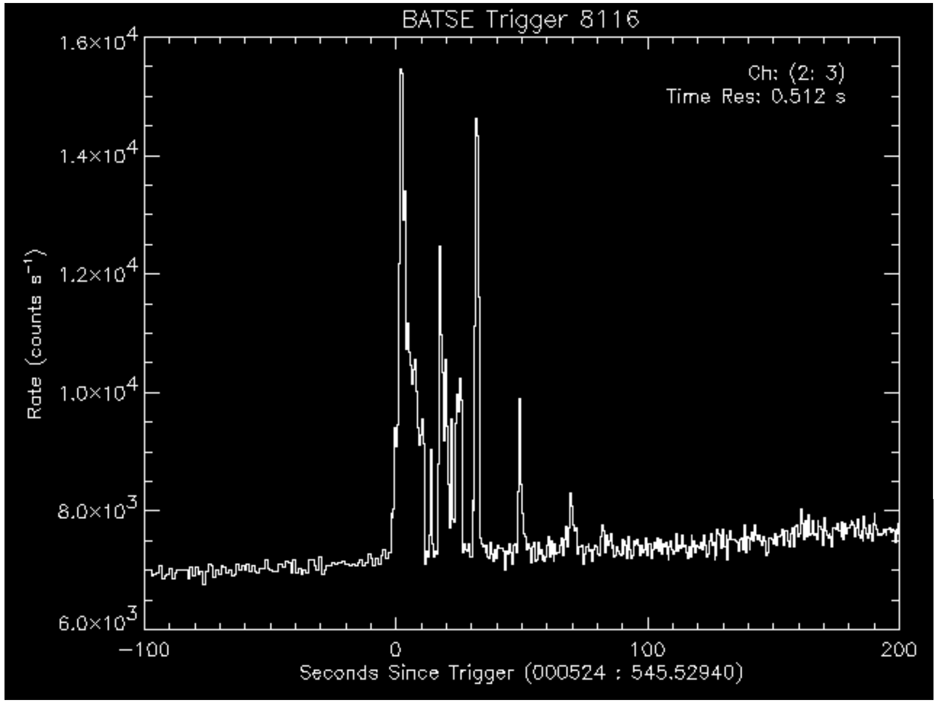

Briggs et al. (1999)

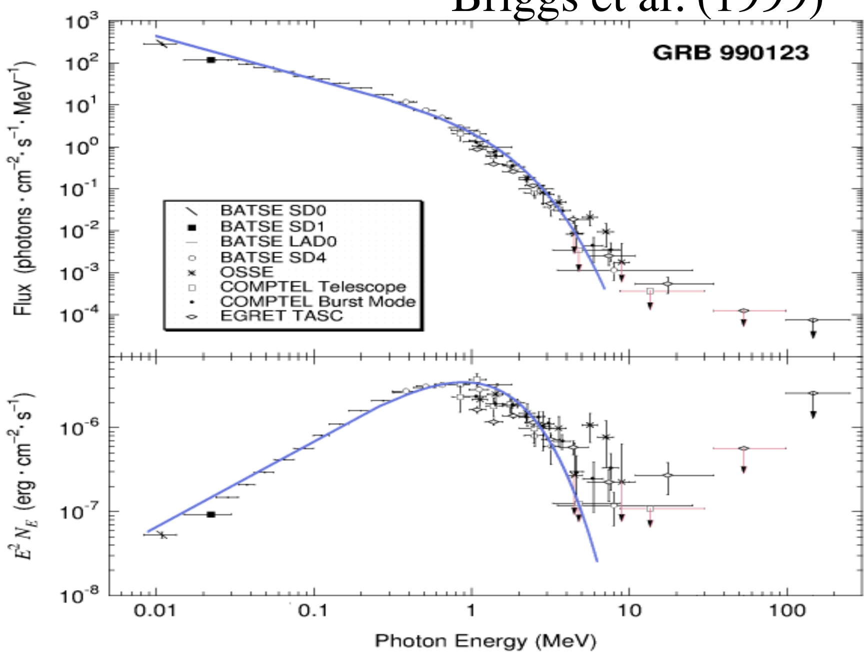

Non thermal spectra

- Fluence (γ): (0.1-10) x 10^{-6} erg/cm^2 ($\Omega/4\pi$)
- Total Energy: E ~ $10^{51} \div 10^{52}$ erg

The compactness problem

$$R_i < c\delta t \qquad \gamma\gamma \to e^+e^-$$

$$\tau_{\gamma\gamma} = \frac{f_p \sigma_T F D_L^2}{R_i^2 m_e c^2} \approx 10^{17} f_p \left(\frac{F}{10^{-6} erg/cm^2}\right)\left(\frac{D_L}{3Gpc}\right)^2\left(\frac{\delta t}{1ms}\right)$$

$$\tau_{\gamma\gamma} >> 1$$

Very High Optical Depth to pair production

$$\Gamma = \frac{1}{\sqrt{1-\beta^2}}$$

Size

Pair fraction

$$R_i < \Gamma^2 c\delta t \quad f_p \to f_p \Gamma^{-2\alpha}$$

$$\tau_{\gamma\gamma} = \frac{f_p \sigma_T F D_L^2}{R_i^2 m_e c^2} \approx \frac{10^{17}}{\Gamma^{4+2\alpha}} f_p \left(\frac{F}{10^{-6} erg/cm^2}\right)\left(\frac{D_L}{3Gpc}\right)^2\left(\frac{\delta t}{1ms}\right)$$

$$\Gamma \approx 10^2 \div 10^3$$

Piran (1999)

Relativistic motion of the emitting region

Superluminal motion

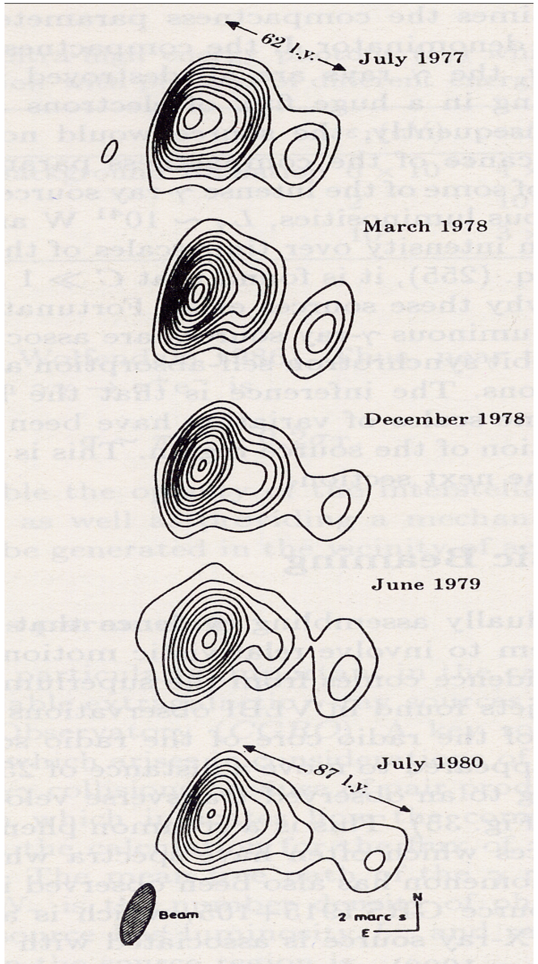

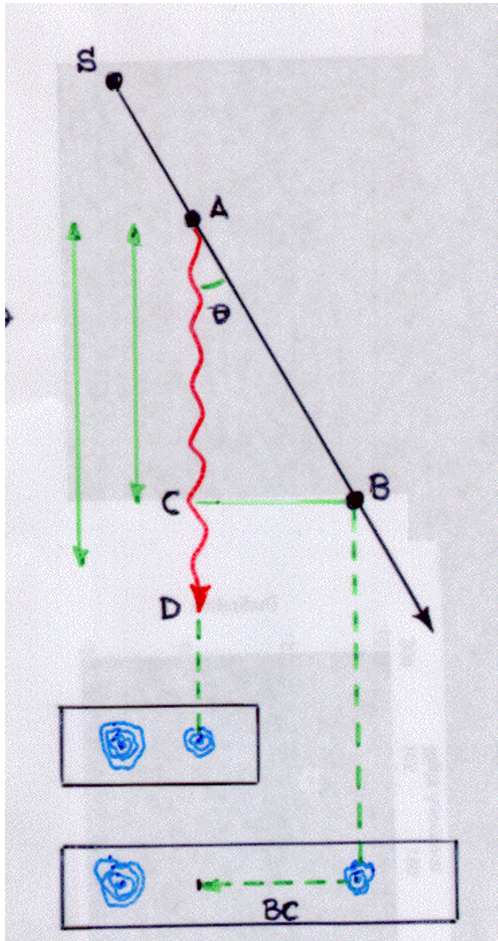

Superluminal motion

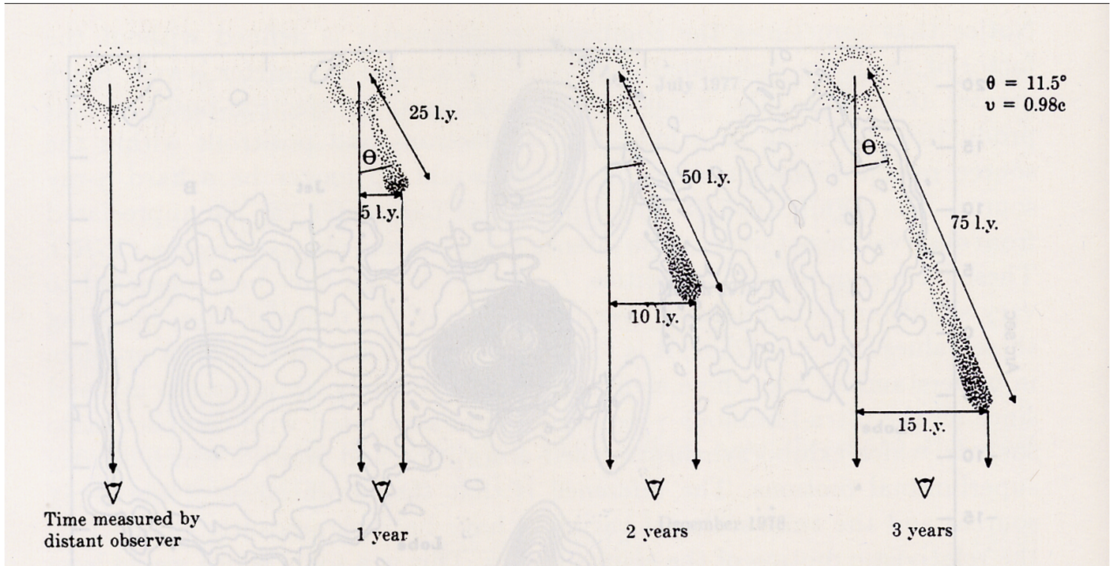

Arrival time of "bullets" emission

$$t'_A = t_A + \frac{D + v\delta t\cos\theta}{c}$$

$$t'_B = t_B + \frac{D}{c}$$

$$\delta t' = \delta t(1 - \beta\cos\theta)$$

$$v_\perp = \frac{v\sin\theta}{1 - \beta\cos\theta}$$

$$\cos\theta = \frac{v}{c}$$

$$\sin\theta = \sqrt{1 - \beta^2}$$

$$v_\perp = \gamma v$$

Relativistic effects

- **Light aberration:** photons emitted at right angles with respect to the velocity vector (in K') are observed in K to make an angle given by $\sin\theta = 1/\Gamma$. This means that in K half of the photons are concentrated in a cone of semi-aperture angle corresponding to $\sin\theta = 1/\Gamma$.

- **Arrival time of the photons**: as discussed above, the emission and arrival time intervals are different. As measured in the same frame K we have, as before, $\Delta t_a = \Delta t_e(1-\beta\cos\theta)$. If $\Delta t'_e$ is measured in K', $\Delta t_e = \Gamma\Delta t'_e$ leading to

$$\Delta t_a = \Gamma(1-\beta\cos\theta)\Delta t'_e \equiv \frac{\Delta t'_e}{\delta} \quad (2)$$

  Here we have introduced the factor δ, referred to as the beaming or Doppler factor. It exceeds unity for small viewing angles, and if so, observed time intervals are *contracted*.

- **Blueshift/Redshift of frequencies**: since frequencies are the inverse of times, we just have $\nu = \delta\nu'$.

Ghisellini astro-ph/9905181

Relativistic effects

$\nu = \delta\nu'$	frequency
$t = t'/\delta$	time
$V = \delta V'$	volume
$\sin\theta = \sin\theta'/\delta$	sine
$\cos\theta = (\cos\theta' + \beta)/(1 + \beta\cos\theta')$	cosine
$I(\nu) = \delta^3 I'(\nu')$	specific intensity
$I = \delta^4 I'$	total intensity
$j(\nu) = \delta^2 j'(\nu')$	specific emissivity
$\kappa(\nu) = \kappa'(\nu')/\delta$	absorption coefficient
$T_B = \delta T'_B$	brightness temperature (size directly measured)
$T_B = \delta^3 T'_B$	brightness temperature (size from variability)

$\delta = \gamma(1-(V/c)\cos\theta)$

Ghisellini astro-ph/9905181

The compactness problem

Light curve variability ~ 1 ms

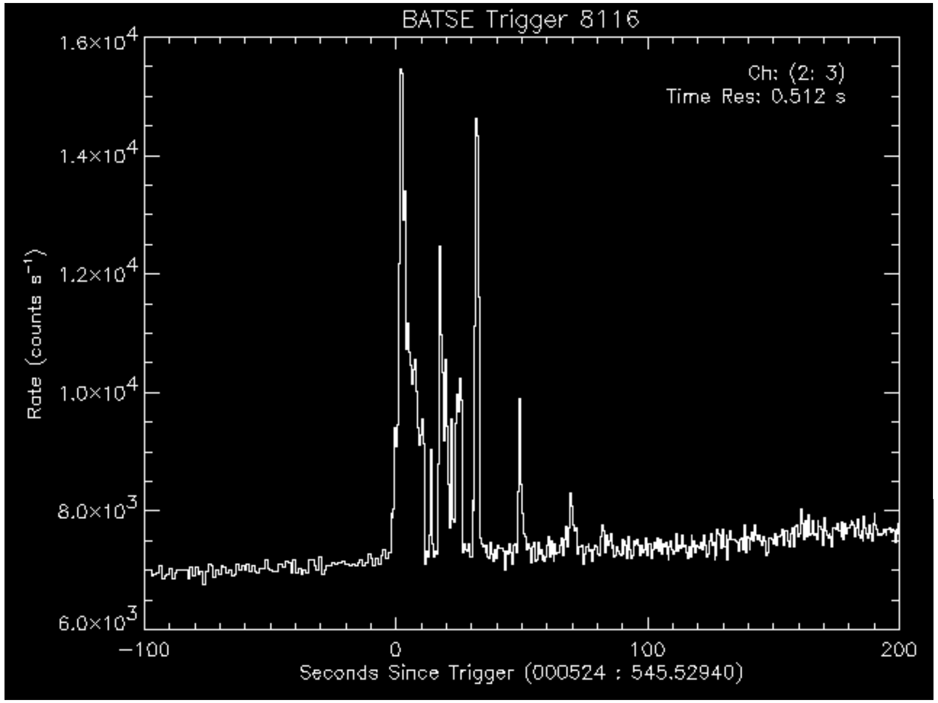

Briggs et al. (1999)

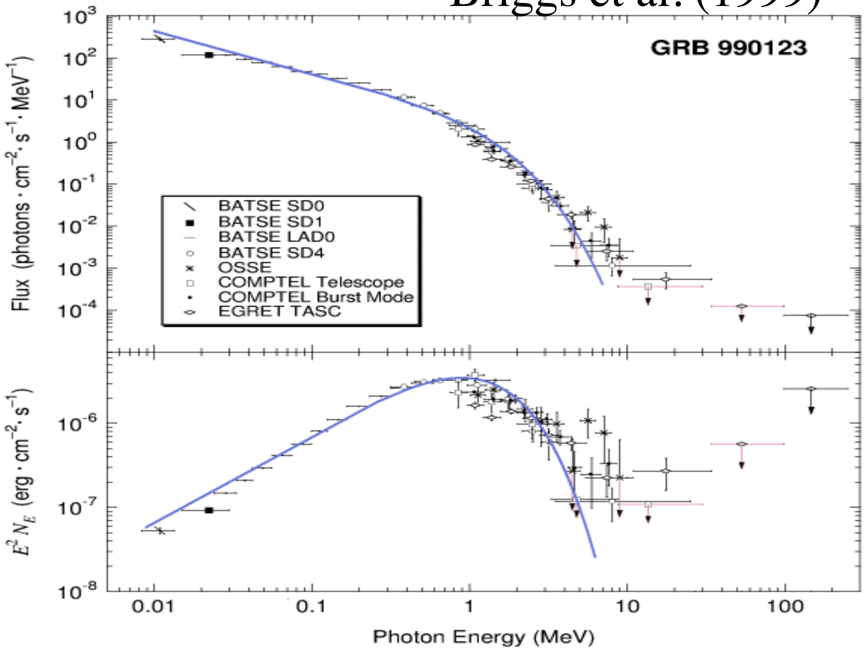

Non thermal spectra

- Fluence (γ): (0.1-10) x 10^{-6} erg/cm^2 ($\Omega/4\pi$)
- Total Energy: E ~ $10^{51} \div 10^{52}$ erg

The Fireball Model

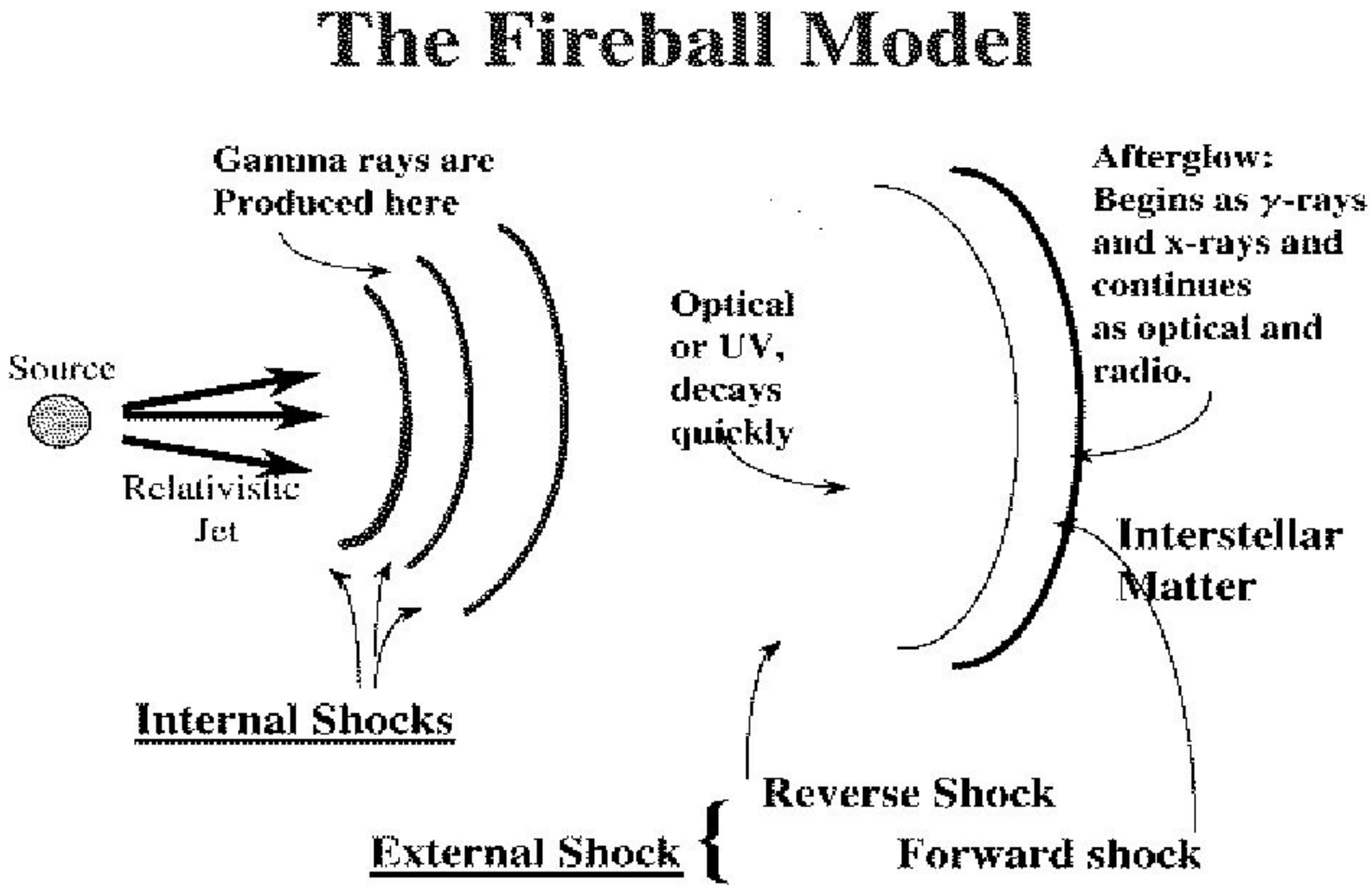

Cartoon by Piran (1999)

The Fireball model

- Relativistic motion of the emitting region
- Shock mechanism converts the kinetic energy of the shells into radiation.
- Baryon Loading problem

External Shock
- Synchrotron & SSC
- High conversion efficiency
- Not easy to justify the rapid variability

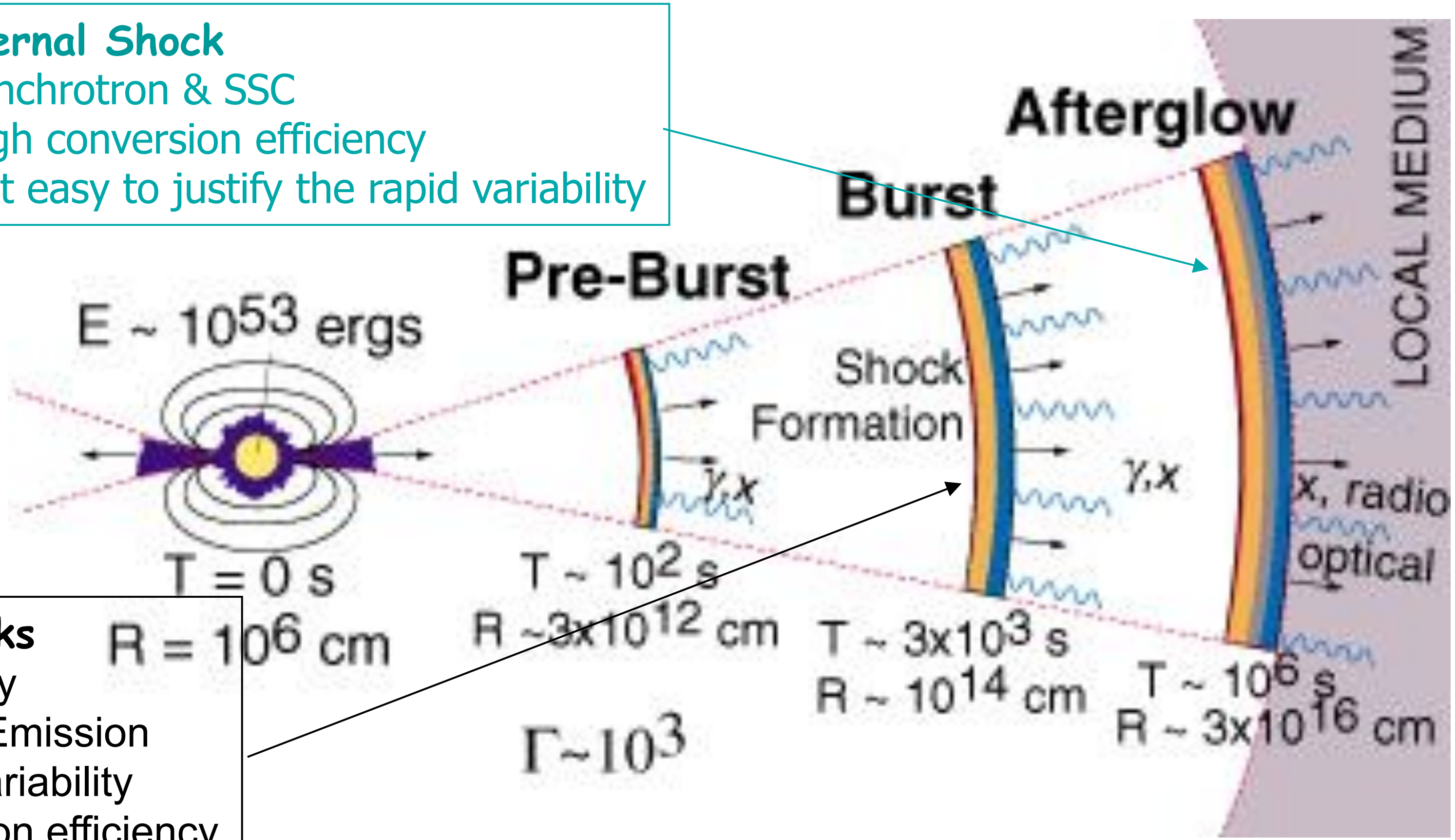

Internal Shocks
- Source activity
- Synchrotron Emission
- Rapid time Variability
- Low conversion efficiency

Afterglow Observations

Harrison et al (1999)

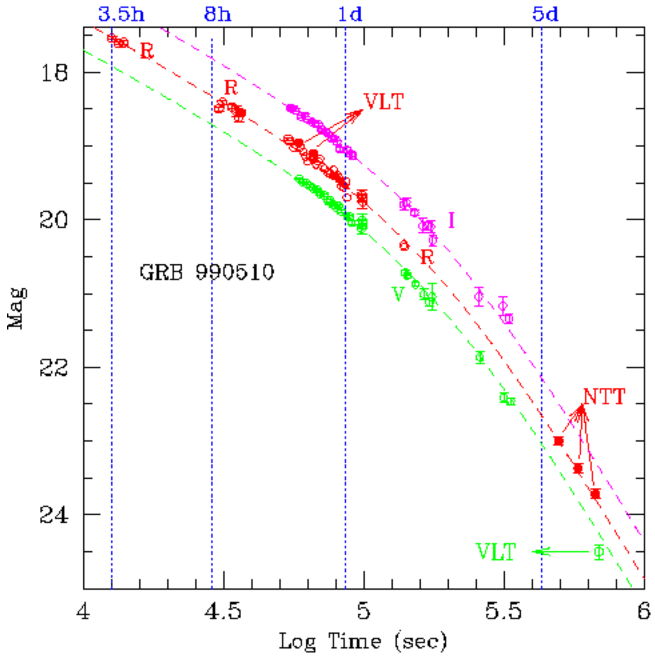

Achromatic Break

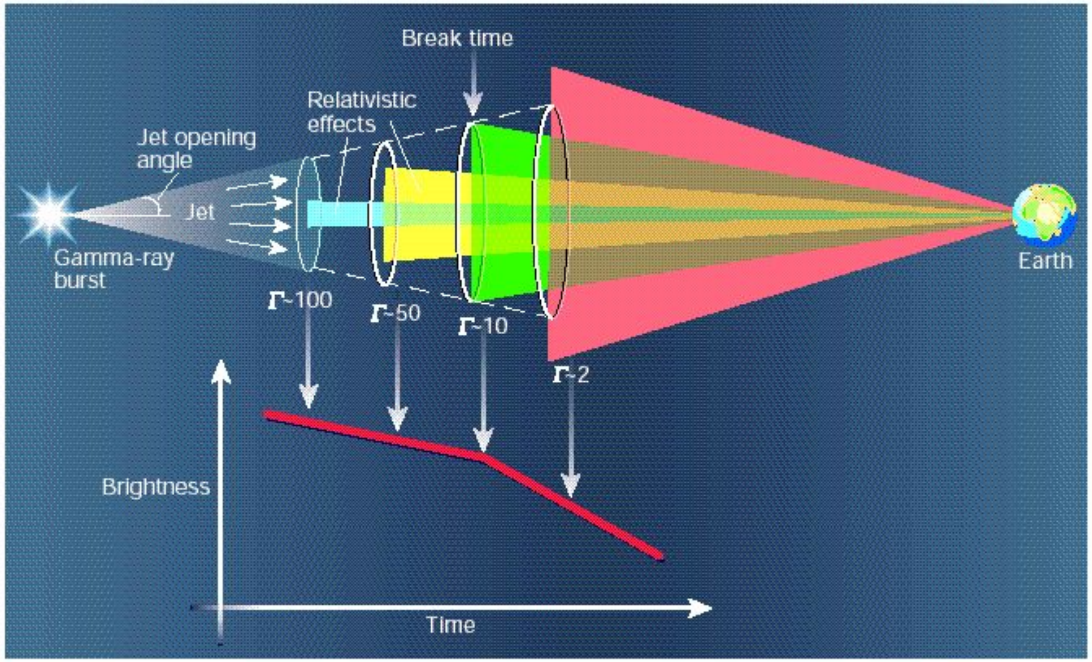

Woosley (2001)

Jet and Energy Requirements

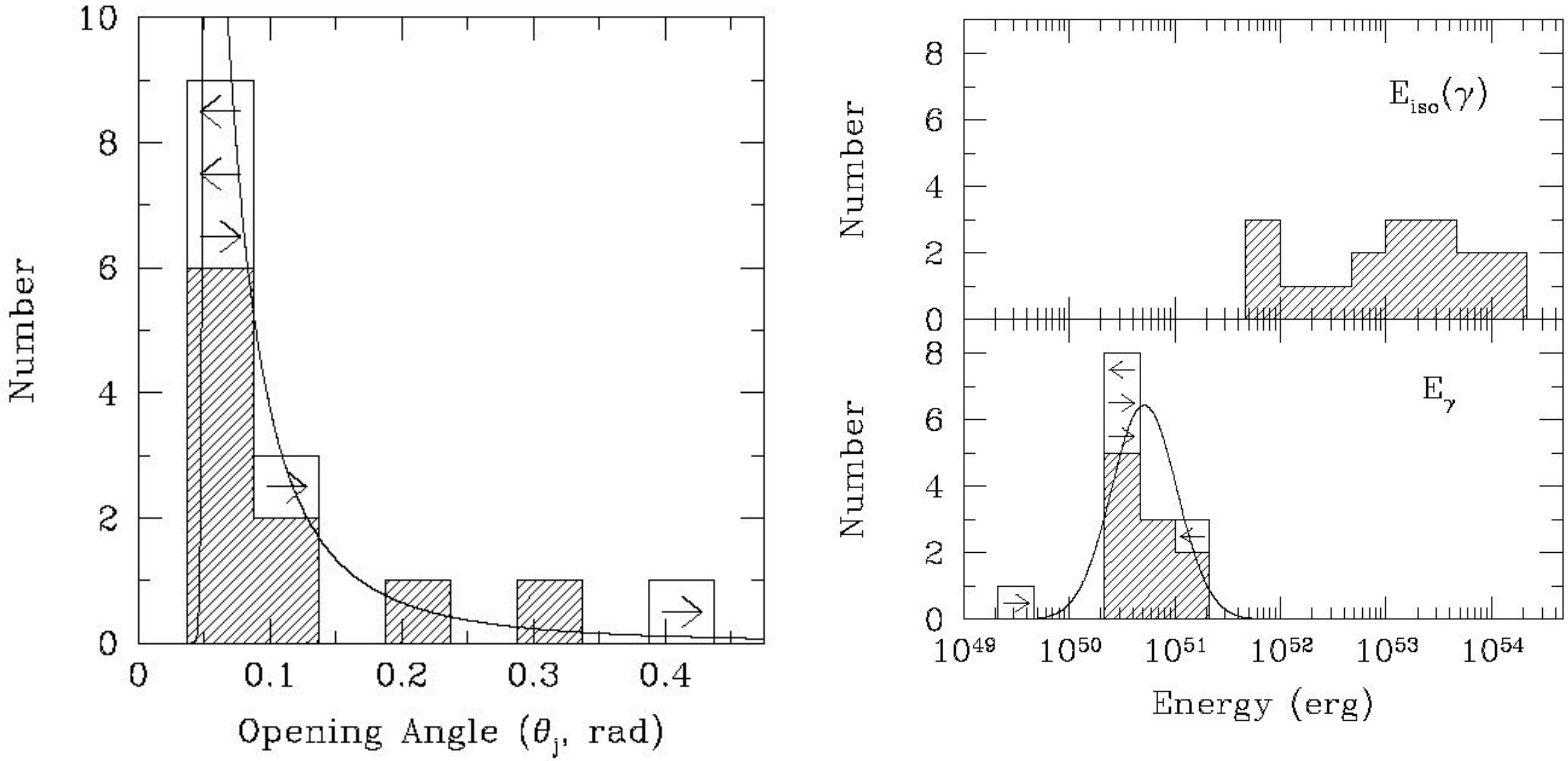

Frail et al. (2001)

Relativistic beaming

Suppose two frames are moving relative to each other with velocity **v** along the z-axis. Then, according to equation (3.10), the component $u_z = dz/dt$ of a velocity u measured in the laboratory frame is

$$\frac{dz}{dt} = \frac{dz' + v\,dt'}{dt' + v\,dz'/c^2} \tag{5.87}$$

or

$$u_z = \frac{u'_z + v}{1 + vu'_z/c^2}. \tag{5.88}$$

Similarly, in the (x- or) y-direction,

$$u_y = \frac{dy}{dt} = \frac{dy'}{\gamma(dt' + v\,dz'/c^2)}, \tag{5.89}$$

which also simplifies to the form

$$u_y = \frac{u'_y}{\gamma(1 + vu'_z/c^2)}. \tag{5.90}$$

Since we wish to determine boosting effects relative to **v**, let us define the angle $\psi \equiv \pi/2 - \theta$. Then, using this angle convention with $u = c$, we infer from

Relativistic beaming

equation (5.90) that

$$\sin\psi = \frac{\sin\psi'}{\gamma(1+\beta\cos\psi')}. \qquad (5.91)$$

A ray leaving the electron in a direction $\theta' = \pi/4$ to $\ddot{\mathbf{d}}$ has a $dP'/d\Omega'$ equal to half its maximum possible value (which occurs at $\theta' = \pi/2$). However, as seen in the laboratory frame, this ray points in a direction much closer to $\mathbf{v}$. According to equation (5.91),

$$\sin\psi \approx \psi \approx \frac{1}{\gamma}. \qquad (5.92)$$

Thus, whereas the power is radiated nearly isotropically in the particle's rest frame, most of it is *beamed* into a narrow cone with half-opening angle $\sim 1/\gamma$ as seen in the laboratory (see also figure 5.8).

Jet breaks

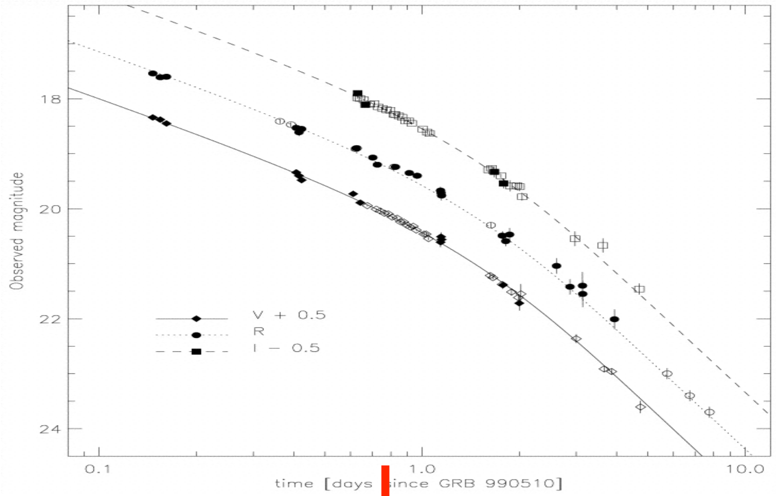

- breaks in the afterglow decay light curves -> collimation ?

$$\theta = 0.09 \left(\frac{t_{jet,d}}{1+z}\right)^{3/8} \left(\frac{n\,\eta_\gamma}{E_{\gamma,iso,52}}\right)^{1/8}$$

$$E_\gamma = (1 - \cos\theta) E_{\gamma,iso}.$$

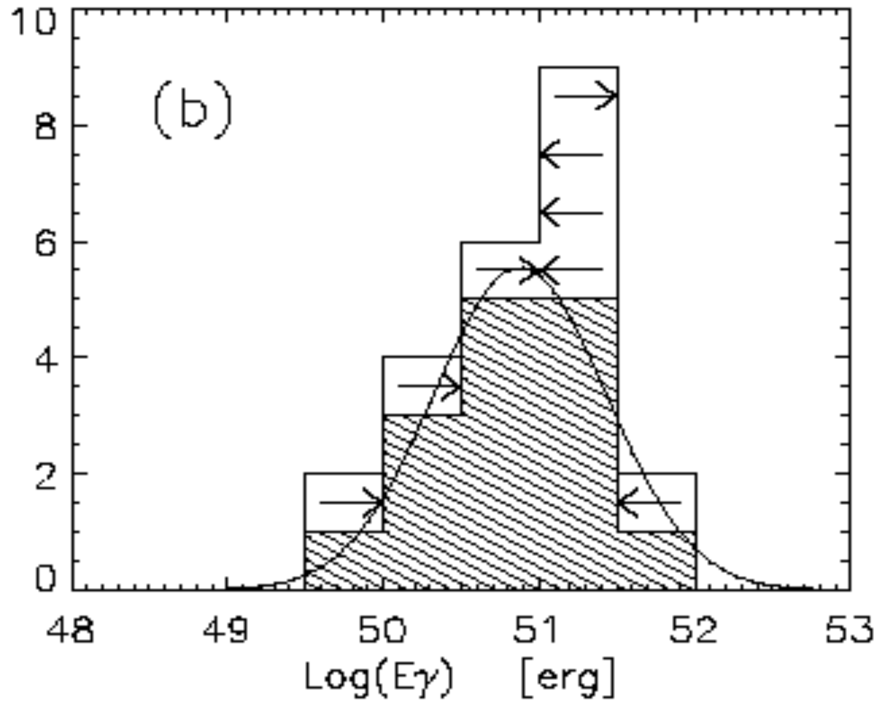

Progenitors

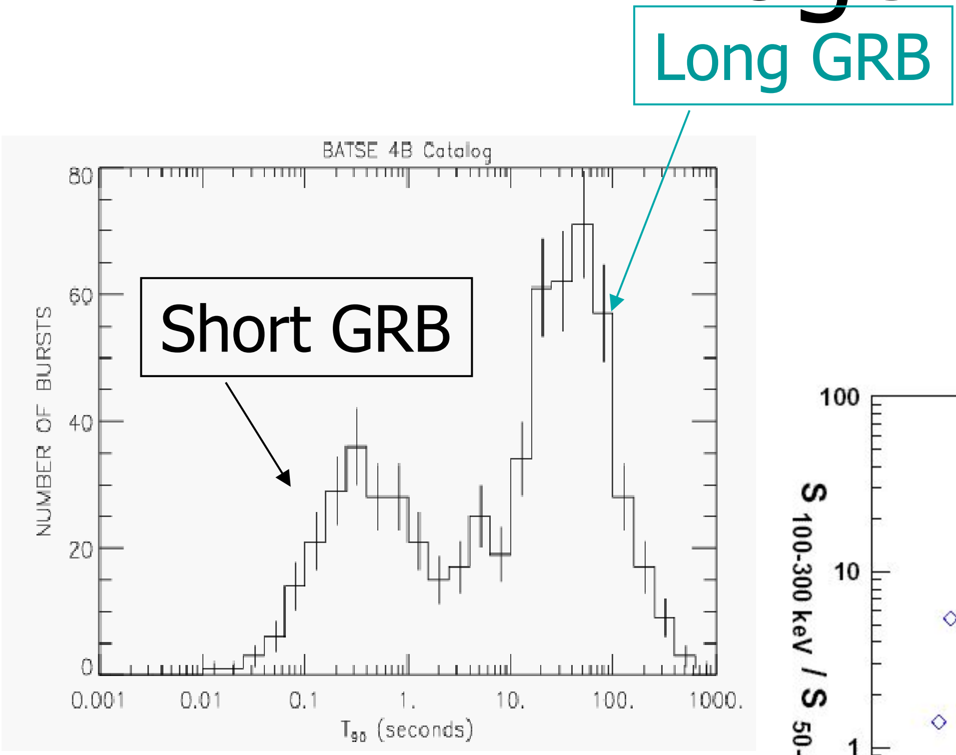

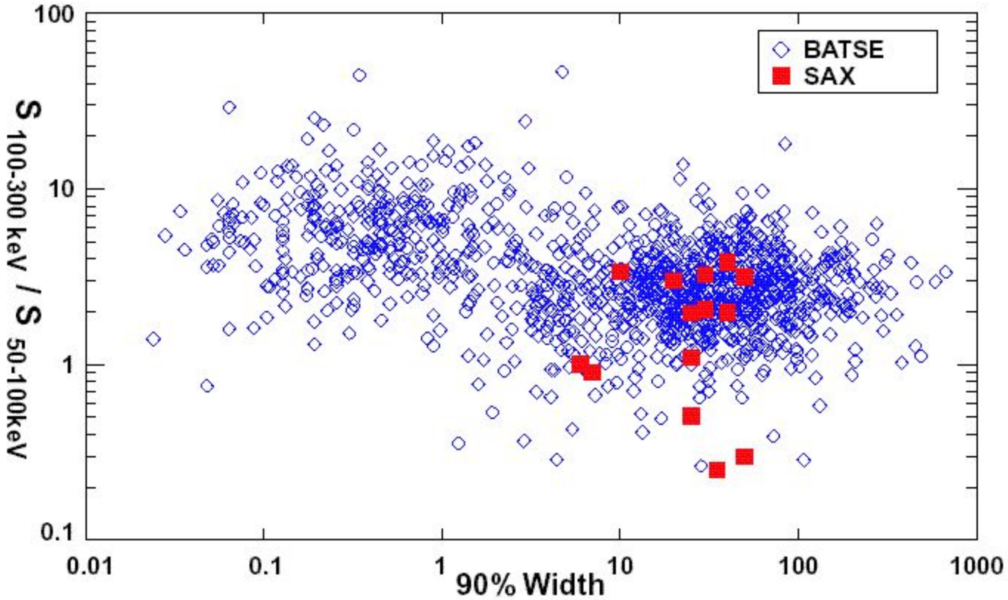

Towards a solution?

Fruchter et al (1999)

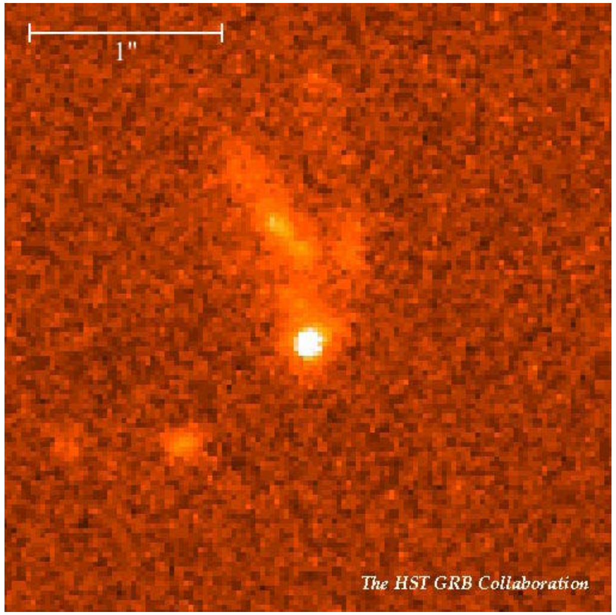

Offset from Host Galaxy

Galama & Wijers (2000)

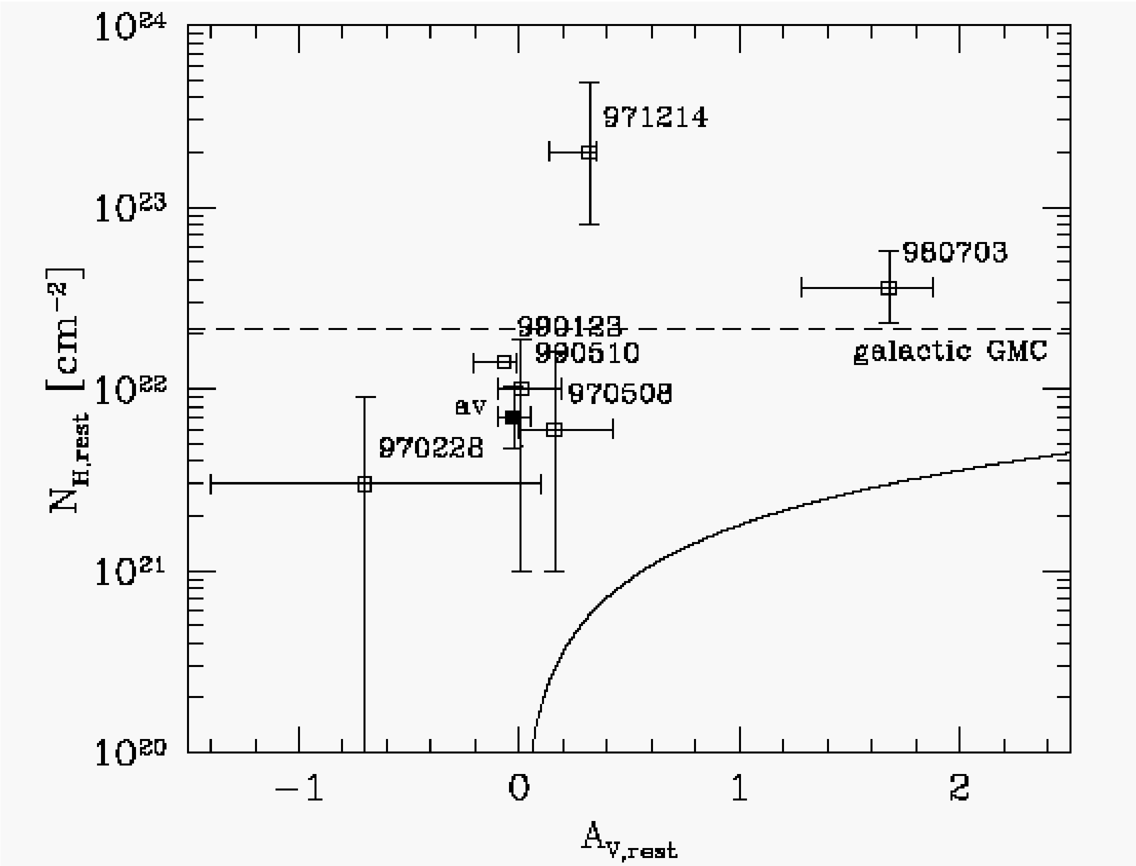

Star forming region density

Towards a solution?

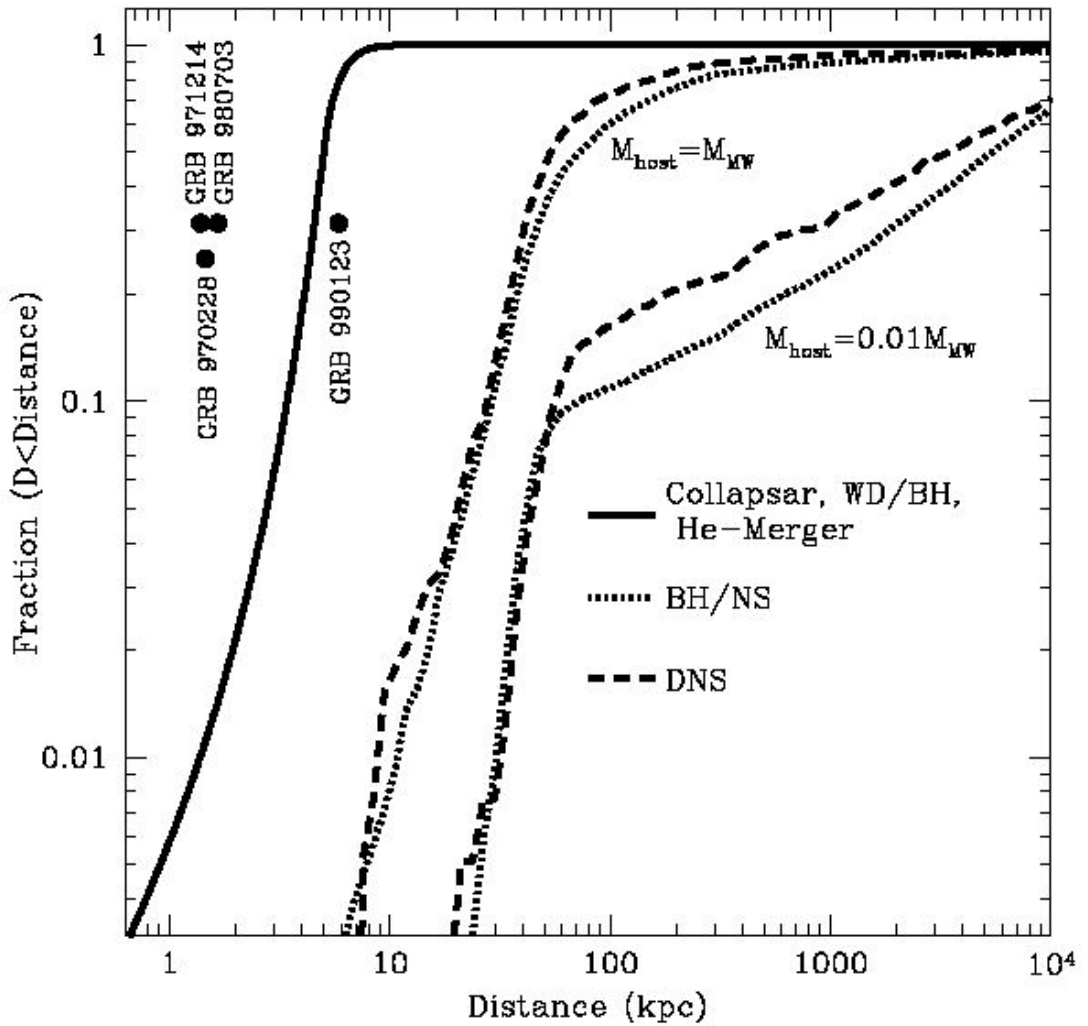

Fryer et al. (1999)

Distance from Host Galaxy

SN- GRB connection

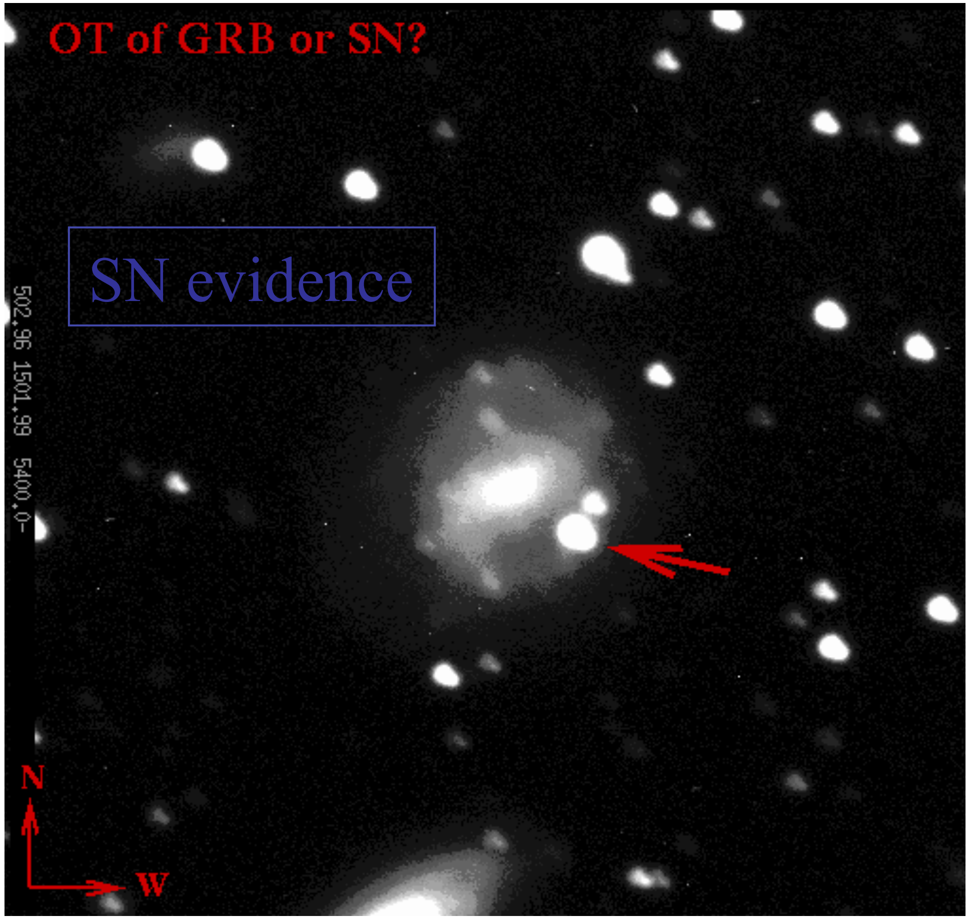

SN 1998bw - GRB 980425

chance coincidence O(10^{-4})

(Galama et al. 98)

GRB & SN first predictions

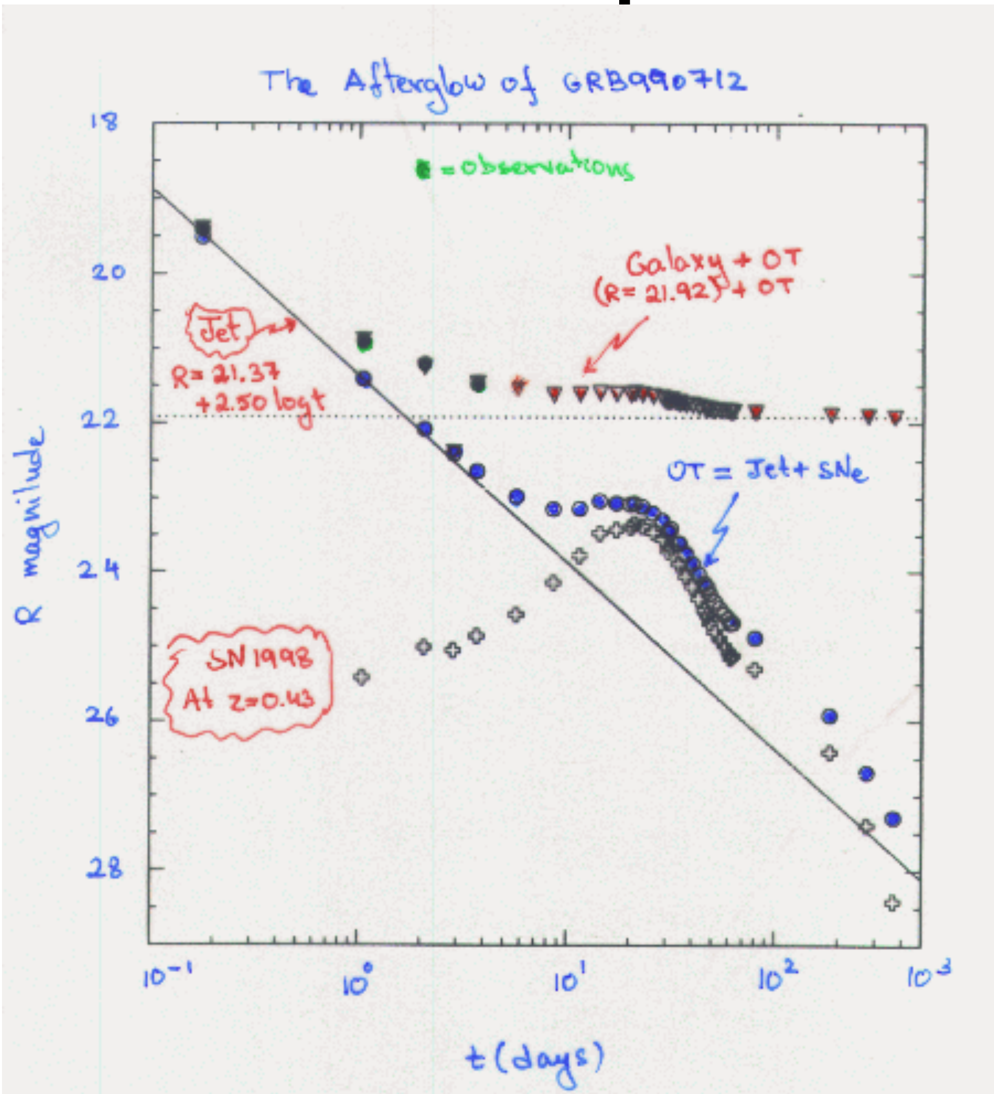

Hjorth, Fynbo, Dar & Courbin (1999)

GRB & SN

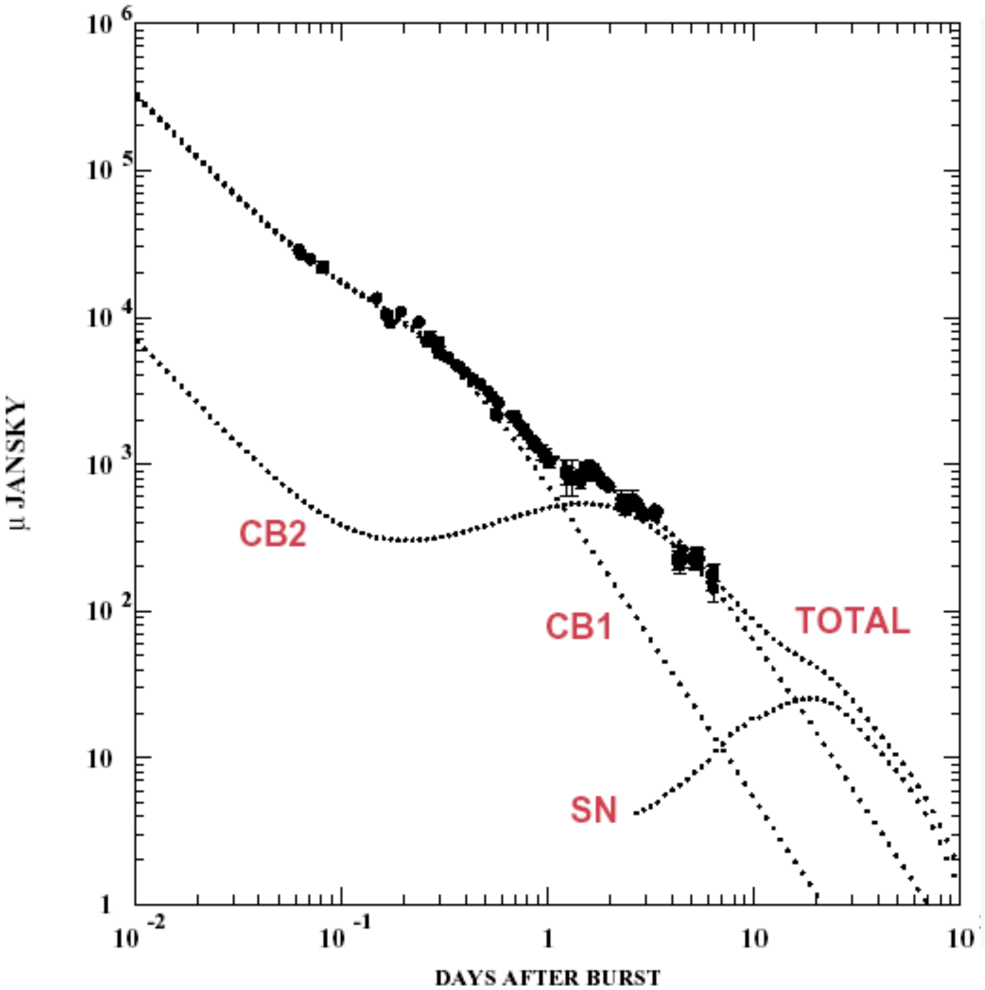

Dado, Dar & De Rujula (2003)

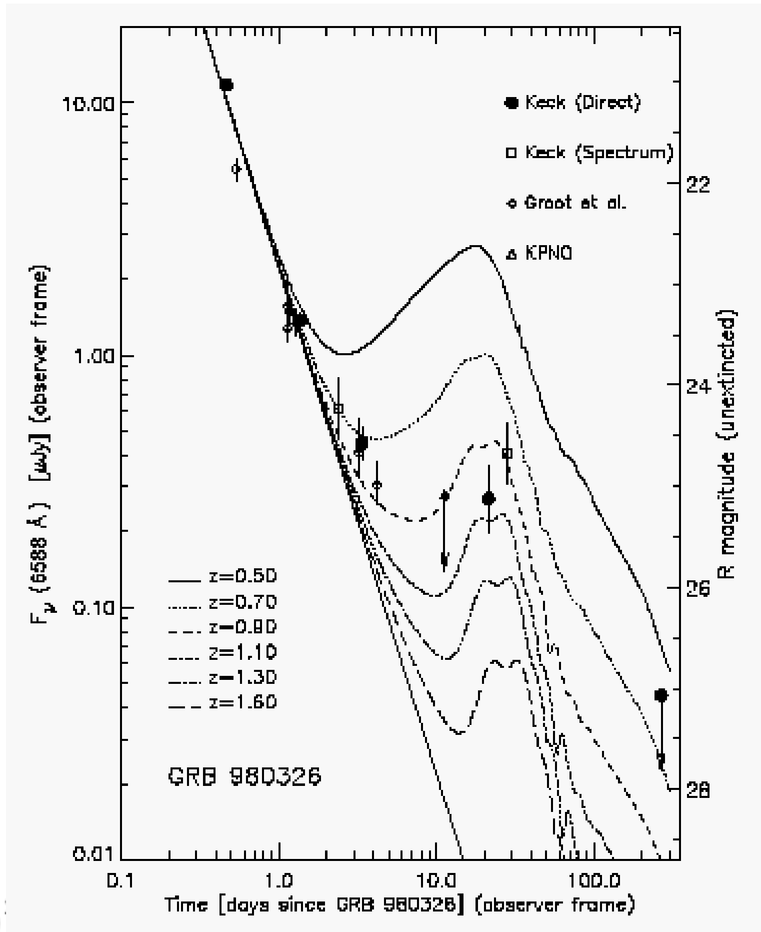

GRB 980326

(Bloom et al. 99)

Hete2

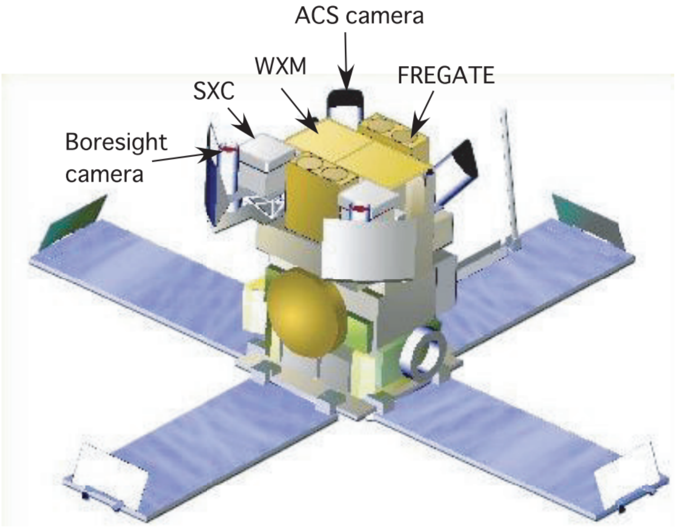

Fig. 1. Schematic drawing of the HETE-2 spacecraft.

2000 - 2008

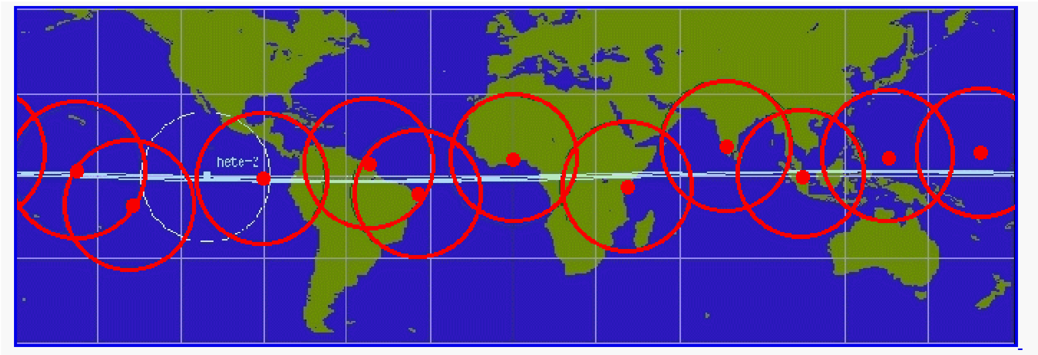

- Two X-ray detectors:
  - Soft X-ray Camera (SXC; 0.5-14 keV).
    Two CCD-based one-dimensional coded-aperature X-ray imagers, one along spacecraft X-direction, the other parallel to Y-direction. Eff. area 7.4 cm^2 per SXC. FOV ~0.9 sr. Spatial resolution less than 30". Spectral resolution 46 eV @ 525 eV, 129 eV @ 5.9 keV.
  - Wide Field X-ray Monitor (WXM; 2-25 keV).
    Two coded-mask one-dimensional position sensitive X-ray detectors oriented orthogonally to each other to measure X and Y positions independently. Eff. area 175 cm^2 each. Spatial resolution less than 10´.Spectral Resolution ~22% @ 8 keV.
- French Gamma-ray Telescope (FREGATE; 6-400 keV).
  4 NaI(Tl) gamma-ray detectors. Eff. area 120 cm^2. FOV ~3 sr. Spectral resolution ~25% @ 20 keV, ~9% @ 662 keV.

HETE-2 Science Instrument Package

French Gamma-ray Telescope
(FREGATE): 5-500 keV; ~π FOV

Wide-Field X-ray Monitor **(WXM):**
2-25 keV; ~5’-10’ localizations

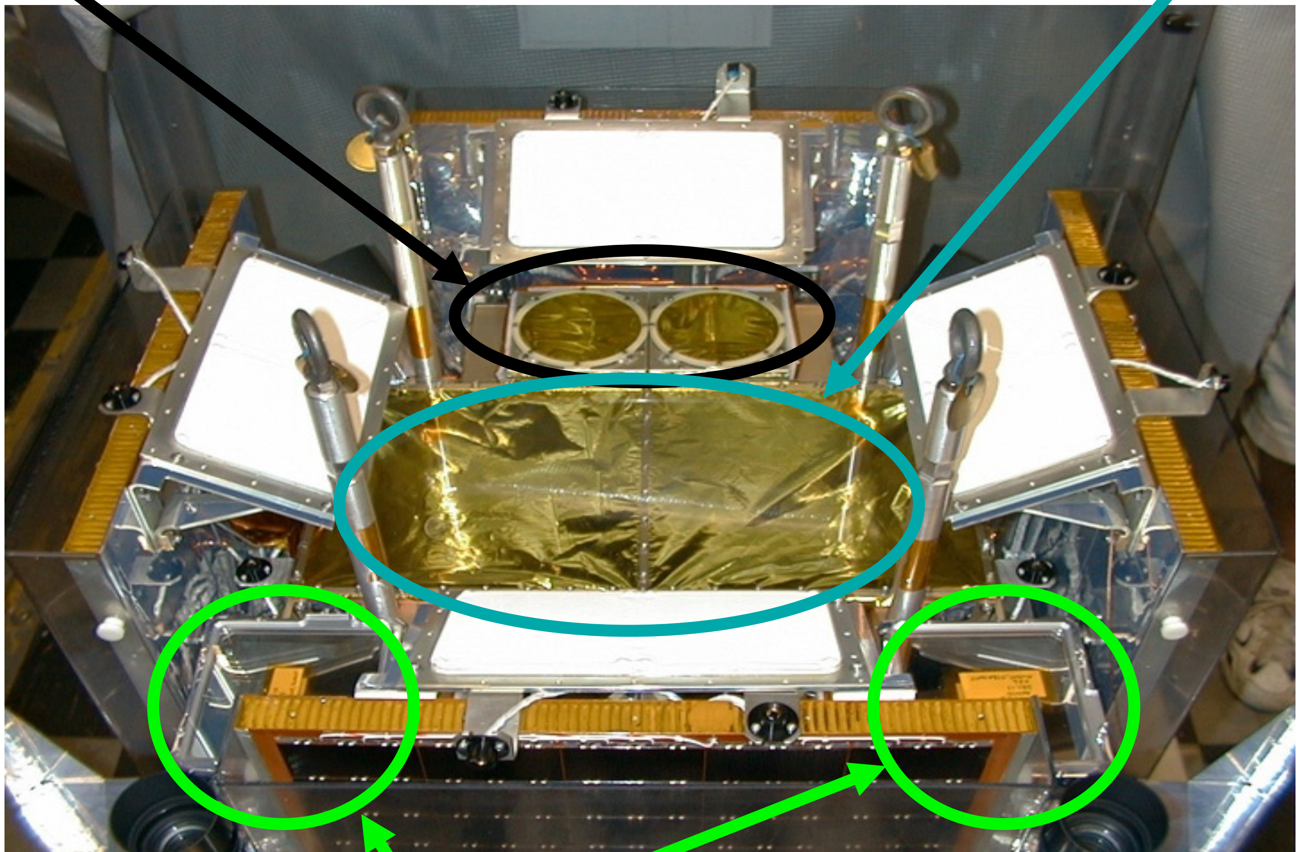

Soft X-ray Cameras **(SXC):**

1-10 keV; ~30” localizations

The Hete-2 detectors

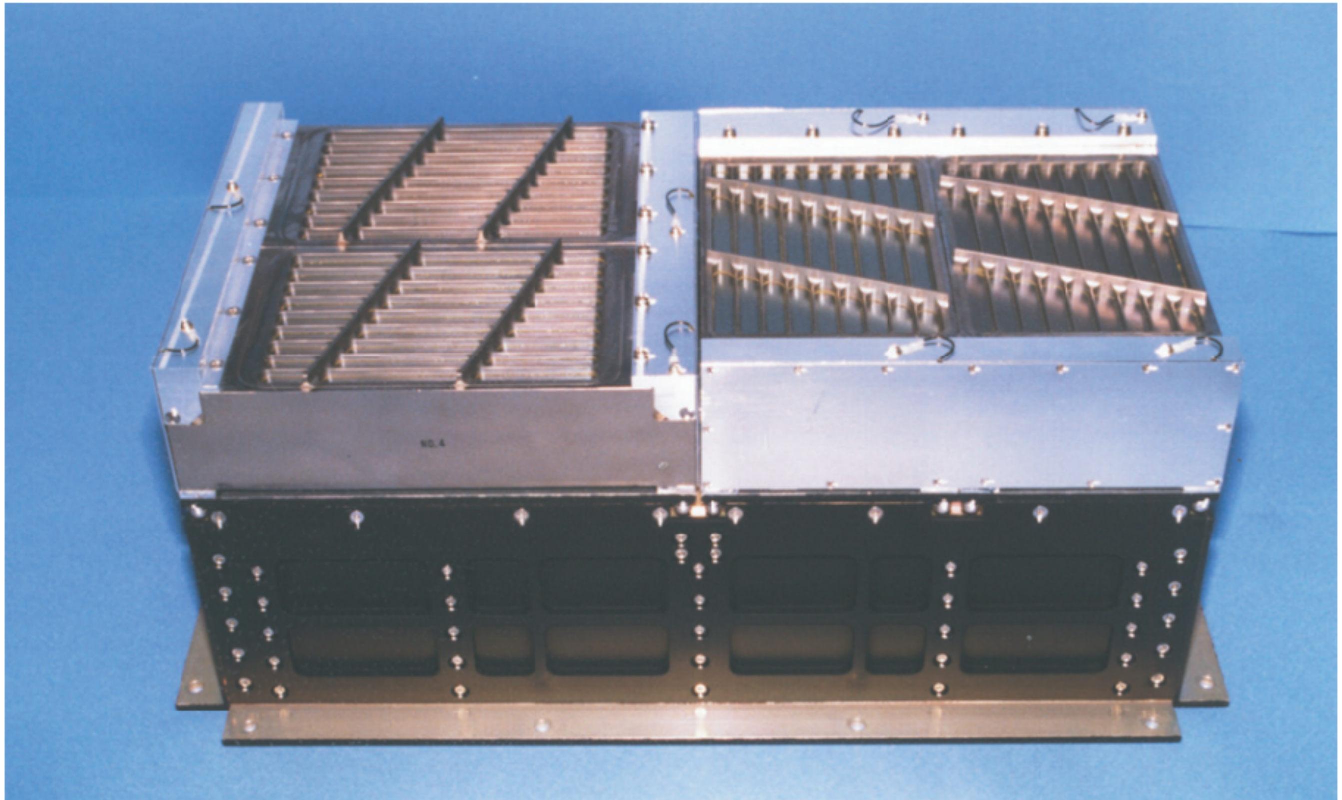

HETE2 Wide Field X-ray Monitor (WXM)

Hete-II results

- The discovery of GRB 030329 -- connecting GRBs with supernovas.
- The discovery of GRB 050709 -- the first short/hard GRB with optical afterglow -- the cosmological origin of this subclass of GRBs.
- Dark bursts…. Some of these dark GRBs fade in the optical very rapidly, others are dimmer but detectable with large (meter class) telescopes.
- The establishment of another subclass of GRBs, the less energetic X-Ray Flashes (XRF), and its first optical counterpart.
- The first to send out arcminute positions of GRBs to the observation community within tens of seconds of the onset of GRB (and in a few instances, while the burst was ongoing).

GRB050709

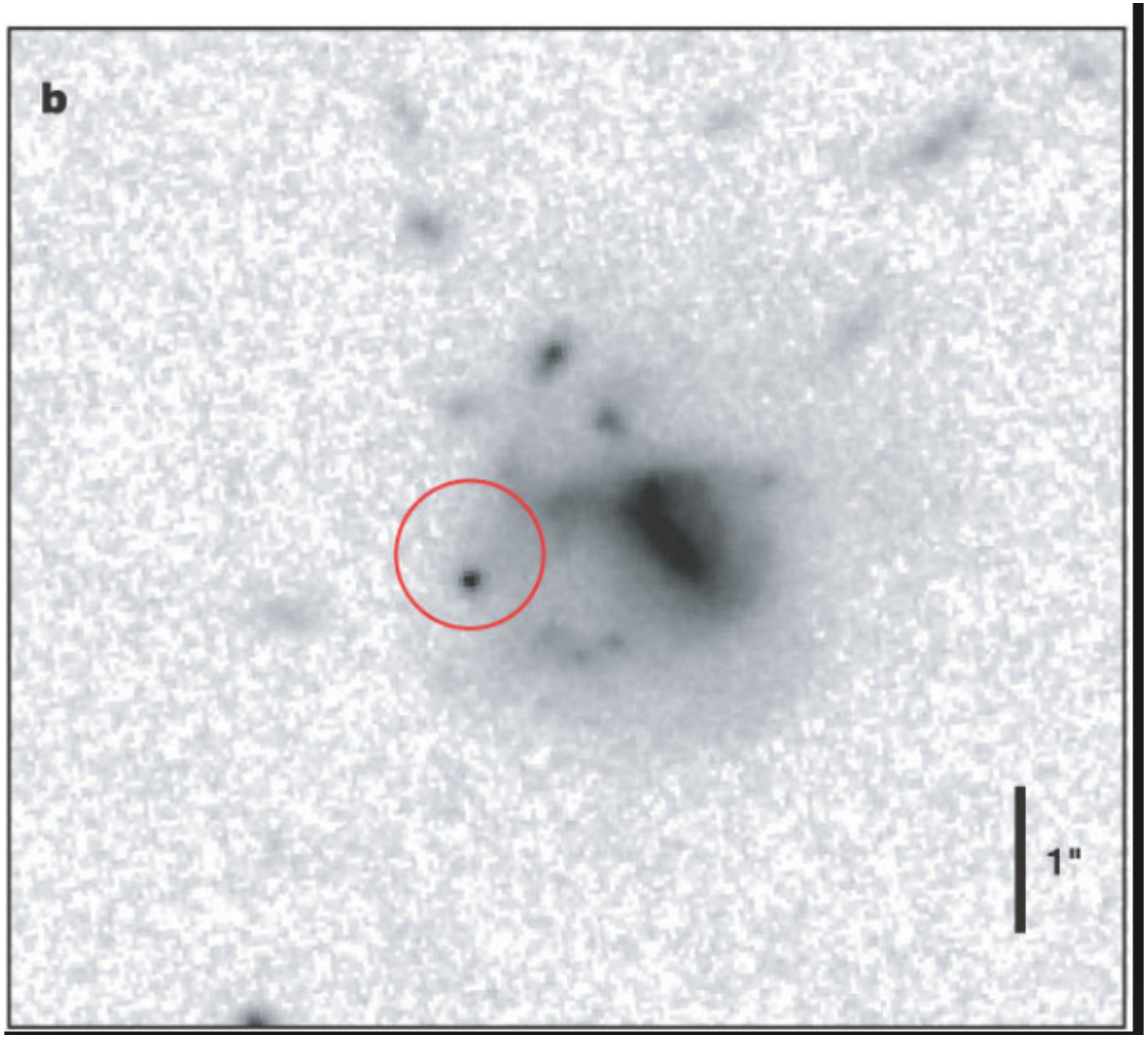

(Fox et al. 2005)

GRB 030329: the “smoking gun”?

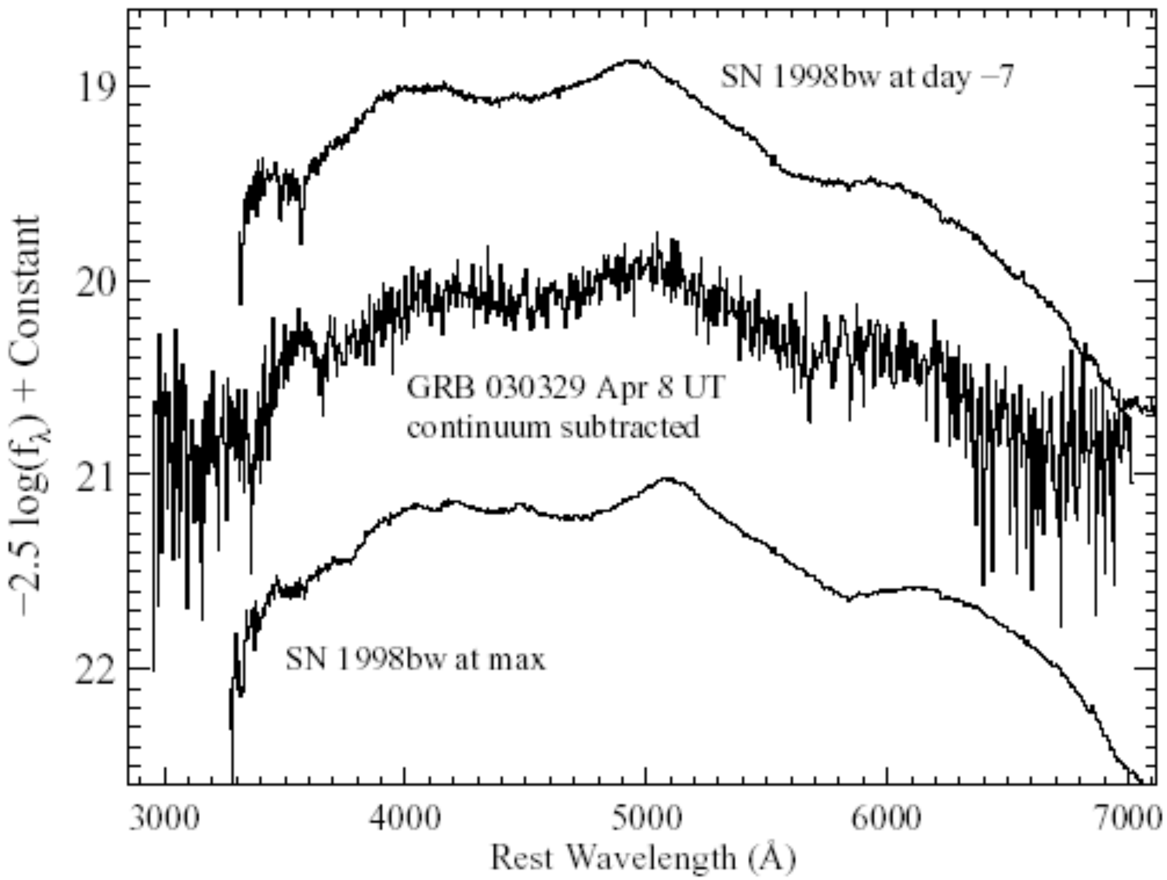

(Matheson et al. 2003)

Classificazione delle SNe

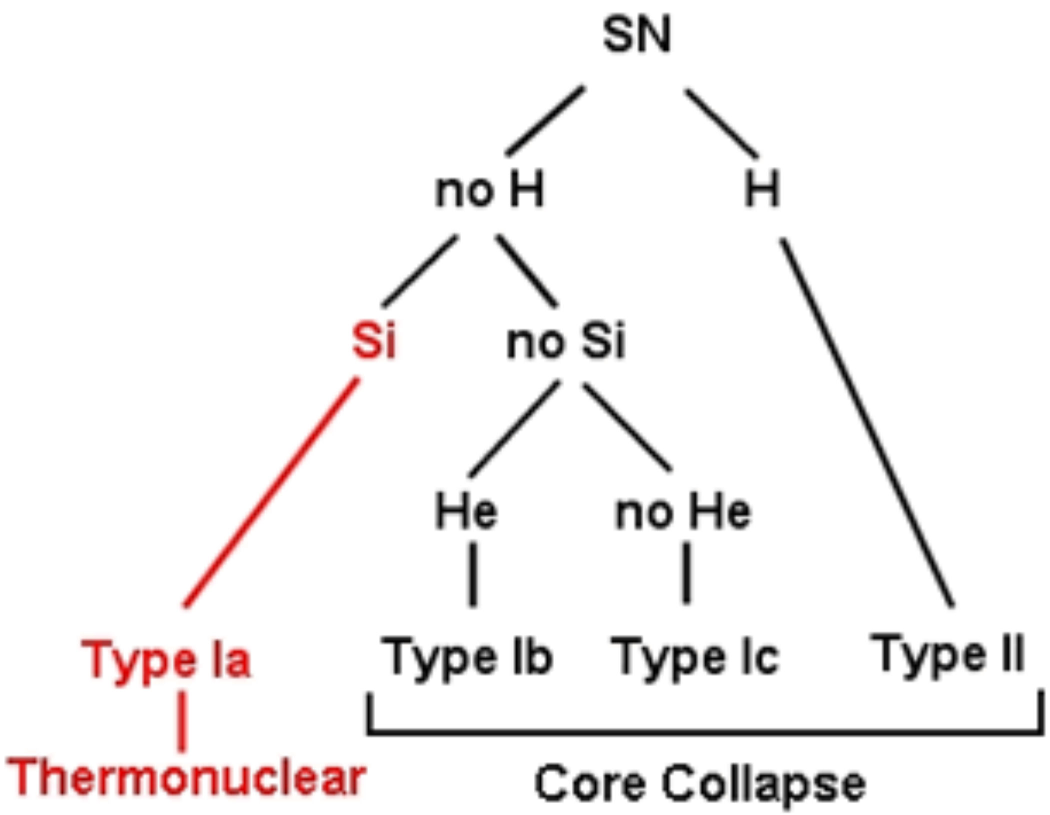

Classificazione delle SNe

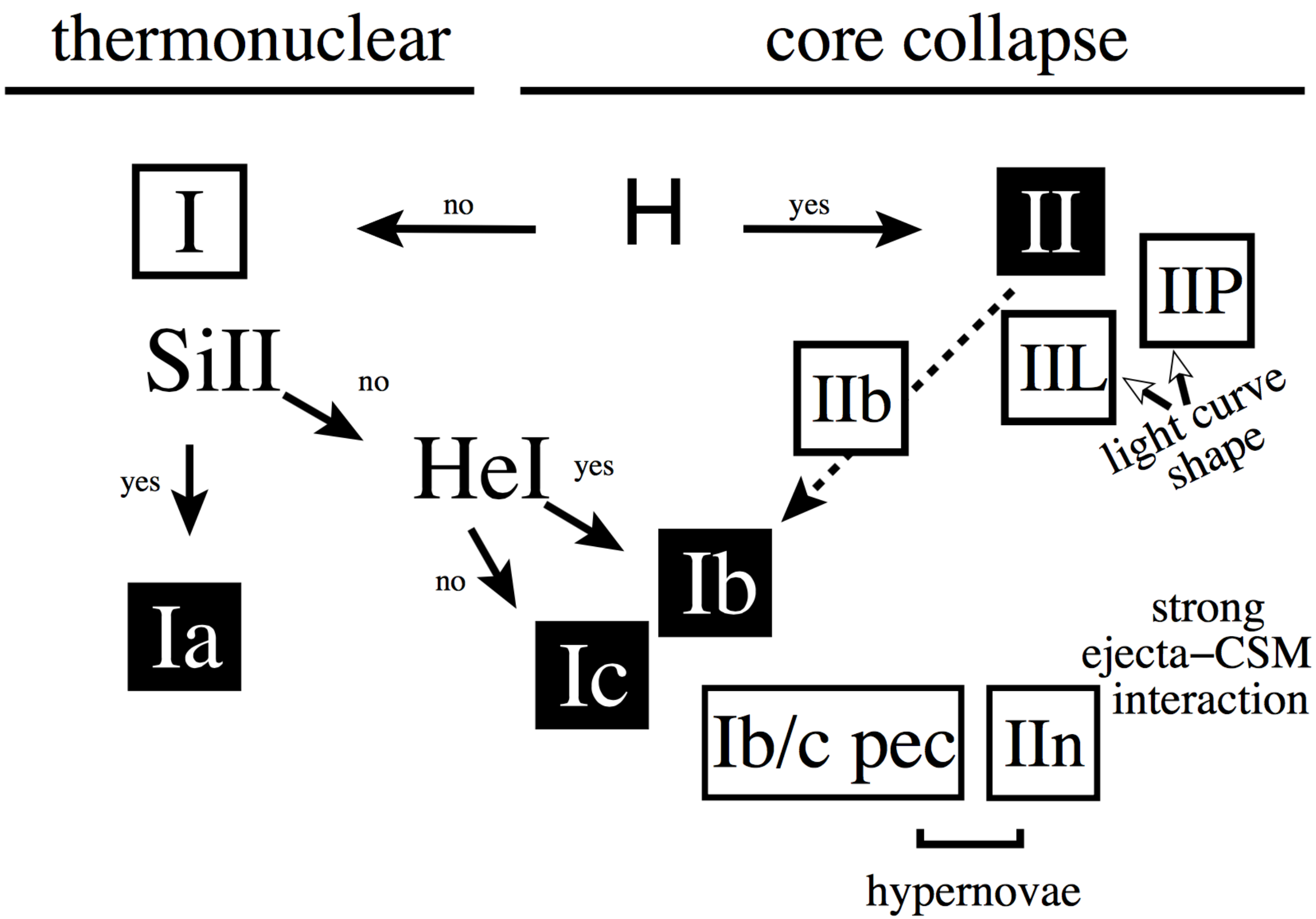

Collapsar model

Woosley (1993)

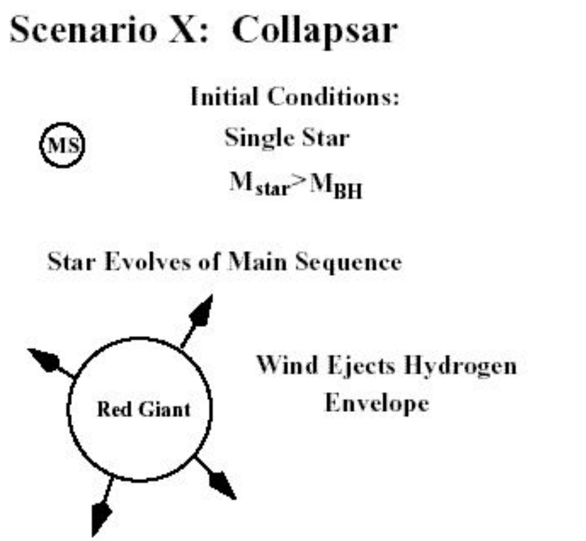

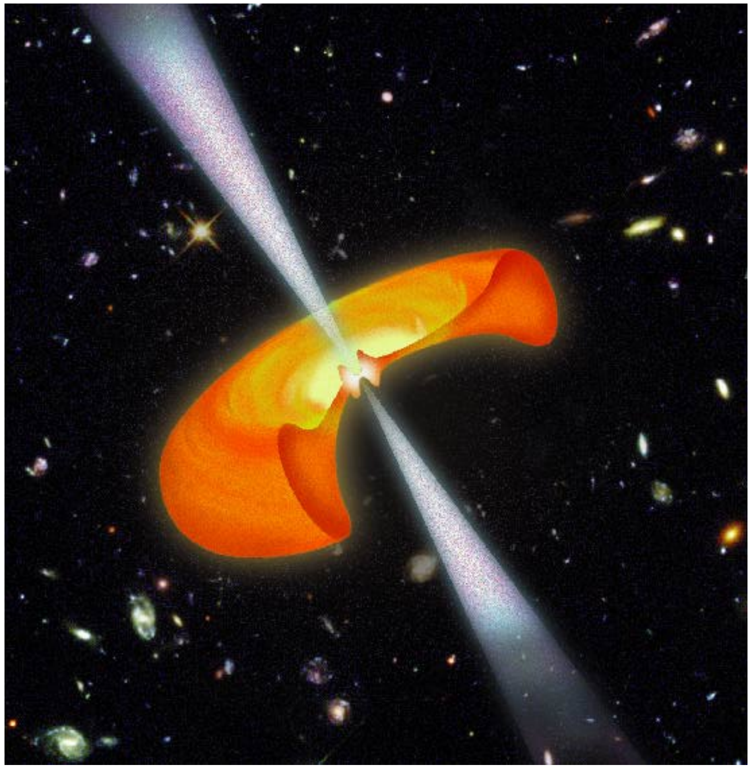

- Very massive star that collapses in a rapidly spinning BH.
- Identification with SN explosion.

Radial transformations

Consider an observer located at a distance R from the point A. The radiation from A reaches the observer at time R/c. The radiation emitted from B takes place at time L/v later and it then travels a distance $(R - L)$ at the speed of light to reach the observer. The trailing edge of the pulse therefore arrives at the observer at a time $L/v + (R - L)/c$. The duration of the pulse as measured by the observer is therefore

$$\Delta t = \left[\frac{L}{v} + \frac{(R - L)}{c}\right] - \frac{R}{c} = \frac{L}{v}\left[1 - \frac{v}{c}\right] . \tag{8.16}$$

The observed duration of the pulse is much less than the time interval L/v, which might have been expected. Only if light propagated at an infinite velocity would the duration of the pulse be L/v. The intriguing point about this analysis is that the factor $1 - (v/c)$ is exactly the same factor which appears in the Liénard–Wiechert potentials (6.19) and which takes account of the fact that the source of radiation is moving towards the observer. The

Radial transformations

relativistic electron almost catches up with the radiation emitted at A since $v \approx c$, but not quite. We can rewrite (8.16) using the fact that

$$\frac{L}{v} = \frac{r_g \theta}{v} \approx \frac{1}{\gamma \omega_r} = \frac{1}{\omega_g}, \quad (8.17)$$

where ω_g is the non-relativistic angular gyrofrequency and $\omega_r = \omega_g / \gamma$ the relativistic angular gyrofrequency. We can also rewrite $(1 - v/c)$ as

$$\left(1 - \frac{v}{c}\right) = \frac{[1 - (v/c)][1 + (v/c)]}{[1 + (v/c)]} = \frac{\left(1 - v^2/c^2\right)}{1 + (v/c)} \approx \frac{1}{2\gamma^2}. \quad (8.18)$$

since $v \approx c$. Therefore, the observed duration of the pulse is

$$\Delta t \approx \frac{1}{2\gamma^2 \omega_g}. \quad (8.19)$$